Vol. 192 No. 1, January 15, 1987 ISSN 0003-2670

ANALYTICA CHIMICA ACTA

UBLISHER'S NOTE

lease note that Vol. 190 No. 2 Cumulative Indexes covering Vols. 171–190) and Vol. 191 (special issue on Chemometrics in Analytical Chemistry) will both appear in May 1987.

International journal devoted to all branches of analytical chemistry

ELSEVIER

ANALYTICA CHIMICA ACTA

International journal devoted to all branches of analytical chemistry
Revue internationale consacrée à tous les domaines de la chimie analytique
Internationale Zeitschrift für alle Gebiete der analytischen Chemie

PUBLICATION SCHEDULE FOR 1987

	J	F	M	A	M	J	J	A	S	O	N	D
Analytica Chimica Acta	192	193	194	195	196	197	198	199	200	201	202	203

Scope. *Analytica Chimica Acta* publishes original papers, short communications, and reviews dealing with every aspect of modern chemical analysis both fundamental and applied.

Submission of Papers. Manuscripts (three copies) should be submitted as designated below for rapid and efficient handling:

Papers from the Americas to: Professor Harry L. Pardue, Department of Chemistry, Purdue University, West Lafayette, IN 47907, U.S.A.

Papers from all other countries to: Dr. A. M. G. Macdonald, Department of Chemistry, The University, P.O. Box 363, Birmingham B15 2TT, England. Papers dealing particularly with computer techniques to: Professor J. T. Clerc, Universität Bern, Pharmazeutisches Institut, Baltzerstrasse 5, CH-3012 Bern, Switzerland.

Submission of an article is understood to imply that the article is original and unpublished and is not being considered for publication elsewhere. Upon acceptance of an article by the journal, authors will be asked to transfer the copyright of the article to the publisher. This transfer will ensure the widest possible dissemination of information.

Information for Authors. Papers in English, French and German are published. There are no page charges. Manuscripts should conform in layout and style to the papers published in this Volume. Authors should consult Vol. 170 for detailed information. Reprints of this information are available from the Editors or from: Elsevier Editorial Services Ltd., Mayfield House, 256 Banbury Road, Oxford OX2 7DH (Great Britain).

Reprints. Fifty reprints will be supplied free of charge. Additional reprints (minimum 100) can be ordered. An order form containing price quotations will be sent to the authors together with the proofs of their article.

Advertisements. Advertisement rates are available from the publisher.

Subscriptions. Subscriptions should be sent to: Elsevier Science Publishers B.V., Journals Department, P.O. Box 211, 1000 AE Amsterdam, The Netherlands. Tel: 5803 911, Telex: 18582.

Publication. *Analytica Chimica Acta* appears in 12 volumes in 1987. The subscription for 1987 (Vols. 192–203) is Dfl. 2700.00 plus Dfl. 300.00 (p.p.h.) (total approx. US $1333.30). All earlier volumes (Vols. 1–191) except Vols. 23 and 28 are available at Dfl. 231.00 (US $102.70), plus Dfl. 17.00 (US $7.60) p.p.h., per volume.

Our p.p.h. (postage, packing and handling) charge includes surface delivery of all issues, except to subscribers in the U.S.A., Canada, Japan, Australia, New Zealand, P.R. China, India, Israel, South Africa, Malaysia, Thailand, Singapore, South Korea, Taiwan, Pakistan, Hong Kong, Brazil, Argentina and Mexico, who receive all issues by air delivery (S.A.L. — Surface Air Lifted) at no extra cost. For the rest of the world, airmail and S.A.L. charges are available upon request.

Claims for issues not received should be made within three months of publication of the issues. If not they cannot be honoured free of charge.

For further information, or a free sample copy of this or any other Elsevier Science Publishers journal, readers in the U.S.A. and Canada can contact the following address: Elsevier Science Publishing Co. Inc., Journal Information Center, 52 Vanderbilt Avenue, New York, NY 10017, U.S.A., Tel: (212) 916-1250.

ANALYTICA CHIMICA ACTA
VOL. 192 (1987)

ANALYTICA CHIMICA ACTA

International journal devoted to all branches of analytical chemistry

ELSEVIER Amsterdam–Oxford–New York–Tokyo

Anal. Chim. Acta, Vol. 192 (1987)

0003-2670/87/$03.50

Printed in The Netherlands

New Editor — Professor W. E. van der Linden

In this issue we welcome Professor Willem van der Linden to the team of editors of Analytica Chimica Acta.

Professor van der Linden taught at the University of Amsterdam from 1962 to 1980. Since 1980, he has been Professor of Chemical Analysis in the Department of Chemical Technology in the University of Twente, The Netherlands. His previous research interests included electroanalytical techniques, especially voltammetry and ion selective electrode procedures. The use of ion selective electrodes as flow-through detectors triggered his interest in flow-injection systems. At present, he is also involved in research in process analytical chemistry. Professor van der Linden has assisted in or been responsible for the organization of a number of successful international conferences, including the first conference on Flow Analysis in Amsterdam in 1979, and the ANATECH conference on applications of analytical chemical techniques to industrial process control in 1986.

Professor van der Linden will strengthen our service to analytical chemists, especially those in Europe. Authors will benefit from his wide knowledge, helpful advice and enthusiasm, and his co-editors look forward to a long and fruitful collaboration.

A. M. G. Macdonald
Harry L. Pardue
Alan Townshend
J. T. Clerc

Analytica Chimica Acta, 192 (1987) 1—8
Elsevier Science Publishers B.V., Amsterdam — Printed in The Netherlands

REMOVAL OF HUMIC ACID AND SURFACTANT INTERFERENCES IN TRACE METAL DETERMINATIONS BY DIFFERENTIAL-PULSE ANODIC STRIPPING VOLTAMMETRY WITH USE OF ADSORPTION AND CHELATE ION-EXCHANGER COLUMNS IN A FLOW-INJECTION SYSTEM

XIURONG YANG, LARS RISINGER and GILLIS JOHANSSON*

Department of Analytical Chemistry, University of Lund, P.O. Box 124, S-221 00 Lund (Sweden)

(Received 14th July 1986)

SUMMARY

A flow-injection differential-pulse anodic stripping voltammetry (d.p.a.s.v.) method is modified so that interferences from humic acids or surfactants are eliminated. The injected, slightly acidic sample is passed through a silica anion-exchanger column to remove compounds with a strong tendency to adsorb to the electrode. The sample then passes to a chelate ion-exchange column containing immobilized 8-quinolinol. The metal ions are retained and later eluted with acid into the voltammetric cell. The results show that the interferences from up to 500 mg l^{-1} humic acid or at least 50 mg l^{-1} Triton X-100 can be removed and that the metal ions can be determined in a range similar to that for normal d.p.a.s.v. methods. The complete cycle time for a determination was 12 min.

Differential-pulse anodic stripping voltammetry (d.p.a.s.v.) is well suited for the determination of trace metals, particularly in environmental samples. The extremely low concentration levels make it necessary to pay particular attention to various kinds of interferences with the methods for trace metals. Among these, there are the well known effects from a number of surface-active compounds and from humic matter. It has been shown [1—5] that if the interferents are present at levels above 0.1 mg l^{-1}, they will affect the response factor of the voltammetric method in a complex and almost unpredictable way.

Various methods or pretreatment schemes are available for the analysis of samples containing, e.g., humic or surface-active interferents. The metal ions can be removed from the sample by extraction or ion-exchange; the organic compounds can be destroyed, at least partially, by chemical oxidation or by u.v.-radiation [6]. All these methods are time-consuming and the total effect is often that the voltammetric methods are considered to be less attractive than, for example, the spectrometric methods, which do not suffer from this kind of interference pattern.

0003-2670/87/$03.50

The medium-exchange method seemed initially to offer a very promising solution. The metals are plated into the mercury and are kept there while the sample solution is replaced by a pure buffer solution. The stripping and thus the actual measurements are made in a solution without interferents. The medium-exchange method can easily be implemented in a flow-injection system [7—13]. It turned out, however, that interferents which could adsorb strongly on the surface of the mercury electrode could not be reduced sufficiently for samples from waters with high humic contents. A completely different method of isolating metal ions from the sample in a flow-injection system has recently been developed. The metal ions are taken up in a small column of a chelate ion-exchanger which is then washed by the carrier solution. An acid plug is next introduced by turning a valve and the metal ions are then eluted with the acid. The method has been used on-line, e.g., for atomic absorption spectrometry [14—16] and with ion-selective electrodes [17].

This paper reports on the properties of a flow injection/d.p.a.s.v. system containing a chelate ion exchanger for increased isolation of metal ions from the sample matrix. The effect of an additional purification step for humic materials, namely an anion exchanger for adsorption, is also reported.

EXPERIMENTAL

Pumping and switching

Trace metal ions were isolated on-line from interfering matrix components in a flow system as shown in Fig. 1. The sample and the acid loops are filled with peristaltic pump A while pump B washes a silica anion-exchanger (SAX) adsorption column with water. It also pumps buffer solution through the chelate ion-exchanger (8-HQ) and the electrochemical cell (Fig. 1a). The ions from the previous sample are simultaneously stripped from the mercury film electrode and quantified by d.p.a.s.v.

The slightly acidic sample is next (Fig. 1b) transported through the SAX column for purification. It is mixed with a buffer to a final pH around 5.5 and passes through the chelate ion-exchanger where the metal ions are retained. The sample matrix is diverted to waste without passing the electrochemical cell to avoid adsorption of interferents on the film electrode.

The content of the acid loop is next transferred to the chelate ion-exchanger (Fig. 1c). The metal ions are eluted and pass the electrochemical cell where the mercury film electrode is kept at a sufficiently negative voltage for plating. The sensitivity is enhanced by using a low flow rate during this step. Stripping is finally made into a flowing buffer solution (Fig. 1a) thus utilizing also the advantage of the medium-exchange method.

The total cycle time was 12 min for 1-ml samples and it was divided into 3, 5 and 4 min for the steps represented by Fig. 1(a), (b), and (c), respectively.

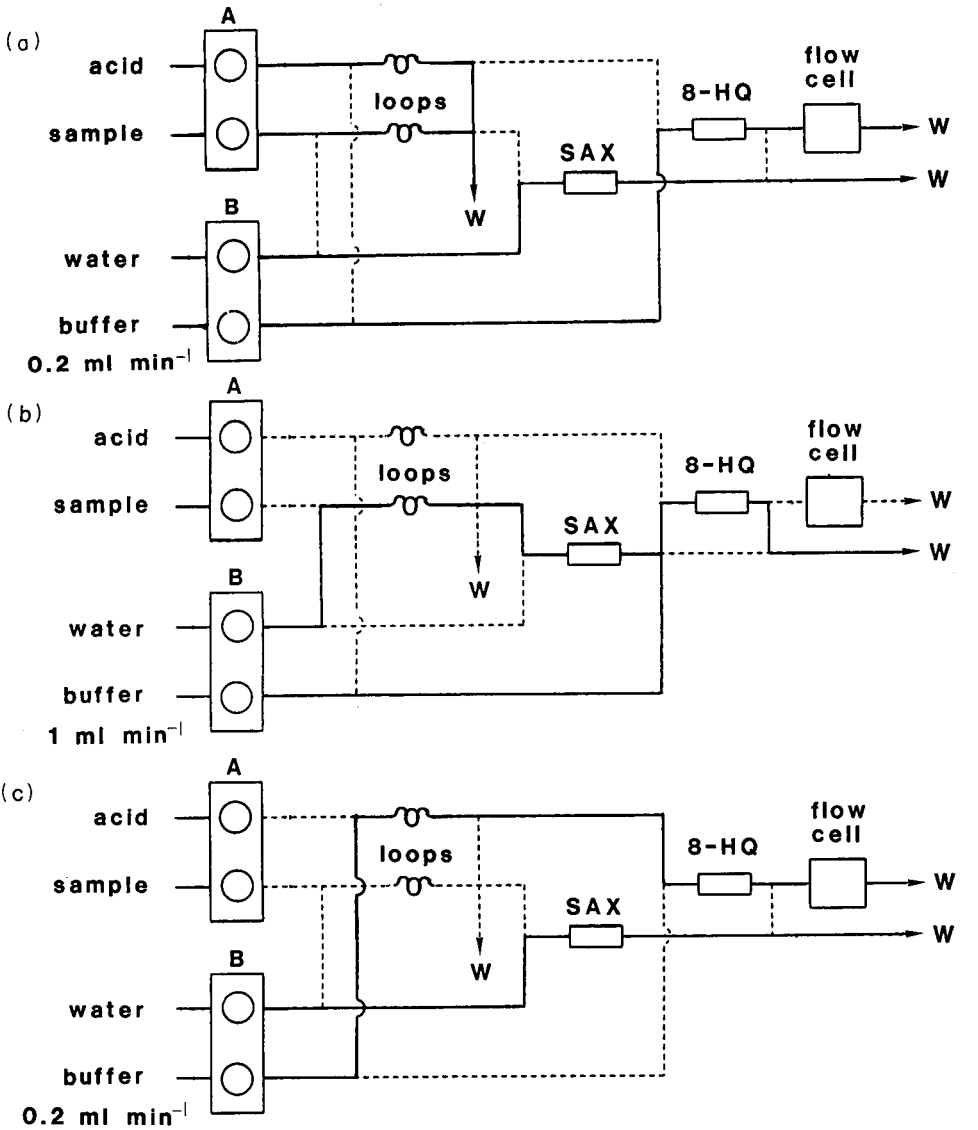

Fig. 1. Switching sequence for the flow injection/d.p.a.s.v. manifold. The connections in use are drawn as solid lines and the inactive with broken lines. (a) Filling of sample (1.0-ml) and acid (250-μl) loops and stripping into a buffer at a low flow rate; (b) transfer of the sample through the SAX and 8-HQ columns with intermediate pH adjustment; (c) elution of the metal ions with acid and plating into a mercury film electrode at a low flow rate.

Components of the flow-injection system

A disposable, strong anion-exchanger (SAX) Bond-Elut (Analytichem International, Harbor City, CA 90710) was filled into a 900-μl column to adsorb impurities. The $-N(CH_3)_3^+$ variety was selected for its lower chelating

strength compared to the $-NH_2$ variety, although the latter has been shown [18—20] to adsorb more humic material. A new column was prepared at least every day, as its capacity is lower in the acidic sample solutions than in the solutions studied earlier. Careful washing as described earlier [20] is necessary, otherwise there will be interferences in the electrochemical measurements.

8-Quinolinol was immobilized on silanized glass with azo coupling; the procedure was essentially that described by Hill [21]. The glass was CPG-10 (particle size 80—125 μm, pore size 70 nm) and was filled into a 100-μl column. This preparation (8-HQ) had about five times higher capacity than the commercially available material.

A confined wall-jet glassy carbon electrode in a holder similar to that described earlier [22] was used. The electrode was polished with aluminum oxide each morning and a mercury film was deposited from a solution containing 8×10^{-4} M Hg(II)/0.2 M KNO_3/10^{-3} M nitric acid during 20 min in a stirred solution. The reference electrode was Ag/AgCl 0.15 M KCl built into the flow cell, its potential was +25 mV vs. SCE. The polarograph was a Princeton Applied Research instrument (model 174) and a sweep rate of 10 mV s^{-1} was normally used.

The valves (Cheminert, LDC/Milton Roy) were made of Kel-F to withstand the acid and were operated from a panel prepared for computer control. The pumphead of pump B was enclosed in a thick-walled plastic box which also contained the valves and the columns. The box was filled with nitrogen which escaped coaxially with the tubing to the cell. There was no need for deoxygenation of the samples because of the medium exchange. The flow-injection system was made from teflon tubings (0.3 or 0.5 mm i.d.).

Chemicals and solutions

Samples and standards were 75 mM in nitric acid to prevent adsorption and chelation of the metal ions, particularly on the SAX column. The sample volume was normally 1.0 ml. The carrier buffer solution (0.2 M sodium acetate/0.3 M NaCl at pH 6.4) adjusted the pH of the dispersed sample to a value where most metal ions were taken up quantitatively by the chelate ion-exchanger [15]. Elution was done with 250 μl of 1 M nitric acid (Suprapur, Merck). The acid is diluted through dispersion and it was therefore too weak to give complete elution of copper ions. A weaker acid could be selected for zinc and a stronger for copper determinations as discussed below.

The buffer solutions were purified from trace metals by passing them through columns containing 4.6 ml of 8-quinolinol on porous glass (Pierce Chemical Co.). The ion-exchange capacity was rather low so the columns had to be regenerated several times a day.

The humic acid (Fluka) had a molecular weight of 600—1000 and an ash content of 10—15%. It was prepared essentially as described previously [18].

RESULTS AND DISCUSSION

System behaviour

The sensitivity of a flow injection d.p.a.s.v. system will depend on the flow rates, cell designs and the normal polarographic parameters. The sensitivity was found to decrease three-fold when the flow rate was increased from 0.25 to 0.97 ml min^{-1} during plating. The rate of the mass transfer to the electrode increases, but the deposition time decreases as the flow rate increases for a given peak in the flow stream. The net result is therefore that the sensitivity decreases with increasing flow rate and a low flow rate should thus be selected during plating.

The flow rate during stripping is much less important as shown by the values given in Table 1. The loss of sensitivity is only about 25% with a flow rate of 1 ml min^{-1} compared to a still solution. A compromise solution, which enhances sensitivity without introducing too much complexity, involves two-speed pumping. A flow rate of 1.0 ml min^{-1} was used for the enrichment step and 0.20 ml min^{-1} during plating and stripping.

The sensitivity is directly proportional to the volume of the sample passing through the chelate ion-exchanger, as shown by the calibration data in Table 2. A sample loop is advantageous for volumes less than about 2 ml, whereas it is more advantageous to use time-controlled pumping [15] for injection of larger volumes. The reason is that it takes a long time to wash out a large loop. The possibility of using a high flow rate during enrichment and a low flow rate during elution gives this method a time advantage over plating directly from a flowing sample solution. For large volumes, the time advantage will approach the ratio of the flow rates.

The sensitivities for some metals are given in Table 3. Plating was normally done at −1.1 V vs. Ag/AgCl in order to prevent hydrogen evolution during elution. Small amounts of hydrogen will not interfere but if a more negative value had been chosen, the bubbles would have interfered with the mass transport during plating and caused irreproducible results. A plating voltage of −1.4 should be used for zinc, and the acid strength must therefore be decreased in order to prevent hydrogen gas interferences. This is possible because zinc can be eluted with about 0.2 M acid. Copper requires a higher acid strength for elution than that normally used in this work, but it can be plated at lower voltages. The acid concentrations and the plating potentials should thus be chosen with due regard to the metals to be determined.

TABLE 1

Normalized peak currents for varying flow rates during stripping[a]

Flow rate (ml min^{-1})	(0.00)	0.26	0.52	0.76	0.97
Normalized current	(1.00)	0.87	0.82	0.79	0.75

[a]Sample 1.0 ml of 10^{-7} M Cd^{2+}.

TABLE 2

The response, defined as the peak current divided by the sample volume and the metal ion concentration, given as a function of the sample volume (10^{-7} M Cd^{2+})

Sample volume (ml)	0.5	1.0	1.5
Response (A M^{-1} ml^{-1})	82	78	81

TABLE 3

The sensitivity, defined as the peak current divided by the metal ion concentration, normalized to a 1.0-ml sample volume

Metal ion	Cd^{2+}	Pb^{2+}	Zn^{2+}
Sensitivity (A M^{-1})	80	76	17

Effect of humic acid and surfactants

Samples containing humic acid as well as metal ions were run through a set-up containing a chelate ion-exchanger but no SAX column. The idea was that the metal ions would be collected on the chelate ion-exchanger, but that most of the humic material would pass to waste. Figure 2 shows that the slope of the calibration curves was strongly affected by the presence of humic material. The sensitivity was found to vary with the amount of added humic acid so that the cadmium peak became lower or higher than that for a pure cadmium standard depending on the conditions. Such a complex influence on the sensitivity has previously been reported, for example, by Sagberg and Lund [2]. The reason for the insufficient isolation of metal ions from the matrix was that a humic acid fraction was adsorbed on the chelate ion-exchanger at pH 5.5. Some of the humic material was eluted when acid was introduced for elution of the metal ions. This behaviour was confirmed with a spectrophotometric detector for chromatography attached to the outlet of the chelate ion-exchanger. Washing the chelate ion-exchanger with buffer for longer times had little effect. Triton X-100 behaved similarly.

A column for pre-adsorption of humic material was therefore included in the system and the results for cadmium are shown in Fig. 3. The calibration plots had identical slopes for pure cadmium solutions and for solutions containing humic acid or Triton X-100, which proves that the effect on sensitivity has been eliminated. The capacity of the SAX column depends on the amount of humic acid in the sample. With 1.0-ml samples containing 500 mg l^{-1} humic acid, the column had to be replaced for every sample.

The different intercepts in the presence and absence of Triton X-100 or humic acid might be due to metal contamination in the materials or to an artefact caused by the SAX column. It was observed that successive blank injections after insertion of a fresh SAX column resulted in decreasing blank responses. It was also observed that different SAX columns resulted in different standard deviations for metal standards. These effects might be due to

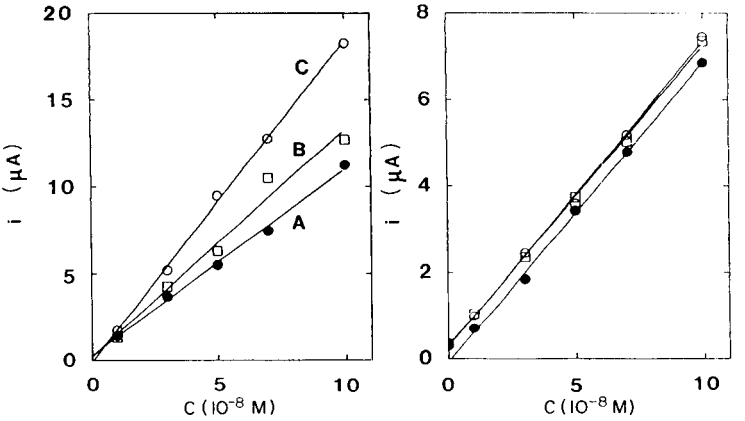

Fig. 2. Response curves for Cd^{2+} in a manifold without the SAX column: (A) Cd^{2+} only; (B) Cd^{2+} + 20 mg l^{-1} Triton X-100; (C) Cd^{2+} + 20 mg l^{-1} humic acid.

Fig. 3. Response curves for Cd^{2+} obtained with the manifold of Fig. 1: (●) Cd^{2+} only; (○) Cd^{2+} + 50 mg l^{-1} Triton X-100; (□) Cd^{2+} + 50 mg l^{-1} humic acid. All standards contained 75 mM nitric acid.

slow decomposition of the column material and release of substances which interfere with the electrochemical detection. These effects on the blanks are small compared to the change in sensitivity caused by humic acid or Triton X-100 in the absence of the SAX column. The inclusion of the SAX column therefore results in a great improvement, although some imperfections remain.

Discussions with G. Marko-Varga about the use of SAX columns are acknowledged. The SAX columns, Bond-Elut, were gifts from Analytichem International. Xiurong Yang thanks the University of Sciences and Technology of China, Heifei, for support. The work was supported financially by the Swedish Natural Research Council.

REFERENCES

1 J. Wang and D.-B. Luo, Talanta, 31 (1984) 703.
2 P. Sagberg and W. Lund, Talanta, 29 (1982) 457.
3 E. Jacobsen and H. Lindseth, Anal. Chim. Acta, 86 (1976) 123.
4 T. Ugapo and W. F. Pickering, Talanta, 32 (1985) 131.
5 C. Zur and M. Ariel, Anal. Chim. Acta, 88 (1977) 245.
6 T. M. Florence, Talanta, 29 (1982) 345.
7 G. Koster and M. Ariel, J. Electroanal. Chem., 33 (1971) 339.
8 E. O. Martins and G. Johansson, Anal. Chim. Acta, 140 (1982) 29.
9 J. Wang and B. A. Freiha, Anal. Chim. Acta, 148 (1983) 79.
10 J. Wang, H. D. Dewald and B. Greene, Anal. Chim. Acta, 146 (1983) 45.
11 J. A. Wise and W. R. Heineman, Anal. Chim. Acta, 172 (1985) 1.
12 C. Wechter, N. Sleszynski, J. J. O'Dea and J. Osteryoung, Anal. Chim. Acta, 175 (1985) 45.
13 H. Gunasingham, K. P. Ang and C. C. Ngo, Anal. Chem., 57 (1985) 505.

14 S. Olsen, L. C. R. Pessenda, J. Růžička and E. Hansen, Analyst (London), 108 (1983) 905.
15 F. Malamas, M. Bengtsson and G. Johansson, Anal. Chim. Acta, 160 (1984) 1.
16 J. F. Tyson, Analyst (London), 109 (1984) 319.
17 L. Risinger, Anal. Chim. Acta, 179 (1986) 509.
18 G. Marko-Varga, I. Csiky and J. Å. Jönsson, Anal. Chem., 56 (1984) 2066.
19 I. Csiky, G. Marko-Varga and J. Å. Jönsson, Anal. Chim. Acta, 178 (1985) 307.
20 E. Hoffmann, G. Marko-Varga, I. Csiky and J. Å. Jönsson, Int. J. Environ. Anal. Chem., 25 (1986) 161.
21 J. M. Hill, J. Chromatogr., 76 (1973) 455.
22 R. Appelqvist, G. Marko-Varga, L. Gorton, A. Torstensson and G. Johansson, Anal. Chim. Acta, 169 (1985) 237.

Analytica Chimica Acta, 192 (1987) 9—16
Elsevier Science Publishers B.V., Amsterdam — Printed in The Netherlands

AMPEROMETRIC SENSOR FOR PYRUVATE WITH IMMOBILIZED PYRUVATE OXIDASE

M. MASCINI* and F. MAZZEI

Dipartimento di Scienze e Tecnologie Chimiche, Il Università di Roma Tor Vergata, Via Orazio Raimondo, 00173 Roma (Italy)

(Received 15th April 1986)

SUMMARY

Several procedures for immobilization of pyruvate oxidase by chemical bonding are reported. Attachment to nylon net was unsatisfactory in terms of yield and stability. Polyazetidine, a new commercially available prepolymer and a new nylon membrane with surface carboxyl groups provided good long-term stability, up to 30 days in the case of the nylon membrane. Under optimal conditions of solution preparation (0.1 mmol l^{-1} thiamine pyrophosphate, 0.5 mmol l^{-1} phosphate, 2.5 mmol l^{-1} calcium and 0.04 mol l^{-1} Tris buffer pH 7.0), linear calibration graphs were obtained until the lowest concentration of 10^{-3} mmol l^{-1} pyruvate and amperometric sensors based on these membranes. With careful standardization, the procedures were suitable for application to blood serum.

Pyruvate is a metabolite involved in the oxidation of carbohydrates. In anaerobiosis, pyruvate and lactate increase in the blood, whereas in aerobiosis the metabolites are converted to carbon dioxide and water. The pyruvate concentration in blood is thus important, being related to the glucose and lactate concentrations and to their variations in connection with several diseases. A good pyruvate sensor can also be exploited in the determination of transaminases [1—4] in blood and of lactate dehydrogenase [5], so that there is considerable interest in developing a reliable sensor [6, 7].

Pyruvate oxidase is a very expensive enzyme and its immobilization reduces the price of pyruvate determinations. However, pyruvate oxidase has never been immobilized through covalent bonding because of deactivation of the enzyme; it has only been entrapped physically in collagen [1], poly(vinyl chloride) [2, 3] and acetylcellulose [4] because of its delicate nature. In this paper, results obtained by chemical immobilization of pyruvate oxidase with recently available supports and materials are reported.

The reaction catalyzed by pyruvate oxidase is

$$\text{pyruvate} + HPO_4^{2-} + O_2 \rightarrow \text{acetylphosphate} + H_2O_2 + CO_2$$

Thus an oxygen sensor or hydrogen peroxide sensor could be used to monitor the reaction. The use of a carbon dioxide sensor would create problems because of the low concentration of pyruvate and the high content of

0003-2670/87/$03.50

hydrogencarbonate in most of the samples. To obtain a pyruvate sensor suitable for clinical purposes, the hydrogen peroxide sensor must be used because the normal range of pyruvate in serum (0.04–0.12 mmol l^{-1}) is too low to be monitored with an oxygen sensor.

EXPERIMENTAL

Materials and apparatus

Pyruvate oxidase (E.C. 1.2.3.3., from *Pediococcus sp.*) was obtained from Boehringer/Mannheim (10 U mg^{-1}), from Sigma (20 U mg^{-1}) and from Toyo Yozo/Shizuoka (21 U mg^{-1}). Cellulose acetate (53% acetyl) and poly(vinyl acetate) with high molecular weight were obtained from Farmitalia Carlo Erba.

Porous filters of mixed esters of cellulose (acetate and nitrate) were obtained from Millipore (Type HA 45). The Biodyne immunoaffinity membrane (nylon 6.6, porosity 0.2 μm) with carboxyl groups on the surface was obtained from Pall Filtration Corp. (Glen Cove, NY). Dialysis membranes (0.001-in. thick with molecular cutoff 12000) were from A.H. Thomas (Philadelphia, PA). Polyazetidine prepolymer solution (Hercules Polycup 172, 12% solids in water) was obtained from M. Delaney (New York 10010). Nylon net (120 mesh cm^{-2}, 100 μm thick, with 35% free surface) was obtained from A. Bozzone (Appiano Gentile, Como, Italy).

The hydrogen peroxide sensor and a flow cell with a dead space of 40 μl were from Instrumentation Laboratory. The platinum wire was 0.5 mm in diameter; the silver foil cathode was 0.5 cm^2 in area. The polarization unit was a voltammetric detector (Metrohm model 641), which was used with a Houston Omniscribe recorder. The peristaltic pump was a Microperpex model 2132 (LKB Bromma, Sweden).

For casting the cellulose membrane, a precision gauge tool was used (Precision Gage and Tool Co., Dayton, OH).

Procedures

Casting the cellulose acetate membrane. To protect the anode from interfering substances which could be oxidized, a cellulose acetate membrane was prepared [7]. Cyclohexanone (40 ml), acetone (60 ml), cellulose acetate (3.96 g) and poly(vinyl acetate) (40 mg) were mixed. The solution was cast on a glass plate to a thickness of 200 μm. After evaporation (30—40 min), the membranes were immersed in water and the membranes were peeled off and stored. The dry membrane was 20 μm thick.

Immobilization of pyruvate oxidase. Immobilization was done by chemical bonding and by physical entrapment in an acetylcellulose membrane.

Four main procedures were tested. First, immobilization on nylon net was examined. This procedure [8] has proved to be effective for a number of oxidases [9—11] but gave very low yields with pyruvate oxidase and very short lifetimes. The second method was physical entrapment on cellulose

acetate filters (Millipore HA 0.45-μm pore size) [1, 5]. The third method was based on a recently available nylon 6.6 filter membrane with carboxyl groups on the surface. The membrane (0.8-cm diameter) was soaked in 0.1 mol l^{-1} 1-ethyl-3(3-dimethylaminopropyl)carbodiimide/0.5 mol l^{-1} phosphate buffer (pH 4.8) for 40 min at room temperature with continuous stirring. Then, the membrane was washed with 0.4 mol l^{-1} hydrogencarbonate buffer (pH 7.0), 1—2 mg of enzyme was mixed with 10 μl of the buffer pH 7.0 on the membrane surface, and the membrane was left in a humid atmosphere at 4°C.

In the fourth method a new prepolymer, polyazetidine(I), which was recently described for the immobilization of *Escherichia Coli* [12], was used. On a dialysis membrane (0.8-cm diameter) 10 μl of the prepolymer solution, as obtained, was mixed with 1 mg of enzyme and spread uniformly. The membrane was then left for 24 h at 4°C. The polyazetidine reacts with various functional groups (carboxyl, hydroxyl, amine, mercaptan and free amine) on another chain of the polymer [12].

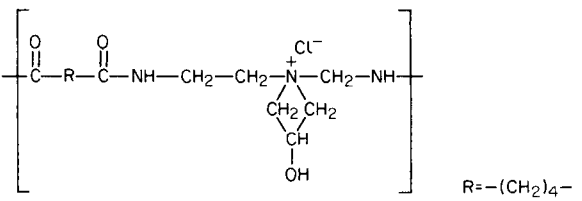

Assembly of the sensor

First, a cellulose acetate membrane was placed on the platinum surface to eliminate interferences from electroactive chemicals (ascorbic acid, etc.). Then a second membrane with immobilized enzyme was placed on the first together with a dialysis membrane to prevent microbial attack of the enzyme and leaching of the enzyme from the second membrane. The three layers were held in position with a rubber O-ring.

The sensor was either immersed in a thermostated vessel to which buffer and pyruvate standard solutions were added, or placed in a flow cell through which suitably treated pyruvate standard solutions were pumped by a peristaltic pump.

RESULTS AND DISCUSSION

Preliminary experiments with pyruvate oxidase obtained from Boehringer failed. The enzyme obtained at different times and from different lots seemed to denature very quickly; no immobilization procedure could be effective with such commercial preparations. The Sigma and Toyo Yozo preparations seem to be identical in results and performance, even though most of the experiments reported were obtained with the Toyo Yozo preparation.

The reaction catalyzed by pyruvate oxidase is affected by various solution parameters. Figures 1 and 2 show a comparison of the four immobilization procedures when the phosphate and calcium chloride concentrations are varied. In both cases, the curves of the pyruvate oxidase activity are bell-shaped for all procedures and critical values of these parameters can be estimated. The behaviour shown in Fig. 1 excludes the use of phosphate buffer

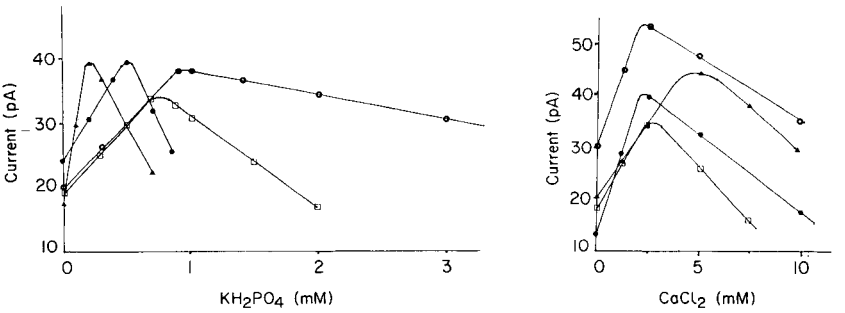

Fig. 1. Response to pyruvate (0.005 $mmol^{-1}$) as a function of phosphate concentration for the different immobilization procedures: (○) carboxyl; (▲) polyazetidine; (●) acetylcellulose; (□) nylon. Conditions: 0.04 mol l^{-1} Tris buffer pH 7.0, 2.5 mmol l^{-1} calcium chloride, 0.1 mmol l^{-1} thiamine pyrophosphate.

Fig. 2. Response to pyruvate concentration (0.005 mmol l^{-1}) as a function of calcium concentration. Symbols and conditions as for Fig. 1, apart from variable calcium and 0.5 mmol l^{-1} phosphate.

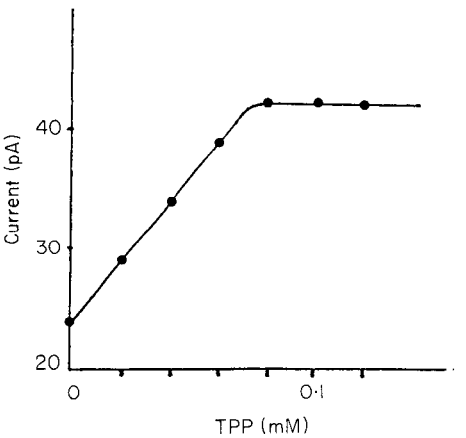

Fig. 3. Response to pyruvate concentration (0.005 $mmol^{-1}$) as a function of thiamine pyrophosphate (TPP) concentration. All immobilization procedures show the same pattern. Conditions: 0.04 mol l^{-1} Tris buffer pH 7.0, 0.5 $mmol^{-1}$ phosphate, 2.5 $mmol^{-1}$ calcium.

because of the low activity of the enzyme at concentrations higher than 1 mmol l^{-1}. Experiments with magnesium ion instead of calcium showed the same pattern, a concentration of around 2.5 mM calcium being optimal. Figure 3 reports the behaviour of pyruvate oxidase in the presence of TPP (thiamine pyrophosphate). This co-enzyme has the same effect for all immobilization procedures. Its concentration should be at least 0.1 mmol l^{-1} in the sample solutions.

The pH and buffer effects in the useful range 6.5—7.5 are shown in Fig. 4. The activity of pyruvate oxidase is low in the presence of citrate; the activity is highest in all procedures when the Tris buffer is used at pH 7.0—7.2.

The calibration graphs in the range 0.001—0.01 mmol l^{-1} pyruvate obtained by addition of standard solutions to a mixture of the appropriate components in a beaker are shown in Fig. 5(a). Calibrations for a flow system are shown in Fig. 5(b). There are only small variations between the different procedures of immobilization and of measurement.

From these experiments, it can be concluded that the cofactor concentrations in the samples for pyruvate determination should be 0.1 mmol l^{-1} TPP, 0.5 mmol l^{-1} phosphate and 2.5 mmol l^{-1} calcium chloride in a Tris buffer (0.04 mol l^{-1}) at pH 7.0. The sensitivity of the sensor depends greatly on the composition of the solution and this makes it necessary to calibrate in the sample matrix with standard solutions or to dilute unknown samples with a suitable buffer, as required.

Figure 6 shows the behaviour of the sensors as a function of time, which is an important feature of a pyruvate sensor. The nylon net sensor failed after a few days and it seems that pyruvate oxidase is inactivated by all procedures in which glutaraldehyde is used in the final step. For the results shown in Fig. 6, the concentration of pyruvate used for the nylon net procedure was increased to obtain a better current value. The activity of the enzyme immobilized by physical adsorption on acetylcellulose decreased with time, as expected for physical immobilization. With the carboxyl membrane, the

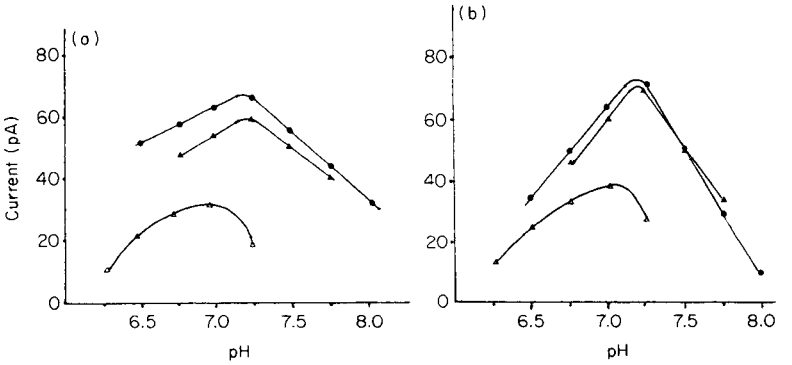

Fig. 4. Effects of pH and buffer: (a) the acetylcellulose and polyazetidine procedures; (b) the carboxylic procedure. Buffer: (●) Tris; (▲) hydrogencarbonate; (△) citrate. All buffers were 0.04 mol l^{-1}; other conditions were 2.5 mmol l^{-1} calcium, 0.5 mmol l^{-1} phosphate, 0.1 mmol l^{-1} TPP, 0.01 mmol l^{-1} pyruvate.

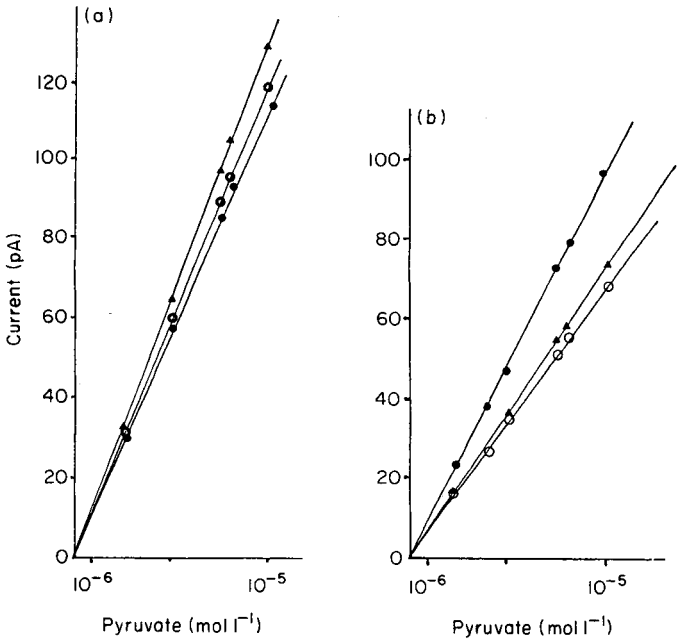

Fig. 5. Calibration graphs for pyruvate: (a) addition of standard solution to a thermostated beaker where a pyruvate sensor was immersed in Tris buffer (0.04 mol l^{-1}) with the other components; (b) flow system through which prepared solutions were pumped. Immobilization method: (○) carboxyl; (▲) polyazetidine; (●) acetylcellulose.

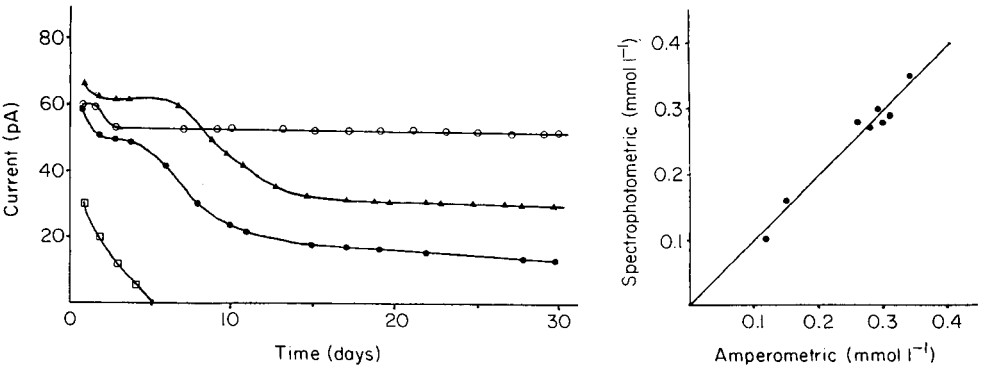

Fig. 6. Lifetime of the different sensors: (○) carboxyl; (▲) polyazetidine; (●) acetylcellulose; (□) nylon. Pyruvate concentration was 5×10^{-6} mol l^{-1}, except with nylon for which the concentration was 10^{-5} mol l^{-1}; Tris buffer (0.04 mol l^{-1}, pH 7.0, with all cofactors as specified.

Fig. 7. Correlation between spectrophotometric measurements and measurements with the pyruvate amperometric sensor (Table 1).

TABLE 1

Comparison of pyruvate concentrations found in serum samples with the pyruvate amperometric sensor (polyazetidine immobilization procedure) and with a clinical spectrophotometric procedure (UV of NADH)

Serum	Pyruvate found (mmol l^{-1})		Serum	Pyruvate found (mmol l^{-1})	
	Amperometric	Spectrophotometric		Amperometric	Spectrophotometric
1	0.34	0.35	5	0.29	0.30
2	0.28	0.27	6	0.31	0.29
3	0.26	0.28	7	0.12	0.10
4	0.30	0.28	8	0.15	0.16

decrease in the signal was only 13% after 30 days while, with the polyazetidine procedure, the decrease was 64% after the same period.

Table 1 reports the results of pyruvate determination in some serum samples from normal and diabetic patients. Spectrophotometric results were obtained in the clinical laboratory from the absorbance of NADH at 340 nm in the presence of lactate dehydrogenase. For the pyruvate sensor prepared by the polyazetidine procedure, 0.5 ml of serum was added to 5 ml of Tris buffer containing all the cofactors. The correlation coefficient was 0.975 ($y = 1.02x - 0.006$). Figure 7 shows the correlation obtained between the sets of data.

Conclusion

Pyruvate oxidase is a very delicate enzyme for immobilization procedures. Chemicals, pH, buffer must be chosen carefully because the activity can vary greatly with the procedure. As reported above, the membranes and the prepolymer, which have recently become commercially available, seem mild enough to preserve the activity of the enzyme, anchoring it firmly to a solid support with high activity for analytical purposes. The concentrations of cofactors, chemicals, buffer and pH are rather critical, but with careful control and standardization, the sensor can be used with clinical samples.

REFERENCES

1 F. Mizutani, K. Tsuda, I. Karube, S. Suzuki and K. Matsumoto, Anal. Chim. Acta, 118 (1980) 65.
2 M. Notsuki, Y. Ishimori, M. Koyama, I. Karube and S. Suzuki, Proc. Int. Chemical Sensors, Kodansha, Fukuoka (Japan) 1983, 654 pp.
3 K. Kihara, E. Yasukawa, M. Hayashi and S. Hirose, Anal. Chim. Acta, 159 (1984) 81.
4 K. Kihara, E. Yasukawa and S. Hirose, Anal. Chem., 56 (1984) 1876.
5 N. Minaura, S. Yamada, I. Karube, I. Kubo and S. Suzuki, Anal. Chim. Acta, 135 (1982) 355.
6 B. Lloyd, J. Burrin, P. Smithe and K. G. M. Alberti, Clin. Chem., 24 (1978) 1724.
7 T. Tsuchida and K. Yoda, Clin. Chem., 29 (1983) 135.

8 M. Mascini, M. Iannello and G. Palleschi, Anal. Chim. Acta, 145 (1983) 213.
9 M. Mascini and G. Palleschi, Anal. Chim. Acta, 145 (1983) 213.
10 M. Mascini, D. Moscone and G. Palleschi, Anal. Chim. Acta, 157 (1984) 45.
11 M. Mascini, S. Fortunati, D. Moscone, G. Palleschi, M. Massi-Benedetti and P. Fabietti, Clin. Chem., 31 (1985) 451.
12 L. L. Wood and G. J. Calton, Biotechnology Dic., 2 (1984) 1081.

Analytica Chimica Acta, 192 (1987) 17—31
Elsevier Science Publishers B.V., Amsterdam — Printed in The Netherlands

AUTOMATIC POTENTIOMETRIC TWO-PHASE TITRATION IN PHARMACEUTICAL ANALYSIS
Part 3. Titrimetric Identification of Drugs

PER-ARNE JOHANSSON* and SIDSEL THELANDER

Astra Pharmaceutical Production AB, Analytical Control, S-151 85 Södertälje (Sweden)

OLLE STÅLBERG[a]

Linköping University, Department of Physics and Measurement Technology, S-581 83 Linköping (Sweden)

(Received 18th July 1986)

SUMMARY

The conditional acidity constant in a liquid-liquid two-phase system ($pK^*_{HA^+}$ value) can be used as an identity parameter for drug compounds. The $pK^*_{HA^+}$ value can be calculated if the phase ratio and the acidity and distribution constants are known. Selectivity is obtained mainly by the choice of the organic phase. An excess of hydrochloric acid is first added to the sample in the two-phase system. The hydrochloric acid and the sample are then titrated sequentially with sodium hydroxide. The proposed titration procedure makes it possible to calibrate the electrodes, determine the $pK^*_{HA^+}$ value(s), quantify one or more compounds, and check the performance of the electrodes in one and the same experimental run. Lidocaine was "identified" and assayed in different dosage forms such as ointment and solution for injection. The results were in agreement with those obtained by liquid chromatography.

In Part 2 of this series [1], it was demonstrated that two-phase acid-base titrations can be conducted instrumentally by the use of ordinary automatic titrators. Examples were given on how the acid-base strength of amines could be regulated in order to obtain longer titration breaks or better selectivity in the titrations. The manipulation of the acid-base strength was discussed in quantitative terms using a conditional acidity constant ($pK^*_{HA^+}$ value).

For an amine, that is distributed to an organic phase only as a base, the conditional acidity constant assumes the following form

$$K^*_{HA^+} = K'_{HA^+}[1 + (V_{org}/V_{aq})K_{D(A)}] \quad (1)$$

where K'_{HA^+} is the (aqueous) acidity constant, $K_{D(A)}$ the distribution constant and V_{org}/V_{aq} the phase ratio. Compounds having the same pK'_{HA^+} values can thus have different $pK^*_{HA^+}$ values; it depends on the magnitude of the individual distribution constants.

---

[a]Present address: Astra Pharmaceutical Production AB, S-151 85 Södertälje, Sweden.

0003-2670/87/$03.50

In liquid chromatography, the retention time or retention volume is normally used as a parameter of identification [2]. The relationship between the retention time, t_R, and the chromatographic parameters can be described [3] by the equation

$$t_R = t_0[1 + (V_s/V_m)K] \quad (2)$$

where t_0 is the retention time of an unretained compound, V_s and V_m are the volumes of the stationary and mobile phases, respectively, and K is the distribution constant for a solute between the two phases.

The equations above are rather similar. In both cases, it is a distribution constant that governs the size of the $K^*_{HA^+}$ and t_R values (provided that the experimental conditions remain unchanged). Accordingly, if t_R can be used as an identity parameter in liquid chromatography, it should not be impossible to use $K^*_{HA^+}$ or $pK^*_{HA^+}$ for the same purpose in titrimetry.

The pK_a or $pK^*_{HA^+}$ value can be calculated graphically from a titration curve as "the pH at 50% neutralization". Today, however, several automatic titrators are commercially available (e.g. [4, 5]) that can store and/or printout the data of measurement of a titration. With such an instrument, connected to, e.g., a personal computer, the $pK^*_{HA^+}$ value could be calculated during or immediately after a titration. At least one automatic titrator that also determines the pK_a value of a sample is already available (Metrohm). In the determination of aqueous pK_a and pK'_{HA^+} values, the electrodes are normally calibrated against two or more pH buffers before the titration. Afterwards, one of the buffers is measured to check the stability of the electrode system [6]. It is questionable, however, if this calibration procedure is the best for the determination of $pK^*_{HA^+}$ values. The liquid-junction potential may not be very reproducible in the two-phase systems and may change when the electrodes are transferred from buffer to sample solution and from one titration to another [1, 7, 8]. A more stable junction potential might be obtained if the electrodes were kept in the same environment during the calibration and the determination of the $pK^*_{HA^+}$ value. Such in situ calibration of pH electrodes has been achieved in aqueous one-phase systems by use of E^0 titrations (see, e.g. [9—11]).

The aim of the present work is twofold: to find a suitable electrode calibration procedure for the two-phase titrations, and to investigate if the conditional acidity constant can be determined accurately and precisely with an automatic titrator so that "titrimetric identification" of a compound becomes possible.

EXPERIMENTAL

Apparatus

An automatic titrator (Titroprocessor 636 with program 102; Metrohm) was used in the titrations. The instrument was provided with a titration head (DV702; Mettler), a rod stirrer (622; Metrohm), 1- or 10-ml burettes and

different pH electrodes (Table 1). The electrodes were used as received, with one exception, where the saturated, potassium chloride solution was replaced by 0.1 M sodium chloride in the salt bridge.

Chemicals and reagents

The hydrochlorides of mepivacaine, lidocaine, pilocarpine, prilocaine and tocainide were all of pharmacopoeial grade. Hexadecylpyridinium chloride (HPC) was recrystallized from water before use in order to remove an impurity with a pK_a about 5 (probably pyridinium hydrochloride). All aqueous solutions were adjusted to an ionic strength of 0.1 or 0.01 M with potassium chloride. (The ionic strength of an aqueous solution of HPC is practically the same as the c.m.c. [12], the latter being about 1×10^{-4} M in 0.1 M NaCl at 25—37° C [13]). The titrants, 0.1 M and 1 M sodium hydroxide and 0.1 M hydrochloric acid, were prepared from Titrisol (Merck) ampoules. Deionized water which had been deaerated with a stream of nitrogen was used in the preparation of all solutions. All other chemicals and reagents were of analytical grade.

Determination of acidity constants

The constants were determined by potentiometric titrations at a temperature of 25.0 ± 0.2° C. The ionic strength was 0.1 or 0.01. The experimental conditions, i.e., concentrations and acidity constants of the compounds, were chosen so that the hydrogen or hydroxyl ion concentrations could be

TABLE 1

pH electrodes used

pH electrode	Type	Liquid junction	Salt bridge electrolyte	Manufacturer	Cat. no.
A	Glass/calomel	Ceramic	Sat. KCl	Radiometer, Denmark	G202B/K401
B	Combination	Ceramic	3 M KCl/AgCl	Ingold, Switzerland	U402-K7
C	Combination	Ceramic	3 M KCl	Metrohm, Switzerland	6.0203.000
D	Glass/calomel	Ceramic	0.1 M NaCl	Radiometer, Denmark	G202B/K401
E	Combination	Platinum wire	3.5 M KCl	Schott-Geräte, West Germany	N 65
F	Combination	Ceramic	3 M KCl	Orion Research, U.S.A.	810200
G	Combination	PTFE sleeve	3 M KCl/AgCl	Ingold, Switzerland	405-88-TEK7
H	Combination	Ceramic	Sat. KCl	Radiometer, Denmark	GK 2401C
I	Combination	Ceramic	3 M KCl/AgCl	Russell pH, Scotland	CW-76

neglected in the calculation of the pK'_{HA^+}, $pK^c_{HA^+}$ and $pK^*_{HA^+}$ values (cf. [14]). the pH value of 50% neutralization, which can be printed out after the titration by the Titroprocessor, then equals the pK'_{HA^+} or $pK^*_{HA^+}$ value. All data of measurement (ml and pH or mV values) were collected during stirring (vigorously in the two-phase systems) by use of the automatic titrator. The instrument was run in the dynamic titration mode using a drift criterion of 7.5 mV min^{-1}. Two approaches were used to calibrate the electrodes: calibration against pH buffers and calibration by E^0 titrations.

Calibration with buffers. The pH meter of the automatic titrator was calibrated with two of the pH standards 4.01, 7.00 and 9.18 (Radiometer) before the titration. About 5×10^{-4} mol of sample (amine, amine mixture or amine hydrochloride) was then titrated with 0.1 M hydrochloric acid or 0.1 M sodium hydroxide from a 10-ml burette. After the titration, the drift of the electrodes was checked against one of the buffers. The drift was <0.02 pH in all aqueous one-phase titrations and 0.02—0.08 pH in most of the two-phase titrations. The initial volume of the aqueous phase was 50.00 ml in the one-phase titrations and 26.00 ml in the two-phase titrations. The volume of the organic phase was 20.00 ml, which gives $V_{org}/V_{aq} = 0.70$ at 50% neutralization. By programming the automatic titrator via the control card, the pK'_{HA^+} or $pK^*_{HA^+}$ value was printed out after each titration.

Calibration by E^0 *titrations.* An equimolar mixture of hydrochloric acid and amine hydrochloride (2 or 3×10^{-4} mol of each) was titrated with 1 M sodium hydroxide from a 1-ml burette. (The larger amounts of sample were used in the aqueous one-phase titrations.) The initial volume of the aqueous phase was 50.30 ml in the one-phase titrations and 30.20 or 30.40 ml in the two-phase titrations. The final volume of added titrant was 1.000 ml in the one-phase systems and 0.600 ml in the two-phase systems. Accordingly, the dilution of the aqueous phase was 2% or less and was considered negligible. In the two-phase titrations, the volume of organic phase was 15.00 ml, giving a nearly constant phase ratio ($V_{org}/V_{aq} = 0.487$—0.493) during the titration of HA^+. Two equivalence points (EP1 and EP2) were obtained in all titrations, unless otherwise stated.

The ml/mV data before EP1 and after EP2 were used to calibrate and check the performance of the electrode system. The following equations (c.f. [15, 16]) were used

$$U_{H_3O^+} = E^0_{H_3O^+} + J_{H_3O^+}[H_3O^+] \tag{3}$$

$$U_{OH^-} = E^0_{OH^-} + J_{OH^-}[OH^-] \tag{4}$$

$$pK^c_W = (E^0_{H_3O^+} - E^0_{OH^-})/59.16 \tag{5}$$

where $U_{H_3O^+} = E - 59.16 \log [H_3O^+]$ and $U_{OH^-} = E + 59.16 \log [OH^-]$, E is the measured potential in mV and $[H_3O^+]$ and $[OH^-]$ are the molar concentrations of H_3O^+ and OH^-. The latter were calculated by use of the formulae

$$[H_3O^+] = (\text{ml EP1} - \text{ml } OH^-)f/V_{aq} \tag{6}$$

$$[OH^-] = (\text{ml } OH^- - \text{ml EP2})f/V_{aq} \tag{7}$$

The E^0 values were obtained by slope analysis using 6—9 points of measurement within a H_3O^+ or OH^- concentration range of (1—7) × 10^{-3} M.

The conditional acidity constant was calculated from the ml/mV data between EP1 and EP2 by use of the equation

$$K^*_{HA^+} = [H_3O^+](\text{ml } OH^- - \text{ml EP1})/(\text{ml EP2} - \text{ml } OH^-) \quad (8)$$

where $[H_3O^+] = (E - E_{H_3O^+})/59.16 = 10$. The standard deviation of the $pK^*_{HA^+}$ values (calculated on 8—12 points of measurement over a mV range of 70—120 mV) was <0.02 log units.

All calculations were done after a titration by using the measuring-point list from the titrator. The list was either printed out or transmitted to a VAX computer (Digital Equipment Corporation) via a RS232 interface [17]. In the first case, a programmable pocket calculator (HP41CV; Hewlett Packard) was used in the calculations. The calculations on the VAX computer were done by use of the RS/1 data analysis system (Bolt Baranek and Newman, Cambridge, MA, U.S.A.).

Assay of Xylocaine and Xyloproct preparations

Use a 1-ml burette and titrate with 1 M sodium hydroxide during vigorous stirring to a final volume of titrant of 0.6 ml. Run the titrator in the dynamic titration mode (7.5 mV min^{-1}) and keep the titration vessel at a constant temperature (25.0 ± 0.2°C). Two equivalence points are obtained; one at about 0.2 ml and the other at about 0.4 ml of titrant.

Jelly and solution for injection. Weigh 3.000 g of sample (containing about 20 mg ml^{-1} lidocaine hydrochloride) into the titration vessel. Add 0.20 ml of 1 M hydrochloric acid, 27.00 ml of aqueous 0.05 M HPC and 15.00 ml of toluene and start the titration.

Ointment. Weigh 0.9400 g of sample into the titration vessel. Dissolve the sample in 15.00 ml of toluene. Add 30.00 ml of 0.05 M HPC, 0.40 ml of 1 M hydrochloric acid and start the titration.

Suppository. Weight one suppository (ca. 2.5 g) into a 50-ml centrifuge tube with stopper. Add 20.00 ml of toluene and shake mechanically for 20 min. (The diluent of the suppository, Hard Fat B.P. 1980, is soluble in toluene, which increases the volume of the toluene phase to 21.65 ml after the extraction.) Separate the solid and liquid phases by centrifugation. Transfer 15.00 ml of the liquid phase to the titration vessel. Add 30.00 ml of 0.05 M HPC, 0.40 ml of 1 M hydrochloric acid and start the titration.

Viscous solution. Weigh 3.600 g of sample into a 50-ml centrifuge tube with stopper. Add 20.00 ml of toluene, 1.0 ml of 2 M sodium hydroxide and 4.0 ml of water. Shake in a shaking machine for 20 min. Separate the phases by centrifugation. Transfer 15.00 ml of the upper (toluene) phase to the titration vessel. Add 30.00 ml of 0.05 M HPC, 0.40 ml of 1 M hydrochloric acid and start the titration.

Calculate the content of lidocaine hydrochloride or lidocaine base from the difference in volume of sodium hydroxide solution between the two equivalence points, taking into account the volume changes or phase ratios in

the extractions. Use the ml/mV data before the first EP and after the second EP for the calibration of the electrodes. The ml/mV data between the two EP values are used for the calculation of the $pK^*_{HA^+}$ value (the identity parameter).

RESULTS AND DISCUSSION

The symbols used are given in Table 2. In the discussion below it has been assumed that the amine is distributed to the organic phase only as the base. Then $C'_{HA^+} = [HA^+]$ and $C'_A = [A] + V_{org}(V_{aq})^{-1}[A]_{org}$ and the conditional acidity constant is defined by Eqn. 1.

Criteria for identification

If the conditional acidity constant is to be of any practical use as an identity parameter, it is desirable that even closely related compounds have different $pK^*_{HA^+}$ values. Generally, the log $K_{D(A)}$ value increases by 0.6 log

TABLE 2

Symbols	Definitions
A, D and HA^+, HD^+	Amines in unprotonated and protonated form, respectively
HY and Y^-	Organic acid in protonated and unprotonated form, respectively
[A] and $[A]_{org}$	Molar concentration of A in aqueous and organic phase, respectively
a_{H^+}	Hydrogen ion activity
C^0_A	Initial total molar concentration of A calculated as being present entirely in the aqueous phase
$C'_A = [A] + V_{org}(V_{aq})^{-1}[A]_{org}$	Total molar concentration of A calculated as being present entirely in the aqueous phase
$K'_{HA^+} = a_{H^+}[A][HA^+]^{-1}$	Mixed acidity constant of HA^+
$K^c_{HA^+} = [H_3O^+][A][HA^+]^{-1}$	Stoichiometric acidity constant of HA^+
$K^c_W = [H_3O^+][OH^-]$	Stoichiometric autoprotolysis constant of water
$K^*_{HA^+} = a_{H^+}C'_A(C'_{HA^+})^{-1}$ or $[H_3O^+]C'_A(C'_{HA^+})^{-1}$	Conditional acidity constant of HA^+ (mixed or stoichiometric)
$K_{D(A)} = [A]_{org}[A]^{-1}$	Distribution constant of A
V_{aq} and V_{org}	Volume of aqueous and organic phase in ml
ml OH^-	ml of 1 M NaOH added by titration
ml EP1	ml of 1 M NaOH to the first equivalence point
f	Factor obtained in the standardization of 1 M NaOH
E	Measured potential in mV
$E^0_{H_3O^+}$	Formal potential of the electrode system obtained in the calibration against $[H_3O^+]$
$J_{H_3O^+}[H_3O^+]$, $J_{OH^-}[OH^-]$	Liquid junction potentials in the acid and alkaline pH range, respectively
μ	Ionic strength
HPC	Hexadecylpyridinium chloride (cetylpyridinium chloride)

units per methyl or methylene group added to a molecule [18]. The $pK^*_{HA^+}$ values of amines in a homologous series can therefore be expected to decrease by 0.6 log units for each additional carbon atom until ion-pair extraction causes levelling of the acid-base strength [1].

Prilocaine (C_{13}), lidocaine (C_{14}) and mepivacaine (C_{15}), which are local anaesthetics, were chosen as model compounds because their $pK^*_{HA^+}$ values differ by even less than 0.6 log units (Table 3). A $\Delta pK^*_{HA^+}$ of 0.3 (when

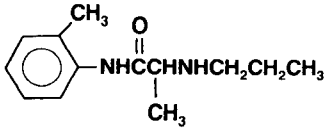

Prilocaine

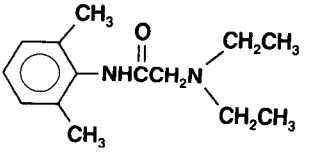

Lidocaine

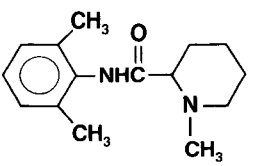

Mepivacaine

toluene is the organic phase) should be sufficient to distinguish between two compounds if $pK^*_{HA^+}$ can be determined with the same precision as an aqueous pK_a value. A scatter of ±0.06 log units can usually be accepted in a titrimetric pK_a determination [6]. Table 3 also shows that a different organic phase might improve the conditions for identification. The $pK^*_{HA^+}$ of lidocaine is separated from the $pK^*_{HA^+}$ values of mepivacaine and prilocaine by 0.73 and 0.81 log units, respectively, in the dichloromethane/water system. Compared with the toluene/water system, however, some selectivity is lost, because mepivacaine and prilocaine have nearly the same $pK^*_{HA^+}$ values ($\Delta pK^*_{HA^+} = 0.08$) when dichloromethane is the organic phase.

Acidity constants based on buffer calibration

The automatic titrator used in this work can calculate the "half-neutralization pH" of a sample. This pH value is under certain conditions (e.g., pH = 4–10, C^0_A = 0.01 M) the same as the pK'_{HA^+} value [14] or, if the titration is done in a two-phase system, the $pK^*_{HA^+}$ value [1].

TABLE 3

pK'_{HA^+} and $pK^*_{HA^+}$ values of some structurally related amines

Amine	pK'_{HA^+}[a]	$\Delta pK'_{HA^+}$	$pK^*_{HA^+}$[b]		$\Delta pK^*_{HA^+}$	
			CH_2Cl_2	$C_6H_5CH_3$	CH_2Cl_2	$C_6H_5CH_3$
Mepivacaine	7.73		4.93	6.25		
		−0.16			0.08	0.30
Prilocaine	7.89		4.85	5.95		
		0.05			0.73	0.32
Lidocaine	7.84		4.12	5.63		

[a]From [19], μ = 0.01, 25°C. [b]Mixed constant, cf. Table 2. Calculated by use of Eqn. 1 and pK'_{HA^+} and $K_{D(A)}$ values given in [19]; V_{org}/V_{aq} = 100.

One-phase systems. The pK_a routine of the titrator was first tested in aqueous solutions in order to get an idea of the accuracy and precision obtainable in the absence of an organic phase. The results are presented in Table 4. The found pK'_{HA^+} values agreed very well with those from the literature and the precision was good. A standard deviation <0.02 log units was obtained in most cases, for three different pH electrodes. Table 4 also shows that the individual pK'_{HA^+} values of two components in a mixture (ΔpK_a = 1.74) can be determined with good accuracy and precision.

Two-phase systems. The results of the $pK^*_{HA^+}$ determinations are presented in Table 5. Only in one case (electrode C) was the accuracy acceptable. The precision was poor throughout; the best standard deviation was ±0.04 log units. The large variations in the $pK^*_{HA^+}$ values obtained for a specific electrode and between different electrodes are consistent with an irreproducible liquid-junction potential. This is probably due to adsorption or precipitation of the surfactant present in the aqueous phase (i.e., hexadecylpyridinium chloride) in the ceramic plug of the reference electrode [1, 8].

The fact that the titration curves were more or less parallelly displaced along the pH axis supported the view that the change in liquid-junction potential generally occurred between the titrations. Only rarely was there an anomalous pH jump in a titration curve, indicating a sudden change of the junction potential during a titration. If the liquid-junction potential really is stable during a two-phase titration, it seemed viable to try to calibrate the electrodes in the same experimental run.

Acidity constants based on E^0 titrations

The method of Budevsky and co-workers [10, 11] for the simultaneous electrode calibration and acidity constant determination was tested. An

TABLE 4

Accuracy and precision in the pK'_{HA^+} determination based on buffer calibration (One-phase system: 0.1 M KCl, $C^0_A + C^0_D$ = 0.01 M, μ = 0.1.)

Amine (A)	C^0_A (× 10^{-3})	C^0_D (× 10^{-3})	pH electrode	pK_a[a]	pK'_{HA^+}		n
					Lit.[b]	This work[c]	
Diethanolamine	10	0	A, B, C	8.88	8.99	9.03 ± 0.014	12
Ethanolamine	10	0	A, B, C	9.50	9.61	9.64 ± 0.019	14
Ethanolamine+ triethanolamine (D)	2—7	8—3	B	—	—	9.65 ± 0.036	11
Triethanolamine	10	0	A, B, C	7.76	7.87	7.90 ± 0.018	12
Triethanolamine+ ethanolamine (D)	3—8	7—2	B	—	—	7.87 ± 0.018	11

[a]From [14]. [b]Calculated by use of $pK_a + 0.512\,\mu^{1/2}/(1 + 1.5\,\mu^{1/2})$ [6]. [c]Mean value and standard deviation of n titrations on the Titroprocessor 636.

TABLE 5

Accuracy and precision in the $pK^*_{HA^+}$ determination based on buffer calibration (Two-phase system; aqueous phase, 0.05 M HPC in 0.1 M KCl; V_{org}/V_{aq} = 0.7; sample, 0.016 M lidocaine HCl)

Organic phase	pH electrode	$pK^*_{HA^+}$[a]		n
		Lit.[b]	This work[c]	
Dichloromethane	B	4.42	4.76 ± 0.32	8
Toluene	B	5.93	6.01 ± 0.21	7
Toluene	C	5.93	5.90 ± 0.04	11
Toluene	D	5.93	5.69 ± 0.21	6

[a]Mixed constant, cf. Table 2. [b]Calculated by use of Eqn. 1 and pK'_{HA^+} and $K_{D(A)}$ values given in [8] and [19], respectively. [c]Mean value and standard deviation of n titrations.

excess of hydrochloric acid is first added to the sample. The hydrochloric acid and the sample acid(s) are then titrated sequentially with sodium hydroxide beyond the second (or last) equivalence point. Some typical titration curves are shown in Fig. 1. In these E^0 titrations, the data of measurement before EP1 are used in the calibration of the electrode pair, the data between EP1 and EP2 in the calculation of the acidity constant, and, finally, the autoprotolysis constant can be calculated using the ml/mV data before EP1 and after EP2 (see Experimental).

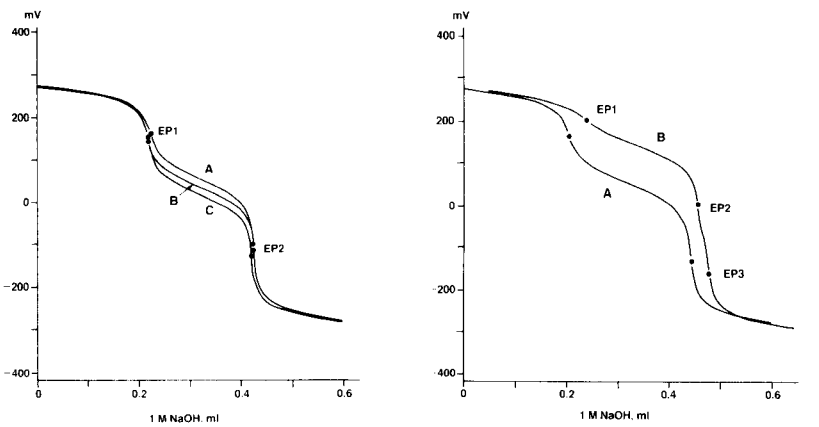

Fig. 1. Two-phase titration of some closely related amines in the presence of hydrochloric acid. EP1, HCl; EP2, amine HCl. (A) Lidocaine; (B) prilocaine; (C) mepivacaine. Aqueous phase, 0.05 M HPC in 0.01 M KCl; organic phase, toluene; V_{org}/V_{aq} = 0.5.

Fig. 2. Two-phase titration of lidocaine hydrochloride and methylparaben in solutions for injection. Hydrochloric acid (2×10^{-4} mol) was added to the sample before titration. EP1, HCl; EP2, lidocaine HCl; EP3, methylparaben. Aqueous phase, 0.05 M HPC in 0.01 M KCl. Organic phase: (A) toluene; (B) dichloromethane; V_{org}/V_{aq} = 0.5. (Curve B has been moved 0.05 ml to the right for clarity.)

The acidity constants determined in the E^0 titrations are stoichiometric constants (Table 2). Levy and Rowland [20] have demonstrated that the thermodynamic pK_a value of many amines, in practice, is the same as the stoichiometric $pK^c_{HA^+}$ value when $\mu \leqslant 0.1$. The following relation [6, 20], which is valid at 25° C, will then apply:

$$pK^c_{HA^+} = pK_a = pK'_{HA^+} - 0.512\,\mu^{1/2}/(1 + 1.5\,\mu^{1/2}) \quad (9)$$

By use of this equation, pK'_{HA^+} values can be converted to $pK^c_{HA^+}$ values or vice versa when it is of interest to compare the constants on the same scale.

One-phase systems. The E^0 titration method was first evaluated in a pure aqueous system using six different pH combination electrodes and the hydrochlorides of pilocarpine and tocainide as test substances. The results are presented in Table 6. As expected, the $E^0_{H_3O^+}$ value varied from one electrode to another while the $pK^c_{HA^+}$ was independent of the type of electrode. The pK^c_W value, however, seemed to change with the electrode. This might be explained by differences in, for example, sodium error or response time between the electrodes. The $pK^c_{HA^+}$ values could be evaluated with the same precision as the pK'_{HA^+} values (cf. Tables 4 and 6). The agreement between the literature and the found $pK^c_{HA^+}$ values was also good.

Two-phase systems. The results of the E^0 titrations in the presence of an organic phase are shown in Table 7. As a rule, there was a larger scatter in the $E^0_{H_3O^+}$ and the pK^c_W values than in the aqueous one-phase system (cf. Table 6). The spread in the pK^c_W value was particularly large for electrode C. This electrode had been in regular laboratory use for much longer than electrodes B or I, the latter being brand new. More important, however, was the fact that neither age nor previous treatment of the electrode seemed to affect

TABLE 6

Accuracy and precision in the $pK^c_{HA^+}$ determination based on E^0 titrations (One-phase system; 0.1 M KCl; sample, HCl + amine HCl, both 6×10^{-3} M)

Amine salt	pH electrode	$E^0_{H_3O^+}$[a] (mV)	pK^c_W		$pK^c_{HA^+}$	
			Lit.	This work	Lit.	This work
Pilocarpine HCl	C	403.1	13.78[b], 13.79[c]	13.75, 13.74	7.04[d]	7.02, 7.05
	E	399.1		13.76, 13.76		7.04, 7.04
	F	382.6		13.70, 13.70		7.01, 7.01
	G	405.2		13.72, 13.72		7.05, 7.05
	H	362.8		13.72, 13.73		7.02, 7.03
Pilocarpine HCl	C—H	—	—	—	—	7.03 ± 0.016[e]
Tocainide HCl	B	397.3		13.76, 13.78	7.71[f]	7.76, 7.77

[a]Mean value of two determinations, which agreed within 1 mV. [b]From [8]. [c]From [21]. [d]Calculated from pK'_{HA^+} = 7.15 (determined in this work according to [7], μ = 0.1) by use of Eqn. 9. [e]Mean value and standard deviation of 10 titrations. [f]Calculated from pK'_{HA^+} = 7.75 (μ = 0.01) [19] by use of Eqn. 9.

TABLE 7

Accuracy and precision in the $pK^*_{HA^+}$ determination based on E^0 titration (Two-phase system; aqueous phase, 0.05 M HPC in 0.01 M KCl or 0.1 M KCl; V_{org}/V_{aq} = 0.5; sample, HCl + Amine HCl, both 6.7 × 10^{-3} M)

Amine HCl	Organic phase	pH electrode	μ	$E^0_{H_3O^+}$ [a] (mV)	pK^c_W [a,b]	$pK^*_{HA^+}$ [c]		n
						Lit. [d]	This work	
Mepivacaine HCl	Dichloro-methane	B	0.1	391—394	13.81—13.85	5.19	5.31 ± 0.010	3
		C	0.1	397—405	13.89—14.03		5.33 ± 0.016	10
Mepivacaine HCl	Toluene	B	0.01	403.7, 399.3	13.73, 13.71	6.49	6.45, 6.45	2
Prilocaine HCl	Toluene	B	0.01	400.4, 398.5	13.62, 13.65	6.21	6.15, 6.17	2
Lidocaine HCl	Toluene	B	0.01	401—404	13.69—13.75	5.89	5.87 ± 0.012	3
		I	0.01	416.7, 417.4	13.72, 13.72		5.85, 5.86	2

[a] The range is given when $n > 2$. [b] Literature value is 13.79 at μ = 0.1 and 13.91 at μ = 0.01 [21]. [c] Stoichiometric constant, cf. Table 2. Mean value and standard deviation of n titrations. [d] Calculated by use of Eqns. 1 and 9; pK'_{HA^+} and $K_{D(A)}$ values obtained from [19].

the $pK^*_{HA^+}$ value. This is illustrated in Table 7 by the $pK^*_{HA^+}$ values for mepivacaine and lidocaine in the dichloromethane/water and toluene/water systems, respectively. The standard deviation was less than 0.02 log units in both cases in spite of the fact that different electrodes were used. Besides, the thirteen E^0 titrations of mepivacaine with dichloromethane as organic phase were done over a period of 6 months; indicating good long-term stability of the $pK^*_{HA^+}$ value.

The $pK^*_{HA^+}$ values obtained in the toluene/water system agreed well with the literature values (Table 7). The titration curves for these amines, which have $\Delta pK^*_{HA^+}$ = 0.29 in the toluene/water system, are shown in Fig. 1. The $pK^*_{HA^+}$ of mepivacaine in the dichloromethane/water system was 0.14 higher than the literature value (Table 7). A likely explanation is that mepivacaine is also extracted into the organic or micellar phase as an ion-pair with chloride [1, 8], because the aqueous phase contained 0.1 M KCl in this case. The $pK^*_{HA^+}$ of mepivacaine was also determined at higher and lower titration speeds than the normal which used a drift criterion of 7.5 mV min^{-1}. Two titrations at a drift criterion of 60 mV min^{-1} gave $pK^*_{HA^+}$ values of 5.30 and 5.28, respectively, with electrode C. At a criterion of 1.875 mV min^{-1}, $pK^*_{HA^+}$ values of 5.37 and 5.36 were obtained. Accordingly, the titration speed does not seem to be a critical factor in these titrations.

Application to drug analysis

The E^0 titration method for the determination of $pK^*_{HA^+}$ values was tested by assaying lidocaine in five different dosage forms (Table 8). Three of the preparations (jelly, ointment and solution for injection) could be titrated directly with sodium hydroxide after the addition of an excess of hydrochloric acid. The suppository and the viscous solution contain other protolytes

TABLE 8

Titrimetric identification and assay of lidocaine in some preparations (Titrant, 1 M NaOH; aqueous phase, 0.05 M HPC in 0.01 M KCl; organic phase, toluene; V_{org}/V_{aq} = 0.5)

Preparation[a]	Form of drug	pH electrode	pK_W^c [b]	$pK^*_{HA^+}$ [c]	Assay[d]	
					Two-phase titrn.	Other method[e]
Jelly[f]	HCl salt	C	13.71, 13.77	5.86, 5.89	19.9, 19.9	19.1, 19.0
Ointment	Base	I	13.71, 13.72	5.88, 5.88	50.7, 50.4	50.0, 49.9
Solution for injection	HCl salt	I	13.74, 13.75	5.88, 5.88	20.4, 20.4	20.2, 20.2
Suppository	Base	B	13.73, 13.70	5.86, 5.86	59.6, 59.6	60.0, 60.3
Viscous solution	HCl salt	C	13.78, 13.63	5.84, 5.89	19.9, 19.9	20.1, 20.5

[a]Trademarks: Xylocaine and Xyloproct. [b]Literature value is 13.91 at μ = 0.01 [21]. [c]Stoichiometric constant, cf. Table 2. [d]mg g^{-1}, mg ml^{-1} or mg/suppository. [e]Liquid chromatography in most cases. [f]Bellows syringe.

such as basic aluminum acetate and methyl *p*-hydroxybenzoate. To avoid interference from these compounds in the assay, the lidocaine base was first isolated by liquid-solid or liquid-liquid extraction (see Experimental).

All titration curves had the same appearance as curve A in Fig. 1. The content of lidocaine in the drug formulations was calculated from the difference in volume of titrant between EP2 and EP1. The titrimetric assay agreed relatively well with the assay using other methods (Table 8), even though the two-phase system had not been optimized for quantitative work. The $pK^*_{HA^+}$ values were all in the range 5.84—5.89 (Table 8). A $pK^*_{HA^+}$ value of 5.87 was earlier obtained for the drug substance in this phase system (Table 7). The good agreement between the "reference" $pK^*_{HA^+}$ value and the found $pK^*_{HA^+}$ values therefore supports the identification of lidocaine in these preparations.

A further example is presented in Fig. 2 which shows a differentiating titration of lidocaine hydrochloride and the preservative methylparaben in injection vials. When toluene was used as organic phase, only the sum of the compounds could be determined (curve A). However, by choosing a different organic phase (dichloromethane), it was possible to titrate lidocaine hydrochloride and methylparaben sequentially in this preparation (curve B). The results of the assay are presented in Table 9 together with data on the identity parameter for lidocaine and methylparaben. The $pK^*_{HA^+}$ values of bulk lidocaine hydrochloride and those obtained for the preparation agreed well (Table 9), thus indicating the identity of lidocaine. A titrimetric identification of methylparaben was not possible in this phase system, however, because the pK^*_{HY} values of methyl- and propyl-paraben were the same (Table 9).

TABLE 9

Titrimetric identification and assay of lidocaine hydrochloride and methyl *p*-hydroxybenzoate (methylparaben) in Xylocaine solution for injection (20 mg ml^{-1})
(Titrant, 1 M NaOH; aqueous phase, 0.05 M HPC in 0.01 M KCl; organic phase, dichloromethane; $V_{org}/V_{aq} = 0.5$)

Sample	pH electrode	pK_W^c [a]	pK_{HY}^* [b]	$pK_{HA^+}^*$ [b]	Assay (mg ml^{-1})	
					Lidocaine HCl	Methyl-paraben
Lidocaine HCl	B	13.96 ± 0.022[c]	—	4.48 ± 0.005[c]	—	—
	I	13.76		4.46	—	—
Methylparaben	B	13.96, 13.99	7.93, 8.03	—	—	—
Propylparaben	B	13.91	7.93	—	—	—
Solution for injection	B	13.99	8.01	4.49	19.5[d]	1.1[d]
	I	13.83	7.96	4.47	19.5[d]	1.1[d]

[a] Literature value is 13.91 at $\mu = 0.01$ [21]. [b] Stoichiometric constants, cf. Table 2. [c] Mean value and standard deviation of 4 titrations. [d] Corresponding results obtained by liquid chromatography were 19.4 and 1.0 mg ml^{-1}, respectively.

Check of electrode performance

Two examples of the electrode calibration in the two-phase systems are shown in Fig. 3. The E^0 plots were mostly slightly curved but the data points at low H_3O^+ and OH^- concentrations were not included in the slope analysis. The main reason for this is that these $[H_3O^+]$ and $[OH^-]$ values are rather uncertain because they were obtained by subtraction of two numbers of almost the same size (cf. Eqns. 6 and 7). The errors are then transferred to the $U_{H_3O^+}$ and U_{OH^-} variables in Eqns. 3 and 4. Other possible explanations of the curvature in the E^0 plots are that equilibrium was not attained or that protolytic impurities (e.g., carbonate) were present.

The slopes of the E^0 plots were in most cases negative with $J_{H_3O^+}$ and J_{OH^-} values ranging from −310 to +210 mV M^{-1} and from −693 to +110 mV M^{-1}, respectively. Liquid-junction potentials of the same order were obtained in Part 1 of this series when the E^0 titrations were done manually [8]. (It should be noted that E^0 values in Part 1 differ by sign and by 59.16 × 3 mV from those in the present work, because another pH meter and concentration units were used.) Generally, the slopes of the E^0 plots were so small that the $J_{H_3O^+}[H_3O^+]$ and $J_{OH^-}[OH^-]$ terms in Eqns. 3 and 4 might even be neglected. For example, omitting the $J_{H_3O^+}[H_3O^+]$ term in Eqn. 3 would only cause an error of about 1 mV or 0.02 log unit in the $pK_{HA^+}^*$ values of the present study. Accordingly, it should be sufficient to look at the pK_W^c value to get an overall check of the electrode performance. The pK_W^c values were therefore included in Tables 6—9.

The pK_W^c values obtained in the one-phase titrations agreed well with the literature values in most cases (Table 6), indicating theoretical or Nernstian

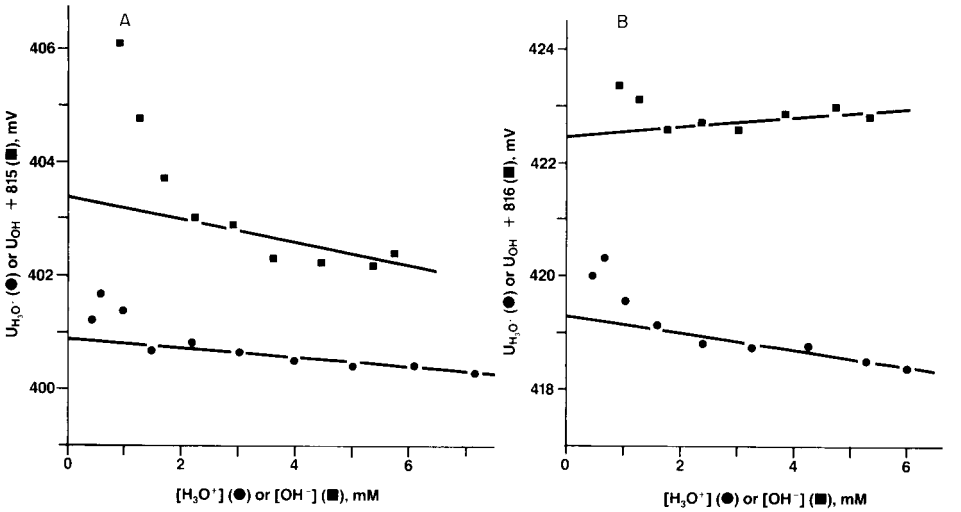

Fig. 3. In situ calibration of pH electrodes in two-phase systems. Plots according to: (•) Eqn. 3; (▪) Eqn. 4. Aqueous phase, 0.05 M HPC in 0.01 M KCl; organic phase, toluene. Samples: (A) suppository (lidocaine base) + HCl with pH electrode B; (B) solution for injection (lidocaine HCl) + HCl with pH electrode I.

behaviour of the electrodes. In the two-phase systems, however, the agreement between found and literature values was usually poor (Tables 7—9). The pK_W^c values obtained when toluene was the organic phase (Tables 7 and 8) were 0.13—0.29 log units lower than the literature value (pK_W^c = 13.91). With dichloromethane as the organic phase, the literature and found pK_W^c values showed better agreement, at least with one of the electrodes (electrode B) (Tables 7 and 9).

The electrode performance, expressed in the form of the pK_W^c value, thus seems to depend on both the organic phase and the individual pH electrode. It should be pointed out, however, that the deviations from the expected pK_W^c value are not necessarily related to the liquid junction of the reference electrode. Deviations will also occur if weak bases or acids are present [8] or if the response of the pH electrode differs from the theoretical 59.16 mV/ $p[H_3O^+]$ that was used in the calculations (Eqns. 3—5).

We thank Dr Göran Östling, Astra Pharmaceutical Production AB, for valuable discussions and Mr Klaus-Ulrich Lipfert, Astra Pharmaceutical Production AB, for writing a FORTRAN program for the data transfer from the Titroprocessor 636 to the VAX computer. Parts of this work were presented at the Workshop on Purity Determination of Drugs (Stockholm 1984) and at the Analytical Days (Lund 1985).

REFERENCES

1 P.-A. Johansson, U. Stefansson and G. Hoffmann, Anal. Chim. Acta, 151 (1983) 49.
2 The United States Pharmacopeia, 21st revision, United States Pharmacopeial Convention, Rockville, MD, 1985, p. 1222.
3 L. R. Snyder and J. J. Kirkland, Introduction to Modern Liquid Chromatography, Wiley, New York, 1974, Chap. 2.2.
4 A. M. Graabaek, Automatic Digital Titration, Radiometer Publication ST 63, Radiometer A/S, Copenhagen, 1978.
5 P. U. Früh, Int. Lab., June 1985, p. 86.
6 A. Albert and E. P. Serjeant, The Determination of Ionization Constants, 3rd edn., Chapman and Hall, London 1984, Chaps. 1—3.
7 E. P. Serjeant, Potentiometry and Potentiometric Titrations, Wiley, New York, 1984.
8 P.-A. Johansson, G. Hoffmann and U. Stefansson, Anal. Chim. Acta, 140 (1982) 77.
9 F. Ingman, A. Johansson, S. Johansson and R. Karlsson, Anal. Chim. Acta, 64 (1973) 113.
10 J. Tencheva, G. Velinov and O. Budevsky, J. Electroanal. Chem., 68 (1976) 65.
11 M. Georgieva, G. Velinov and O. Budevsky, Anal. Chim. Acta, 90 (1977) 83.
12 C. Tanford, The Hydrophobic Effect: Formation of Micelles and Biological Membranes, 2nd edn., Wiley, New York, 1980, pp. 67—68, Chap. 7.
13 G. J. Papenmeier and J. M. Campagnoli, J. Phys. Chem., 91 (1969) 6579.
14 D. D. Perrin and B. Dempsey, Buffers for pH and Metal Ion Control, Chapman and Hall, London, 1979, pp. 157—166.
15 D. Dyrssen, Sven. Kem. Tidskr., 64 (1952) 213.
16 A. Liberti and T. S. Light, J. Chem. Educ., 39 (1962) 236.
17 L. S. Palmer, Drug Inf. J., 20 (1986) 43.
18 S. S. Davis, Sep. Sci., 10 (1975) 1.
19 P.-A. Johansson, Acta Pharm. Suec., 19 (1982) 137.
20 R. H. Levy and M. Rowland, J. Pharm. Pharmacol., 24 (1972) 841.
21 H. S. Harned and W. J. Hamer, J. Am. Chem. Soc., 55 (1933) 2194.

Analytica Chimica Acta, 192 (1987) 33—40
Elsevier Science Publishers B.V., Amsterdam — Printed in The Netherlands

THE ACCURACY AND PRECISION OF THE CLASSICAL TECHNIQUE FOR LOCATING THE POINT OF MAXIMUM SLOPE ON A POTENTIOMETRIC TITRATION CURVE

LOUIS MEITES*

Department of Chemistry, George Mason University, 4400 University Drive, Fairfax, Virginia 22030 (U.S.A.)

NICOLANGELO FANELLI and PAOLO PAPOFF

C.N.R. Istituto di Chimica Analitica Strumentale, c/o Dipartimento di Chimica e Chimica Industriale dell'Università, Via Risorgimento, 35, 56100 Pisa (Italy)

(Received 8th July 1986)

SUMMARY

When it is applied to data simulating those that might be obtained in the titration of either a strong acid or a monobasic weak acid with a strong base at the same concentration, the classical technique for locating the end-point of a potentiometric titration has a bias that is statistically indistinguishable from zero. Its precision depends on the standard error of measurement of the volume of reagent but exhibits no detectable dependence on the standard error of measurement of the pH. If the acid is strong, the precision is improved by decreasing its concentration; if the acid is weak, the precision is improved by increasing its pK_a value or by decreasing its concentration.

The classical technique for locating the end-point of a potentiometric titration was devised by Hostetter and Roberts [1] and by Kolthoff and Furman [2, 3]. It is based on the coordinates V_j, E_j ($j = 1—4$) of four points, of which two must precede the point of maximum slope while the other two follow it. In the neighborhood of that point, the titration curve is approximated by three line segments, the slopes of which are taken to be

$$S_k = (E_{k+1} - E_k)/(V_{k+1} - V_k) \quad (1)$$

where E is a measured potential and V the corresponding volume of reagent that has been added. Assigning these values of the slope to the midpoints of the corresponding intervals of volume, where $V = (V_k + V_{k+1})/2$, yields three points on the first-derivative curve. This is approximated by two line segments, and a similar treatment gives the coordinates of two points on the second-derivative curve: one for which $\Delta^2E/\Delta V^2$ is positive, and another for which it is negative. Linear interpolation between these two values is performed to find the value of V at the point of maximum slope, which is considered to correspond to the end-point.

0003-2670/87/$03.50

It has been known for quite a long time that the point of maximum slope on a potentiometric titration curve does not coincide with the equivalence point of the titration [4], except for so-called "asymmetrical" titration curves under very restrictive conditions [5]. Moreover, although much experience has shown that the error incurred by using the classical technique to locate the point of maximum slope is generally too small to have any practical significance, it seems obvious that the precision with which that point can be located must be governed both by the slope of the titration curve in the vicinity of the equivalence point and by the random errors of measurement, which afflict both the potential (or, in an acid-base titration, the pH) and the volume of reagent that has been added. Despite the frequency with which the technique is applied to titrimetric data, there seems to have been no prior inquiry into its accuracy and precision. This paper presents the results of such an inquiry.

THEORY AND PROCEDURE

The solution being titrated was assumed to have a volume of exactly 25 cm^3 and to contain either (a) a strong acid, for which the concentration was varied from 0.1 M to 3.16×10^{-5} M in different calculations, or (b) a monobasic weak acid, for which the value of pK_a and the concentration were varied from 3 to 6 and from 0.1 M to 0.01 M, respectively, in different calculations. It was always assumed that the concentration of the reagent is equal to the concentration of the acid being titrated, that $pK_w = 14.00$, and that the measured pH is equal to $-\log_{10}[H^+]$ (i.e., that the single-ion activity coefficient of hydrogen ion is equal to unity and that the liquid-junction potential is negligibly small).

According to these assumptions, exactly 25 cm^3 of reagent must be added to reach the equivalence point. The nominal volumes of reagent added at the four important points were always taken to be 24.85, 24.95, 25.05, and 25.15 cm^3. Of course these volumes will not be exactly attained in any practical titration, and the measurements of pH will also be inexact. The effects of the corresponding standard errors of measurement, σ_V and σ_{pH} respectively, were investigated by assigning different values to them in different calculations.

"Data" were synthesized in the following way. Two random numbers, e_1 and e_2, taken from a normally distributed population having a mean equal to 0 and a variance equal to 1, were generated by the technique of Abramowitz and Stegun [6] and Lohnes and Cooley [7]. The product $e_1\sigma_V$ was added to the first nominal volume of reagent (24.85 cm^3) to obtain the "actual" volume of reagent added at the first point. For that volume, the equation for the titration curve was solved to obtain the corresponding values of $[H^+]$ and the pH, and the product $e_2\sigma_{pH}$ was added to the latter to obtain the "actual" value of the pH. Finally, because the numbers of significant digits in the "actual" values could not be obtained in any real titration, and would

not be transcribed if they were obtained, both the volume and the pH were rounded off. The volume was always rounded off to the nearest 0.01 cm^3; the pH was rounded off to 0.001 if $\sigma_{pH} < 0.01$ or to 0.01 if $\sigma_{pH} > 0.01$. It appeared to be immaterial whether the pH was rounded to 0.001 or to 0.01. The technique described above was applied to the rounded values to compute the volume required to reach the point of maximum slope. This procedure is considered to yield the most realistic and accurate approximation to real data that can be obtained.

One of the unexpected conclusions to be drawn from the results obtained is that the precision of the volume required to reach the end-point is independent of the standard error of the measurements of pH under otherwise fixed conditions. In part, this is because the above equations are forgiving in a way that a human chemist might not be. Consider a titration of 25 cm^3 of 0.01 M strong acid with 0.01 M strong base. The first line of the following table shows the successive volumes of base used in these calculations. The second shows the corresponding theoretical values of the pH. The third shows a hypothetical set of pH values that might be obtained if the standard error of the measurements of pH were very large.

Volume, cm^3	24.85	24.95	25.05	25.15
pH, theoretical	4.522	5.000	9.000	9.476
pH, "measured"	4.322	7.500	6.300	9.576

Although different human chemists would probably react in different ways to the "data" on the first and third lines, it may be doubted whether many of them would be inclined to trust the equations given above, and it seems possible that some might take the end-point to lie in some other portion of the titration curve. Nevertheless, the above equations yield 24.9994 cm^3 for the volume of reagent required to reach the end-point. This behavior is at least partly responsible for the conclusion mentioned above.

When the results of 100 "titrations" had been computed in this way, their mean was stored, another set of 100 "titrations" was generated and treated similarly, and so on until 1000 means had been obtained. These were then averaged to obtain the mean error of 100 000 "titrations", and the standard error of a single result was calculated from the standard deviation of the 1000 means. The mean and standard errors are denoted as E and s, respectively, in the tables that follow.

Some of the calculations were performed in BASIC, using Tektronix Model 4051 and IBM PC microcomputers; others were performed in FORTRAN with a Radio Shack TRS-80 Model II microcomputer.

RESULTS AND DISCUSSION

Table 1 summarizes the results obtained in "titrations" of strong acids. In titrations of 0.1 M acid with 0.1 M base, the average relative standard error of the volume required to reach the end-point is 0.022% if σ_V (the standard

TABLE 1

The accuracies and precisions of "titrations" of strong acids
(The first two lines give the initial concentration of the acid, of which 25 cm^3 is titrated with strong base of the same concentration. The first two columns give the standard errors of measurement of the volume of base and the pH; E and s denote the mean error of 100 000 titrations and the standard error of a single result, respectively.)

σ_V (cm^3)	σ_{pH}	Initial concentration of acid (M)									
		0.1		0.01		0.001		0.0001		0.00003162	
		10^5E (cm^3)	10^3s (cm^3)	10^5E (cm^3)	10^3s (cm^3)	10^5E (cm^3)	10^3s (cm^3)	10^5E (cm^3)	10^3s (cm^3)	10^5E (cm^3)	10^3 (cm
0.005	0.001	−0.36	5.34	0.75	5.41	−0.14	5.00	−39	3.33	−401	4.7
	0.002	3.7	5.53	−3.7	5.28	−3.0	4.89	−40	3.42	−398	4.4
	0.005	−4.8	5.50	1.4	5.31	−3.0	5.11	−41	3.37	−399	4.7
	0.01	4.6	5.58	−0.15	5.43	−2.3	4.85	−40	3.36	−402	4.4
0.01	0.001	4.1	9.24	2.5	9.44	6.8	8.83	−40	4.06	−404	4.4
	0.002	1.6	9.02	−8.0	9.58	−4.7	8.40	−39	4.00	−408	4.4
	0.005	15	9.28	5.0	9.74	−1.8	8.60	−43	4.18	−401	4.5
	0.01	−0.48[a]	10.0[a]	−9.7	9.56	−2.1	8.43	−42	4.14	−402	4.1
	0.02	7.4	9.76	−8.1	9.38	—	—	—	—	—	—
	0.05	5.6	9.78	−0.84	9.30	—	—	—	—	—	—
	0.1	0.53	10.2	2.8	9.25	−3.8	8.57	—	—	—	—
	0.2	—	—	1.3	9.34	−2.6	8.25	−43	4.33	—	—
	0.5	—	—	8.5	9.42	—	—	−41	4.10	—	—
0.015	0.001	6.6	13.2	17	15.3	0.76	12.9	−45	4.91	−407	4.6
	0.002	−5.2	13.5	−14	14.7	3.9	12.5	−43	4.84	−408	4.5
	0.005	2.3	16.5	8.0	15.9	−0.67	12.8	−46	4.71	−411	4.3
	0.01	−3.3	16.0	4.6	16.1	−1.4	13.3	−48	4.72	−407	4.4
0.02	0.001	3.0	30.2	—	—	—	—	—	—	—	—

[a]These values are the means for two closely agreeing sets of results: one in which the "measured" pH values were rounded to 0.001, and another for which they were rounded to 0.01.

error in a measurement of the volume of base) is 0.005 cm^3, 0.039% if σ_V is 0.01 cm^3, and 0.059% if σ_V is 0.015 cm^3. In none of these cases does the uncertainty σ_{pH} in the measurements of pH have any detectable effect on the precision of the end-point. The value (0.039%) that corresponds to σ_V = 0.01 cm^3 may be compared with the relative standard error of 0.025% obtained by non-linear regression analysis under comparable conditions, though with a rather different data-acquisition schedule [8]. Because the calculations that are performed in regression analysis are based on a larger number of points, they yield results having relative standard errors that are smaller than those of the measurements. The procedure based on regression analysis also provides values of K_t, the equilibrium constant for the reaction that occurs during the titration, which the present technique cannot do.

The values of σ_V given above correspond to 0.02, 0.04, and 0.06%, respectively, of the volume that is consumed at the equivalence point. Hence the standard error of the result is essentially identical with that of the measurements of volume when the acid is both strong and fairly concentrated. This

would not be surprising if it were true only for small values of σ_{pH}, for the titration curve obtained under these conditions is so steep in the vicinity of the equivalence point that an uncertainty of a few thousandths or hundredths of a unit in each of the pH values could hardly be expected to have an appreciable effect. However, the results given for $\sigma_V = 0.01$ cm^3 show that it remains true up to $\sigma_{pH} = 0.5$, and Table 1 also contains a number of other results that support the same conclusion. With 0.1 M solutions, every mean error is much smaller than the standard error of a single result, so that the bias of the technique is negligible.

The results for 0.01 M solutions are scarcely distinguishable from those for 0.1 M solutions, but at concentrations below 0.01 M the precision improves appreciably as the concentrations decrease. The improvement is smallest if σ_V is small, but is dramatic if $\sigma_V = 0.015$ cm^3, where the average standard error of a single result is 0.0148 cm^3 for 0.1 M and 0.0155 cm^3 for 0.01 M solutions, but decreases to 0.0129 for 0.001 M, 0.00480 for 0.0001 M, and 0.00451 for 3.16×10^{-5} M solutions, in which both the standard error of a single result and the mean of a set of 100 000 individual results are independent of the standard error in the measurements of volume as well as of the standard error in the measurements of pH.

At the same time, the mean errors exhibit a just detectable trend: although they never reach statistical significance at any substantial level of confidence, there is a systematic variation of the fraction of them that are negative. With 0.1 M solutions, there are only 5 means that are negative out of 16; with 0.01 M solutions, there are 7 out of 17; with 0.001 M solutions, there are 11 out of 14; and with 0.0001 and 3.162×10^{-5} M solutions, all of the means are negative.

In the most dilute of these solutions, the overall mean of the errors in the 1.2 million titrations summarized in Table 1 is -0.00404 cm^3. Since 25 cm^3 of base is needed to reach the equivalence point, the average error corresponds to the consumption of 99.984% of the stoichiometric volume of base. With 0.0001 M solutions, the corresponding figures are -4.20×10^{-4} cm^3 and 99.9983%, respectively, and are a little less certain than the foregoing ones because there is a small dependence on σ_V at this concentration. According to Meites and Goldman [4], the points of maximum slope are reached under these conditions by adding 99.984% of the stoichiometric volume of base if both solutions are 3.16×10^{-5} M, or 99.9984% of that volume if both solutions are 1×10^{-4} M. The negative errors that arise in very dilute solutions should therefore be regarded, not as errors, but as accurate reflections of the discrepancy between the point of maximum slope and the equivalence point. The discrepancy decreases rapidly as the solutions become more concentrated, and is too small to be detected in this way at concentrations above 1×10^{-4} M.

In titrations of strong acids with strong bases, the technique provides (1) unbiased estimates of the location of the point of maximum slope, or of the equivalence point as long as the solutions are not too dilute, and

(2) precision that is equal to, or better than, the precision of the measurements of the volume of reagent.

Although a standard error on the order of 0.01—0.015 cm^3 should not be difficult to attain by the careful use of a conventional 50cm^3 buret, few chemists who conduct such titrations expect to achieve, or succeed in achieving, relative precisions like those shown in Table 1. Other sources of error are of course responsible.

Table 2 shows the results obtained for titrations of 0.1 M solutions of monobasic weak acids for which the values of pK_a range from 3 to 6. For $pK_a = 3$, they are indistinguishable from the results for 0.1 M solution of a strong acid, which is to be expected because there is very little difference between the corresponding titration curves in the neighborhoods of their equivalence points. Increasing the value of pK_a for a weak acid has much the same effects as decreasing the concentration of a strong acid: there is a small decrease of the standard error of the volume consumed at the end-point, and there is an increasing preponderance of negative values for the mean error of 100 000 "titrations". The point of maximum slope precedes the equivalence

TABLE 2

The effects of pK_a on the accuracies and precisions of "titrations" of 0.1 M solutions of weak acids

(The first two lines give the value of pK_a for the acid, of which 25 cm^3 of an 0.1 M solution is titrated with 0.1 M strong base. The first two columns give the standard errors of measurement of the volume of base and the pH. E and s, both given in cm^3 as in Table 1, denote the mean error of 100 000 titrations and the standard error of a single result, respectively.)

σ_V (cm^3)	σ_{pH}	pK_a							
		3		4		5		6	
		10^5E	10^3s	10^5E	10^3s	10^5E	10^3s	10^5E	10^3s
0.005	0.001	−0.86	5.49	3.2	5.31	−1.5	5.15	−8.9	4.63
	0.002	0.76	5.49	−1.9	5.34	−6.6	4.97	−7.0	4.43
	0.005	−0.74	5.42	0.36	5.30	0.93	4.87	−7.9	4.58
	0.01	−2.5	5.33	0.45	5.20	0.58	5.04	−11.5	4.38
0.01	0.001	4.7	9.24	−4.0	9.80	−0.55	8.84	−13	7.26
	0.002	2.6	9.17	−2.6	9.11	−0.26	8.58	−12	7.37
	0.005	6.9	9.78	4.0	9.33	−7.2	8.78	−9.2	7.48
	0.01	2.6	9.08	−3.0	9.13	−0.66	8.74	−6.0	7.22
	0.02	—	—	3.1	9.00	−4.3	8.83	—	—
	0.05	—	—	−2.2	9.53	−3.6	8.49	—	—
	0.1	—	—	−5.3	9.58	—	—	—	—
	0.2	—	—	−8.8	9.44	—	—	—	—
0.015	0.001	−17.9	16.4	−8.3	15.7	−36.6	12.7	−35	9.9
	0.002	−6.3	16.9	−0.13	15.4	3.7	13.7	—	—
	0.005	3.0	16.7	5.9	16.2	3.7	13.7	—	—
	0.01	−1.7	16.6	−13	15.7	−5.4	13.1	—	—

point in these titrations [4]: extrapolating the values given by Meites and Goldman indicates that $f = 0.999\,999$ at the point of maximum slope in the titration of an 0.1 M solution of an acid, for which $pK_a = 6$, with 0.1 M base. The average of the nine values of E in the next to the last column of Table 2 is $f = 0.999\,995$. The agreement is less exact than it is for very dilute solutions of strong acids, where the average result is identical with the theoretical location of the equivalence point. The discrepancy reflects the fact that E is not independent of σ_V for a fairly concentrated solution of a weak acid, although it is independent of σ_V for very dilute solutions of strong acids.

Table 3 shows how the results are affected by diluting the acid and base from 0.1 M to 0.01 M if $pK_a = 3$ or 5. If $pK_a = 3$ the effect is very small, as is also true for a strong acid, but if $pK_a = 5$ the precision is improved by dilution. In general, the precision of the technique is improved by a decrease of the slope of the titration curve in the region that is of interest.

Conclusions

The following conclusions may be drawn. First, the precision of the technique is so high that there is very little justification for preferring any of the more sophisticated and more complicated techniques (such as those that involve cubic- or spline-fitting) occasionally proposed. In the titration of 3×10^{-5} M strong acid with equally concentrated strong base, the variation of pH is rather small: between $f = 0.99$ and $f = 1.01$ it increases less than 0.5. Nevertheless, the relative standard error of the technique is only about 4.5×10^{-3} cm^3/25 cm^3 = 1.8×10^{-4}, or 0.018%.

TABLE 3

The effects of pK_a on the accuracies and precisions of "titrations" of 0.01 M solutions of weak acids

(The first two lines give the value of pK_a for the acid, of which 25 cm^3 of 0.01 M solution is titrated with 0.01 M strong base. The first two columns give the standard errors of measurement of the volume of base and the pH. E and s denote the mean error of 100 000 titrations and the standard error of a single result, respectively.)

σ_V (cm^3)	σ_{pH}	pK_a			
		3		5	
		10^5E (cm^3)	10^3s (cm^3)	10^5E (cm^3)	10^3s (cm^3)
0.005	0.001	−1.4	5.20	−12	4.57
	0.002	−2.5	5.15	−7.4	4.41
	0.005	−3.4	5.18	−17	4.02
	0.01	−3.2	4.95	−11	4.37
0.01	0.001	−1.0	9.36	−8.0	7.36
	0.002	1.7	9.01	−9.5	7.31
	0.005	2.2	9.38	−12	7.15
	0.01	8.5	9.29	−6.1	7.44
0.015	0.001	4.7	16.3	−16	9.6

Secondly, over a wide range of conditions, the precision increases moderately as the slope in the vicinity of the equivalence point decreases.

Finally, the inaccuracy of the technique, expressed as the difference between the end-point and the point of maximum slope, is negligible under all conditions. For very dilute solutions of strong acids, and for very weak acids, the end-point precedes the equivalence point because, and to nearly the same extent as, the point of maximum slope precedes the equivalence point.

This work was aided by the generous support of the Consiglio Nazionale delle Richerche, to which one of us (L. M.) is indebted for a visiting fellowship during the summer of 1985.

REFERENCES

1 J. C. Hostetter and H. S. Roberts, J. Am. Chem. Soc., 41 (1919) 1337.
2 I. M. Kolthoff, Rec. Trav. Chim. Pays-Bas, 47 (1928) 397.
3 I. M. Kolthoff and N. H. Furman, Potentiometric Titrations, 2nd edn., Wiley, New York, 1931, pp. 94—96.
4 L. Meites and J. A. Goldman, Anal. Chim. Acta, 29 (1963) 472.
5 L. Meites and J. A. Goldman, Anal. Chim. Acta, 30 (1964) 18.
6 M. Abramowitz and I. A. Stegun, Handbook of Mathematical Functions, U.S. Government Printing Office, Washington, DC, 1964, p. 953.
7 P. R. Lohnes and W. W. Cooley, Introduction to Statistical Procedures, Wiley, New York, 1968, p. 90.
8 H. C. Smit, L. Meites and G. Kateman, Anal. Chim. Acta, 153 (1983) 121.

Analytica Chimica Acta, 192 (1987) 41—48
Elsevier Science Publishers B.V., Amsterdam — Printed in The Netherlands

POTENTIOMETRIC DETECTION OF HALIDES AND PSEUDOHALIDES IN ANION CHROMATOGRAPHY

JAMES E. LOCKRIDGE, NANCY E. FORTIER, GABRIELLA SCHMUCKLER[a] and JAMES S. FRITZ*

Ames Laboratory and Department of Chemistry, Iowa State University, Ames, Iowa 50011 (U.S.A.)

(Received 22nd May 1986)

SUMMARY

A small piece of silver wire, coated with an insoluble silver salt, can be used as a selective potentiometric detector for halides in ion chromatography. Several coated electrodes were examined by electron microscopy and their response to various anions evaluated in a flow-injection system. A silver/silver chloride electrode was found to be a selective and reproducible detector for chloride, bromide, iodide, thiocyanate and thiosulfate separated by ion chromatography. Calibration curves were non-linear and had slopes ranging from 40 to 60 mV per concentration decade in the range 0.1—2 mM. A working range of 0.05—2 mM was used. This electrode is also satisfactory when gradient elution is used in ion chromatography.

Modern ion-exchange chromatography, or ion chromatography as it is now called, is the leading analytical method for determining anions in aqueous samples. Most frequently, detection of eluted anions is by conductivity or spectrophotometry. In a few cases, potentiometric detection of eluted anions has been used. Franks and Pullen [1] used a small silver/silver chloride electrode in conjunction with a reference electrode for the selective detection of halides in anion-exchange chromatography. Deguchi et al. [2] used a similar detection system for gel chromatography. In both papers, the detectors worked well, but the speed and quality of the chromatographic separations were distinctly inferior to those now attainable.

Trojanowicz and Matuszewski [3] obtained good results in the potentiometric determination of chloride with a flow-injection system. Hershcovitz et al. [4] used a silver wire coated with silver salicylate for potentiometric detection of halides and thiocyanate in ion chromatography. Alexander et al. [5] and Loscombe et al. [6] successfully used a copper electrode for the potentiometric detection of a number of anions and cations in ion chromatography.

In the present work, several types of silver electrodes, each coated with an insoluble silver salt, are evaluated for potentiometric detection of anions.

---

[a]Present address: Department of Chemistry, Technion, Haifa 32000, Israel.

0003-2670/87/$03.50

The surface characteristics of the most promising were studied by electron microscopy. The practical advantages of these electrodes as detectors in chromatography are demonstrated for both isocratic and gradient elution.

EXPERIMENTAL

Equipment

The high-performance liquid chromatographic (h.p.l.c.) equipment consisted of an Eldex Model AA-94 dual-channel pump, a Rheodyne Model 7000 injection valve with a 20-μl sample loop, and a Li-Chroma-Damp III pulse dampener. The leads from the potentiometric cell (see below) were connected to a Corning Model 12 pH meter. The recorder output of the pH meter was connected to a Fisher Model 5000 chart recorder. For gradient work, a Tracor Model 980A low-pressure solvent programmer was used.

Column. The anion-exchange columns tested were a 4.6 mm × 50 mm TSK gel column and an XAD-1 column functionalized and packed in this laboratory. Neutral XAD-1 particles (20—26 μm) were functionalized via chloromethylation followed by amination with trimethylamine as in Barron and Fritz [7]. Conditions were chosen such that a final capacity of 84 μeq g^{-1} would be obtained. A 400 × 2 mm glass column was packed with a 40% ethylene glycol diluent.

Potentiometric cell. The holder for the silver electrode was made from two Omnifit polypropylene tube fittings, a coupler and a teflon spacer as in Fig. 1. One fitting held the column effluent delivery tube. The other held a larger-bore polypropylene tube which tightly surrounded the silver-wire electrode. The column effluent passed through one fitting, around the silver electrode and out through a hole drilled into the center of the coupler. The fittings were tightened against the teflon spacer and effluent was allowed to exit the electrode compartment via a notch in the electrode side of the spacer. The calomel reference electrode was placed 2.0 mm downstream of silver electrode.

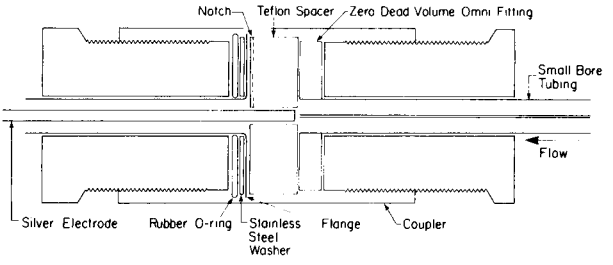

Fig. 1. Sectional view of the silver electrode holder. Silver electrode diameter, 0.8 mm; inlet tubing diameter, 0.3 mm i.d.; distance from electrode to end of inlet, 0.5 mm.

Electron microscopy

A JEOL JSM-35 scanning electron microscope (SEM) in the secondary electron mode, with an accelerating voltage of 20 kV and a beam current of 65 μA, was used to obtain the micrographs. Specimens were mounted on brass discs with double-stick tape and coated with gold/palladium (ca. 15 nm thick) in a Polaron E5100 sputter coater. Images were recorded on Polaroid Type 665 film.

RESULTS AND DISCUSSION

Preparation and preliminary evaluation of electrodes

Electrodes coated with a thin layer of a silver anion precipitate were prepared by electrical oxidation of a silver wire in an aqueous solution of the selected anion for a period of 3—7 min. In some cases, the precipitate layer was formed by immersing a silver wire in a solution of iron(III) chloride [3].

Silver wire electrodes coated with AgCl, AgBr, AgI, Ag_3PO_4, Ag_2S and AgSCN were evaluated for detection of various anions with a flow-injection system, using the sensing electrode arrangement shown in Fig. 1. A 0.01 M solution of sodium perchlorate was pumped through the system at a flow rate of 4.5 ml min^{-1} and a small volume (20 μl) of test solution was injected. Figure 2 shows the response and repeatability for several different anions with a Ag/AgCl electrode. The response and repeatability were equally good with a Ag/AgSCN electrode, but were not as good with the other electrodes evaluated.

The surface of several of the electrodes was examined by electron microscopy. Figure 3 shows portions of the surfaces at high magnification. Electrode coatings of smaller particle sizes were observed to have faster kinetics in flow-injection experiments. Silver sulfide is an exception to this trend; it has small particles but shows slower kinetics when used as an electrode. These preliminary evaluations indicated that either the Ag/AgCl or Ag/AgSCN electrode should be a satisfactory detector for a flow-injection system or for ion chromatography.

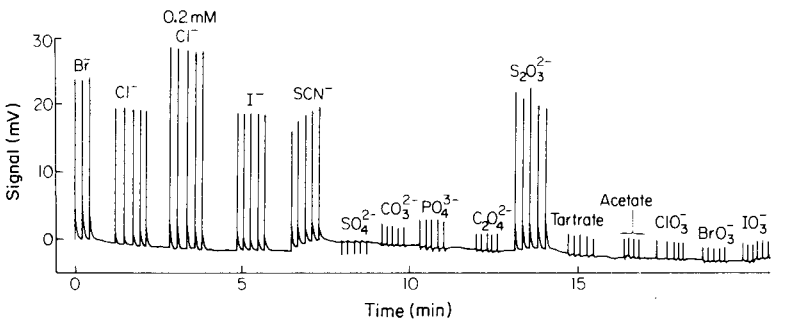

Fig. 2. Responses of a flow-injection system with a Ag/AgCl electrode. Carrier was 0.01 M sodium perchlorate at 4.5 ml min^{-1}; all samples were 0.1 mM unless indicated.

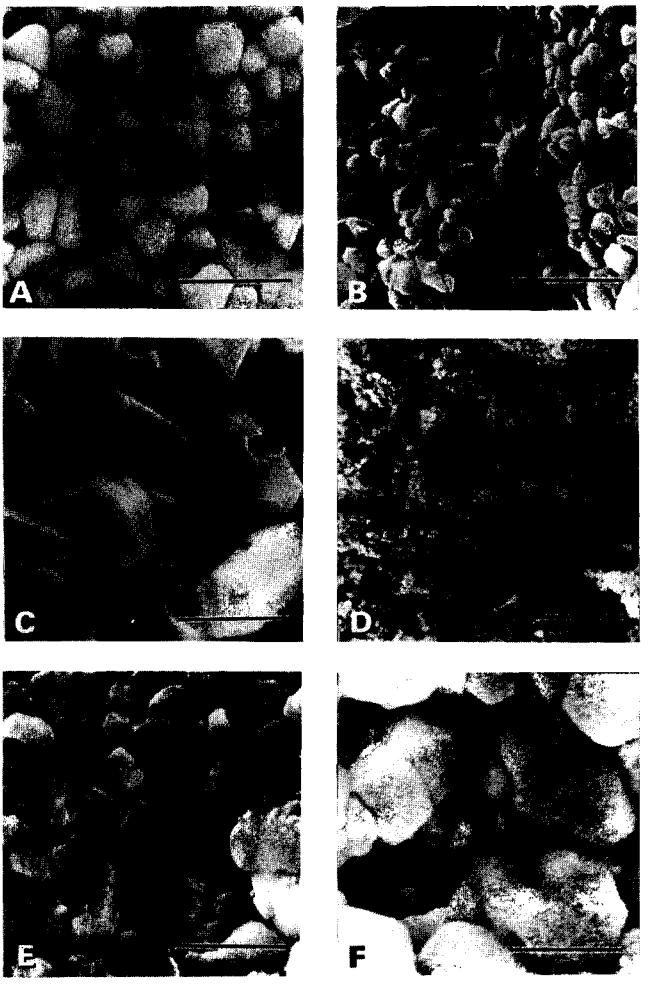

Fig. 3. Electron micrographs of silver/silver anion electrodes: (A) AgCl; (B) AgSCN; (C) AgI; (D) Ag_2S; (E) Ag_3PO_4; (F) AgBr. Each was prepared by passing 100 μA for 7 min through a solution containing the appropriate anion X^{n-}, a silver wire anode, and a platinum cathode. Bars correspond to 2 μm.

Ion chromatography with isocratic elution

A silver/silver chloride electrode in conjunction with a saturated calomel reference electrode was used for detection of various anions separated by ion chromatography. A dilute aqueous solution of sodium perchlorate or sodium sulfate served as the eluent. The baseline was found to be unstable until several samples had been injected. However, it was found that a new silver/silver chloride electrode could be conditioned by dipping (and rinsing with water) 3 or 4 times into a solution containing 1 mM concentrations of each of the halides and pseudohalides. Electrodes so treated quickly gave a steady base-

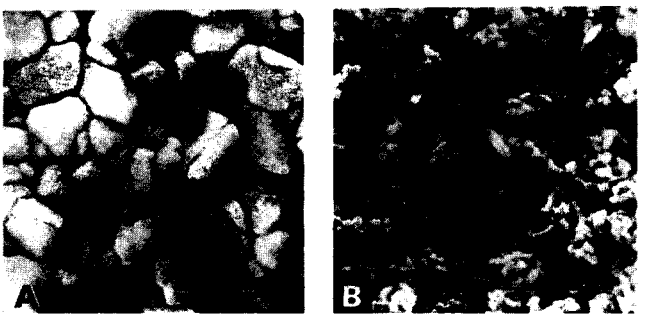

Fig. 4. Electron micrographs of Ag/AgCl electrodes prepared by dipping a silver wire into an aqueous iron (III) chloride solution for 4 min. (A) Fresh electrode; (B) electrode conditioned by dipping several times in a solution containing 10^{-3} M each of I^-, Br^-, Cl^-, SCN^-, $S_2O_3^{2-}$, SO_4^{2-}, PO_4^{3-}. Bars correspond to 2 μm.

line. Figure 4A shows an electron micrograph of a fresh silver/silver chloride electrode. Comparisons with Fig. 4B shows that the surface of the conditioned electrode is a composite of many silver salts covering the underlying silver chloride precipitate.

Use of an ion-selective electrode as a detector in ion chromatography has the advantage that many anions are not detected (or are detected with very low sensitivity) and will not interfere in the determination of the detected anions. Figure 5 shows the chromatographic separation with potentiometric detection of 1.0 mM chloride, bromide, iodide, thiocyanate and thiosulfate; the sample also contained 1.0 mM concentrations each of nitrate, phosphate, carbonate, sulfate and acetate which were not detected. A 4.5 mM solution of sodium perchlorate was used as the eluent and injection volumes were 20 μl. Sodium sulfate eluents also gave good separations of several inorganic anions when used in conjunction with the silver/silver chloride potentiometric detector. Table 1 compares the retention times of halide and other ions with the sulfate and perchlorate eluents. The retention times relative to chloride are also shown; these show perchlorate to be the more efficient eluent for iodide, chloride, bromide and thiocyanate. Thiosulfate is eluted more efficiently with the sulfate eluent.

Calibration curves were prepared for peak area and peak height against anion concentration and logarithm of anion concentration, respectively. The calibration plots varied less from one anion to another when peak height was used. Figure 6 shows the curves obtained for peak height plotted against log concentration. While not linear, the curvature is sufficiently slight for use as practical calibration curves. The working range is approximately 0.05 to 2.0 mM. Some previous authors [1, 2] noted linear calibration plots (detector response vs. concentration), but others [4] found predominantly logarithmic curves. The combined influence of concentration, solubility product, adsorption and rate effects determines the peak potentials [4].

The electrode response is a function of the total ionic strength of the solution in the detector cell as well as the analyte activity. Thus, the slope of a calibration curve is expected to change with the concentration of eluent used.

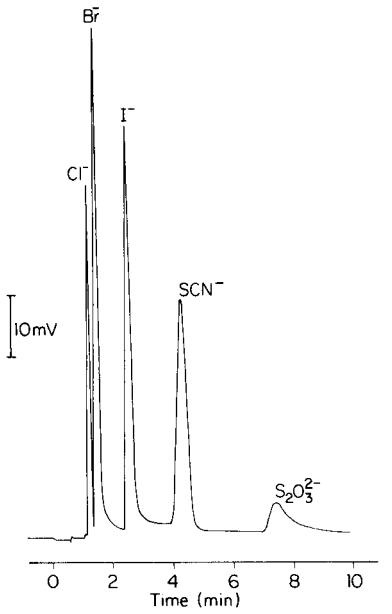

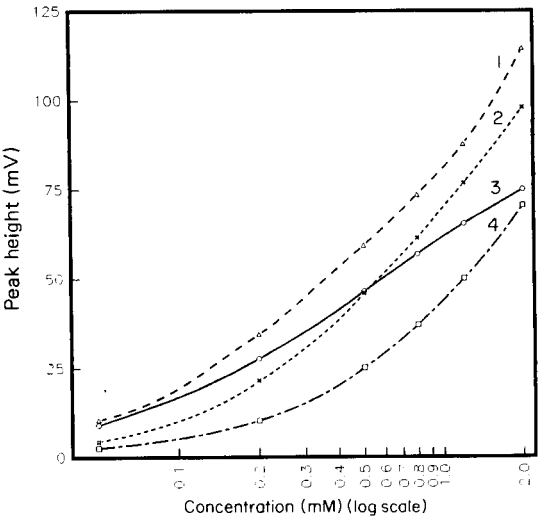

Fig. 5. Typical chromatogram with potentiometric detection at a Ag/AgCl electrode. Eluent, 4.5 mM sodium perchlorate at 1.6 ml min^{-1}; injection volume, 20 μl; analyte concentrations, 1.0 mM.

Fig. 6. Calibration plots of peak height vs. log concentration: (1) bromide; (2) iodide; (3) chloride; (4) thiocyanate. Eluent as in Fig. 5.

TABLE 1

Comparison of retention of anions with sulfate and perchlorate eluents[a]

Ion	Relative retention[b]		Actual retention time (min)	
	5.0 mM ClO_4^-	10.0 mM SO_4^{2-}	5.0 mM ClO_4^-	10.0 mM SO_4^{2-}
Cl^-	1.00	1.00	2.08	1.41
Br^-	1.48	2.18	3.07	3.07
I^-	2.84	8.37	5.9	11.8
SCN^-	4.54	—	9.44	—
$S_2O_3^{2-}$	7.83	3.01	16.28	4.25

[a]TSK anion exchange column; eluent flow rate 1.6 ml min^{-1}; Ag/AgCl detector. [b]Relative to chloride (= 1.00).

It may also change for samples containing a high concentration of undetected anions.

The reproducibility of peak areas of chloride, bromide, iodide and thiocyanate was checked by separating a sample containing these ions ten times,

and by separating a sample containing these anions plus equimolar amounts of phosphate, nitrate, sulfate, carbonate and acetate ten times. The means ($\bar{x}$) and standard deviations (s) are given in Table 2. The results show only a minor effect of the undetected anions at the concentrations used.

TABLE 2

Reproducibility of peak areas[a]

Ion (1.0 mM)	Peak areas (arbitrary units)			
	No foreign ions		With foreign ions[b]	
	$\bar{x}$	s	$\bar{x}$	s
Cl^-	26.5	3.9	26.6	1.3
Br^-	51.2	2.5	53.1	1.5
I^-	68.1	2.4	66.0	1.1
SCN^-	74.3	3.0	72.5	2.3

[a]Mean and standard deviation of 10 runs. [b]PO_4^{3-}, NO_3^-, SO_4^{2-}, CO_3^{2-}, acetate, each at 1.0 mM.

Ion chromatography with gradient elution

The use of eluent concentration gradients in ion chromatography has been quite difficult when conductivity and spectrophotometric detectors are used. Most papers published in ion chromatography have used isocratic elution. However, gradient elution would be advantageous for separation of samples containing both early- and late-eluting anions.

The fact that an ion-selective electrode gives little or no response to many ions suggests the possibility of programming the eluent concentration throughout the chromatographic run. Figure 7 shows the separation and detection of five ions using a gradient of 3.5 to 10.0 mM sodium perchlorate. Compared to the same separation in Figure 5, the peak shape for thiosulfate is much improved and the time required for separation is significantly less.

Conclusions

A small silver/silver chloride electrode rapidly attains a reproducible potential with varying concentrations of halides in a flowing system. This suggests the use of such an electrode for rapid determination of various halides in flow-injection systems. However, individual halides and pseudohalides can be separated by ion chromatography and measured potentiometrically with a silver/silver chloride electrode. Gradient elution is also possible in the latter case.

The microscopy was done in the Bessey Microscopy Facility, Department of Botany, Iowa State University. One of the authors (N.E.F.) thanks Bruce Wagner and Harry Horner for valuable advice and assistance with the micrographs. J.E.L. thanks Dr. Dennis Johnson for his thoughtful discussions

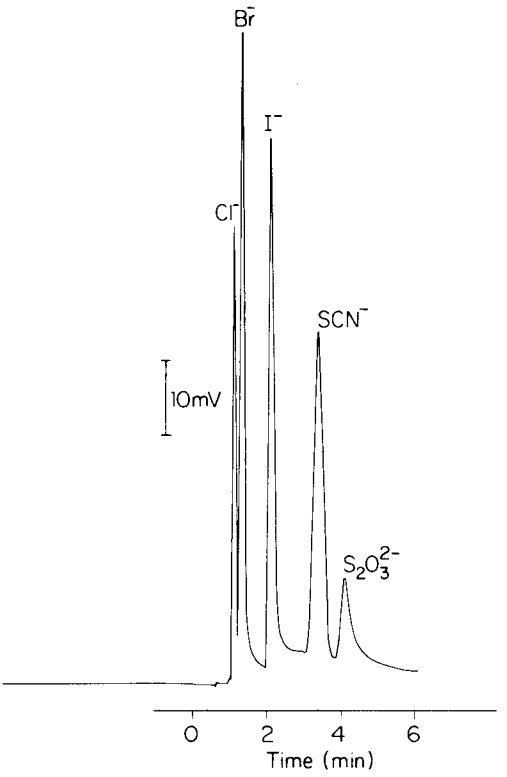

Fig. 7. Gradient elution with potentiometric detection. Eluent: 3.5—10.0 mM sodium perchlorate at 1.6 ml min^{-1}; injection volume, 20 μl; analyte concentrations, 1.0 mM.

and invaluable comments. The Ames Laboratory is operated for the U.S. Department of Energy by the Iowa State University under Contract W-7405-ENG-85. This work was supported by the Director of Energy Research Office of Basic Energy Sciences.

REFERENCES

1 M. C. Franks and D. L. Pullen, Analyst, 99 (1974) 503.
2 T. Deguchi, T. Kuna and H. Nagai, J. Chromatogr., 152 (1978) 349.
3 M. Trojanowicz and W. Matuszewski, Anal. Chim. Acta, 151 (1983) 77.
4 H. Hershcovitz, C. Yarnitzky and G. Schmuckler, J. Chromatogr., 252 (1982) 113.
5 P. W. Alexander, P. R. Haddad and M. Trojanowicz, Anal. Chem., 56 (1984) 2417; Chromatographia, 20 (1985) 179.
6 C. R. Loscombe, C. B. Cox and J. A. W. Dalziel, J. Chromatogr., 166 (1978) 403.
7 R. E. Barron and J. S. Fritz, Reactive Polymer, 1 (1983) 215.

Analytica Chimica Acta, 192 (1987) 49—61
Elsevier Science Publishers B.V., Amsterdam — Printed in The Netherlands

GAS CHROMATOGRAPHIC STATIONARY PHASE PROPERTIES OF TWO ROOM-TEMPERATURE LIQUID ORGANIC SALTS

KENNETH G. FURTON[a], SALWA K. POOLE and COLIN F. POOLE*
Department of Chemistry, Wayne State University, Detroit, Michigan 48202 (U.S.A.)
(Received 14th July 1986)

SUMMARY

The gas chromatographic properties of two room-temperature liquid organic salts, triethyl-n-hexylammonium triethyl-n-hexylboride (TEHAB) and stearylmethyldipolyoxethyl(15)ammonium chloride (Ethoquad 18/25), are described. Triethyl-n-hexylammonium triethyl-n-hexylboride could be used up to temperatures of 130° C but showed poor stability towards air and undesirable reactivity towards some dipolar and proton donor/acceptor solutes when used as a column packing material. In contrast, Ethoquad 18/25 had a maximum column operating temperature of 280° C, or 300° C after vacuum conditioning. From a calculation of McReynolds' phase constants and the molar free energy, enthalpy, and entropy of solution for polarity test probes, it was established that Ethoquad 18/25 showed intermediate selectivity for dipolar and proton-donor solutes compared to results for conventional non-ionic phases. Ethoquad 18/25 is an excellent phase for the profiling of essential oils.

Liquid organic salts represent a new class of polar solvents receiving increasing attention as selective phases for gas and liquid chromatography. This interest arises from the ability of liquid organic salts to enter into unusually strong dipole and proton donor/acceptor interactions that are much stronger than similar interactions observed with non-ionic solvents. The chromatographic properties of the liquid organic salts have been reviewed recently [1].

Elevated temperatures are usually required to liquefy most organic salts. Although this is not prohibitive in their use in gas chromatography, it inhibits the intercomparison of spectroscopic and chromatographic data used to gain an understanding of the fundamental processes governing retention. For studies in this area, organic salts which are liquid at room temperature offer substantial advantages in terms of experimental convenience. However, very few such liquid organic salts are known [2, 3]. Recent studies have used alkylammonium nitrate and thiocyanate salts which are liquid at room temperature but have restricted temperature ranges for chromatographic studies [3—6]. The best characterized group of such liquid organic salts from a spectroscopic viewpoint are the tetraalkylammonium tetraalkylborides introduced by Ford et al. [6]. An extensive collection of spectroscopic data is

[a]Present address: Department of Chemistry, University College Swansea, Swansea (Great Britain).

0003-2670/87/$03.50

available for triethyl-n-hexylammonium triethyl-n-hexylboride (TEHAB), reviewed in reference [2], although no chromatographic data are available for this salt. A further advantage of TEHAB is that it should provide an unusual opportunity to assess the importance of electrostatic interactions in establishing the chromatographic selectivity of liquid organic salts. In TEHAB, each ion consists of a charged core surrounded by aliphatic hydrocarbon groups. This structure permits electrostatic, ion-dipole, ion-induced dipole, and dispersive interactions but prevents hydrogen bonding or any Lewis acid/base interactions between solvent ions and between solutes and the liquid organic salt. Because Lewis acid/base interactions were frequently the dominant interaction observed in previous chromatographic studies of liquid organic salt/solute interactions [3, 5, 7], their absence in TEHAB should provide some insight into the relative chromatographic importance of the other available forces.

The liquid organic salts studied to date have been invariably low-molecular-weight substances with their upper column temperature limits established more frequently by their vapor pressures than by thermal decomposition [1]. A high-molecular-weight organic salt, liquid at room temperature, was sought to test the hypothesis that liquid salts of low vapor pressure might provide the largest liquid ranges available for gas chromatography. However, very few high-molecular-weight liquid organic salts have been described in the literature. One salt, stearylmethyldipolyoxethyl(15)ammonium chloride (Ethoquad 18/25 with $x + y = 15$; average molecular weight = 994) might meet the above requirements and provide some useful insight into the desired properties of new salts purposefully synthesized for gas chromatography [8].

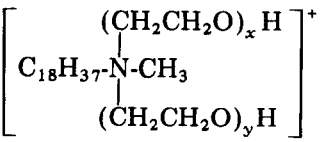

EXPERIMENTAL

Chemicals

Ethoquad 18/25 was obtained from Armak Industrial Chemicals (Chicago, IL, U.S.A.). Triethyl-n-hexylammonium triethyl-n-hexylboride was prepared as described by Ford et al. [6]. The viscous, straw-yellow liquid was further purified by treating a dichloromethane solution of the salt with decolorizing charcoal followed by preparative normal-phase high-performance liquid chromatography (h.p.l.c.). All manipulation of the reactants and salt must be done in an inert atmosphere. The colorless salt has m.p. <-78°C (it forms a glass on cooling without showing a defined melting point). The thin-film infrared spectrum of the neat salt showed characteristic absorptions at 2924, 2838, 2785, 1463, 1437, 1397, 1072, 1012, 879, 846, 793, and 726 cm^{-1}. The proton n.m.r. in acetonitrile produced multiplets at 3.0–3.4 (NCH_2), -0.18 (BCH_2) with all other CH_2 and CH_3 groups absorbing between 0.6 and 1.8 ppm. The carbon-13 n.m.r. in $CDCl_3$ gave the following characteristic signals: *N*-ethyl (C_1 = 53.41, C_2 = 7.71), *B*-ethyl (C_1 = 18.22, C_2 =

11.56), *N*-hexyl (C_1 = 57.62, C_2 = 21.88, C_3 = 26.07, C_4 = 31.16, C_5 = 22.42, C_6 = 13.85), and *B*-hexyl (C_1 = 27.88, C_2 = 28.17, C_3 = 36.21, C_4 = 32.96, C_5 = 23.22, C_6 = 14.44). Fast-atom-bombardment mass spectra of the neat salt gave prominent ions at *m/z* = 556 (<1%) $[A(AB)]^+$, *m/z* 186 (100%) $[A]^+$, *m/z* = 156 (13%) $[A—C_2H_6]^+$, *m/z* = 100 (7%) $[A—C_6H_{14}]^+$, and *m/z* = 86 (17%) $[C_6H_{10}NH_2]^+$ where A is the cation and B the anion.

Chromatography and data treatment

For h.p.l.c., a Varian 5000 liquid chromatograph and a Micro-Pak Si-10 (30 cm × 4 mm i.d.) column (Varian) were used. Separations were done isocratically using dichloromethane and u.v. detection at 230 nm. For preparative applications, the same conditions were used with a 25 cm × 9.4 mm i.d. semipreparative column and a flow rate of 4.0 ml min^{-1}.

Column packings containing from 3 to 20% (w/w) of organic salt on Chromosorb W-AW (100—120 mesh) were prepared by using the rotary evaporator technique and dichloromethane as the slurry solvent. After being coated, the damp packing was dried in a fluidized-bed drier and then packed into glass columns 1—3.0 m long (2.0 mm i.d.) with the aid of vacuum suction and gentle vibration. As far as is practical, the column packing material containing TEHAB should be handled only in a nitrogen atmosphere. For column evaluation, a Varian 3700 gas chromatograph with heated, on-column injectors, a temperature-programable column oven, and a flame-ionization detector was used. Separation conditions are given in the legends to tables and figures.

McReynolds' phase constants were calculated in the usual way, using 3 m (2 mm i.d.) columns packed with 10% (w/w) of organic salt at 120°C with a carrier-gas flow rate of 20 ml min^{-1} of nitrogen [9]. The phase constants are approximate for TEHAB and are corrected for interfacial adsorption in the case of Ethoquad 18/25. The reference retention-index values on squalane were taken from McReynolds [10]. The net retention volume (V_n) per gram of column packing corrected to 20°C was calculated for the phase-loading studies according to the equation suggested by Martin [11]:

$$V_n/g = (t_R - t_M)\, F_0\, (T_c/T_a)\, [1 - (P_W/P_a)]\; 3/2\; [(P^2 - 1)/(P^3 - 1)]$$
$$(293/T_c)\, (1/W) \qquad (1)$$

where t_R is the solute retention time, t_M the column dead time (assumed equal to the retention time of methane at T_c), F_0 the carrier gas flow rate at the column outlet measured with a soap-film meter, T_c the column operating temperature (K), T_a the ambient temperature (K), P_W the vapor pressure of water at T_a, P_a the ambient pressure, P the column pressure drop (P_i/P_a), P_i the column inlet pressure, and W the weight of column packing.

RESULTS AND DISCUSSION

Triethyl-n-hexylammonium triethyl-n-hexylboride

The preparation of TEHAB requires more than average attention to detail. If colorless batches of salt are to be obtained, then all solutions must be

stripped of oxygen, the reaction conducted under an inert atmosphere, and starting materials of the highest purity used. Preparative h.p.l.c. was required for final purification. However, brief exposure to the atmosphere converts the colorless batches of the salt to a straw-yellow color. This problem was investigated in some detail.

The colorless salt and the straw-yellow product have identical infrared, n.m.r., and mass spectra; their only distinguishing features are their visible absorption spectra and the presence of impurity peaks revealed by liquid chromatography (Fig. 1). Continuous exposure to the atmosphere produces a dramatic change in the infrared spectra (Fig. 2). Most noticeable for relatively short exposure times is the appearance of strong absorption bands at 1569 and 1397 cm^{-1} with some weaker bands appearing in the fingerprint region. Upon further exposure to the atmosphere, a strong band appears at 2406 cm^{-1} in the region associated with B—H stretching vibrations. The broad band appearing above 3000 cm^{-1} may be due to the uptake of water by the salt. Heating the salt above 180°C caused a rapid disappearance of the band at 2406 cm^{-1}, suggesting that it is associated with a more volatile decomposition product.

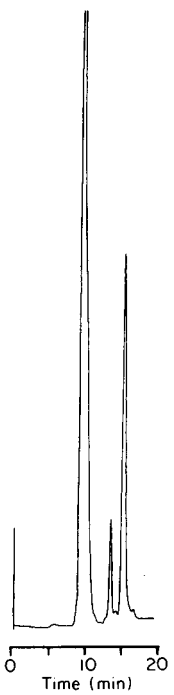

Fig. 1. Separation of impurities from TEHAB by normal-phase h.p.l.c. with dichloromethane as the mobile phase.

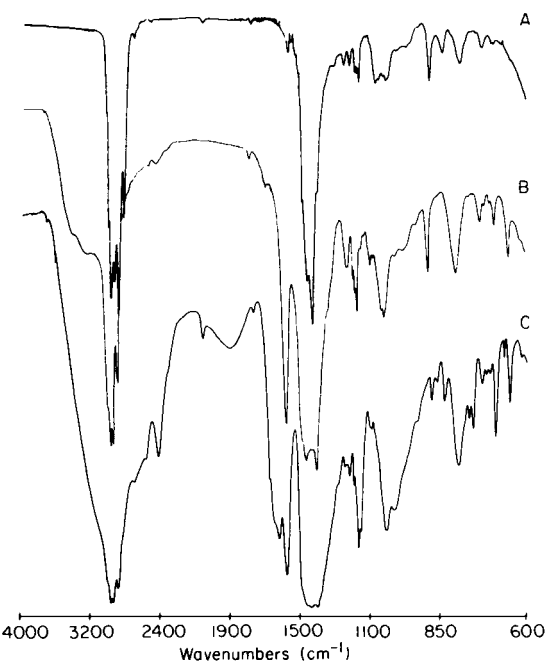

Fig. 2. Changes in the infrared spectra of TEHAB induced by exposure to the atmosphere for various periods of time: (A) initial spectrum; (B) after 1 week; (C) after several weeks.

Brief exposure to the atmosphere during routine laboratory manipulations results in the formation of a slightly discolored product which seems to be more resistant to oxidation than the pure salt. Changes in the infrared spectra may not be discernible at this stage. The straw-yellow product, when exposed continuously to the atmosphere, slowly darkens in color, eventually becoming orange. This is accompanied by a reduction in the viscosity of the salt and the appearance of new bands in the infrared spectra.

In the initial report, Ford et al. [6] claimed that the tetraalkylammonium tetraalkylborides were reasonably stable to heat, light, oxygen, and water. In a later paper, Ford and Hart [12] stated that TEHAB is not stable in air indefinitely and the material used in most experiments was pale yellow because of a trace of an unknown decomposition product. From studies of reaction kinetics of methyl iodide in various solvents, including TEHAB, Ford et al. [13] concluded that the fast initial disappearance of methyl iodide was due to reaction with an impurity in TEHAB, the initial concentration of which was in the 0.01—0.03 M range. From these results and our own studies, it is concluded that TEHAB is very susceptible to atmospheric oxidation, even for batches of salt of very high initial purity. The oxidation mechanism was not evaluated further, but may proceed by more than one step, involving the rapid and initial formation of trace concentrations of a colored product which is either more slowly converted, or inhibits the conversion of TEHAB to the major by-products recognized in the infrared spectra.

To make an initial evaluation of the gas chromatographic properties of TEHAB, sufficient pure material could be obtained by preparative h.p.l.c. Column packings were prepared in an inert atmosphere. Under these conditions, no discoloration of the salt was observed either during the preparation or use of the column. Ford et al. [6] noted that TEHAB could be heated in a sealed tube for 1 h at 200°C without change in color or infrared and nuclear magnetic resonance spectra. For columns prepared with TEHAB, it was found here that the maximum allowable column temperature was 130°C, this limit being established by the vapor pressure of the salt and not by decomposition. The TEHAB columns showed acceptable chromatographic efficiency (1800—2300 effective plates per meter) with slightly lower values being observed for hydrocarbons. The general chromatographic properties of TEHAB can be judged from the separations shown in Fig. 3.

The chromatographic properties of a series of test solutes together with their boiling points and dipole moments are summarized in Table 1. The elution order of the test solutes can be established by first ranking the solutes by boiling point and then taking account of differences in dipole moments. For the substituted benzenes, the influence of the dipole moment (μ_D) seems to be quite small. For example, iodobenzene (b.p. = 189°C, μ_D = 1.36—1.43) is retained longer than *o*-dichlorobenzene (b.p. = 179°C, μ_D = 2.2) and chlorobenzene (b.p. = 132°C, μ_D = 1.55) and ethylbenzene (b.p. = 136°C, μ_D = 0.37) have similar retention properties. The influence of dipole-dipole and dipole-induced dipole interactions is more clearly demonstrated

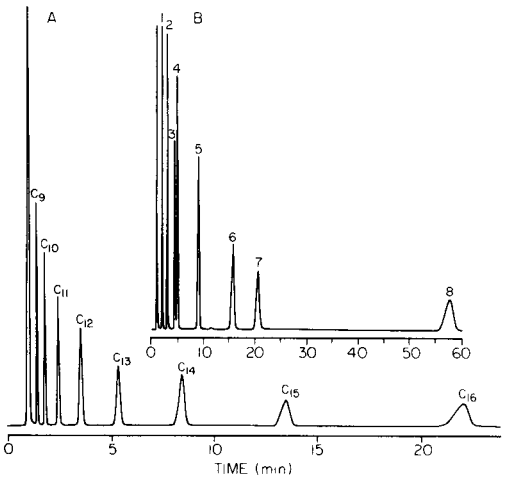

Fig. 3. Separation of C_9 to C_{15} n-alkanes (A) and a mixture of substituted benzenes (B) on a 3 m (2 mm i.d.) column of 10% (w/w) TEHAB on Chromosorb W-AW (100—120 mesh). The flow rate was 15 ml min^{-1} and the column temperature 120°C for (A) and 100°C for (B). Peak identification for (B): (1) benzene; (2) toluene; (3) ethylbenzene, (4) chlorobenzene; (5) bromobenzene; (6) *o*-dichlorobenzene; (7) iodobenzene; (8) acetophenone.

TABLE 1

Chromatographic and physical properties of test solutes[a]

Test solute	Specific retention volume (cm^3)	McReynolds' constant	Boiling point (°C)	Dipole moment[b]
Benzene	21.3	346	80.1	0.03—0.11
2-Pentanone	43.3	503	102	2.82
Pyridine	73.1	528	115.5	2.37
2-Methyl-2-pentanol	43.6	442	121.5	
2-Octyne	22.5	168	138	
Dioxane	36.0	442	101	0.45
cis-Hydrindane	45.3	133	159[c]	
Toluene	35.8		110.6	0.33
Ethylbenzene	57.3		136	0.37
p-Xylene	57.6		138	0.10
Chlorobenzene	62.6		132	1.55
Bromobenzene	124.7		155.5	1.55
o-Dichlorobenzene	211.8		179	2.2
Iodobenzene	276.8		189	1.36—1.43
Acetophenone	712.1		202	3.10

[a]Stationary phase, TEHAB; column temperature, 120°C. [b]Data from [14]. [c]This is the boiling point for the *trans* isomer.

by the McReynolds' test probes. For example, dioxane (b.p. = 101°C, μ_D = 0.45) is easily separated from 2-pentanone (b.p. = 102°C, μ_D = 2.82). The largest values for the McReynolds' constants are associated with the test probes having the largest dipole moments. Lewis acid/base interactions are not possible with TEHAB so that proton donor/acceptor interactions should not be an important consideration in the retention of such probes as 2-methyl-2-pentanol and pyridine. The difference in the retention characteristics between the McReynolds' test probes and the substituted benzene derivatives may be due to specific interactions between TEHAB and the benzene ring. Ford and Hart [15] noted large aromatic solvent-induced shifts in the n.m.r. spectra of TEHAB, which they interpreted in terms of specific complex formation involving the preferential alignment of the π-electrons of the aromatic molecule with the cation. Similar effects were not observed with non-aromatic solvents.

During the course of the present evaluation of the stationary phase properties of TEHAB, certain consistent problems were observed. The test solutes n-butanol, nitropropane, iodobutane, nitrobenzene, benzyl alcohol, and aniline had poor peak shape and were not eluted quantitatively from the column. The nature of these interactions (whether totally with the phase or with unshielded active sites on the support) is unclear, but from the practical standpoint, these interactions limit the usefulness of TEHAB for the separation of polar solutes. For similar reasons, no further studies of the retention of polar solutes for a comparison with spectroscopic data were undertaken; the reliability of the chromatographic data would be in question and any correlations developed would be of a spurious nature. On account of the wealth of spectroscopic data available for TEHAB and its unique physical and structural characteristics, this conclusion is unfortunate. There are no alternative salts known that might be substituted for TEHAB at the moment.

Ethoquad 18/25

Ethoquad 18/25 is used commercially as a surface-active agent and as a cationic wetting, foaming and emulsifying agent [8]. DeStefano and Keough [16] recommended Ethoquad 18/25 as a calibration compound for high-mass fast-atom-bombardment (FAB) mass spectrometry. This latter study also provided useful information about the molecular weight distribution of the commercial product which has an average molecular weight of 994. The most intense ion in the FAB mass spectra corresponds to a molecular weight of m/z = 768 ($x + y = 11$) with a bell-shaped curve extending to m/z = 1209 ($x + y = 21$). This is in keeping with its chromatographic properties. Columns prepared from Ethoquad 18/25 can be safely used up to temperatures of 280°C and, after vacuum conditioning, up to 300°C. In both cases, the column temperature limit is established by the vapor pressure of the salt and not by thermal decomposition. The efficiency of the Ethoquad 18/25 columns met general expectations providing 1000—2000 effective theoretical plates per meter depending on the phase loading and test probe used for the

measurement. These values are not significantly different to those measured for columns prepared with conventional non-ionic phases and the same batch of support. Thus, Ethoquad 18/25 provides column packings of reasonable efficiency and the widest liquid operating temperature range of all organic salts studied to date [1].

TABLE 2

McReynolds' constants for Ethoquad 18/25

Probe	Symbol	Gas/liquid partition coefficient	Retention index	Corrected retention index	Phase constant	Corrected phase constant
Benzene	X'	34.4	834	850	181	196
Butanol	Y'	92.9	1002	1018	412	428
2-Pentanone	Z'	38.0	860	866	233	239
Nitropropane	U'	104.5	1027	1038	375	385
Pyridine	S'	107.0	1034	1042	335	343
2-Methyl-2-pentanol	H'	78.7	978	990	288	300
2-Octyne	K'	69.0	961	968	120	127
Dioxane	L'	55.3	921	930	267	276
cis-Hydrindane	M'	140.1	1081	1088	75	93
Octane		25.6				
Nonane		46.3				
Decane		84.0				
Undecane		150.3				

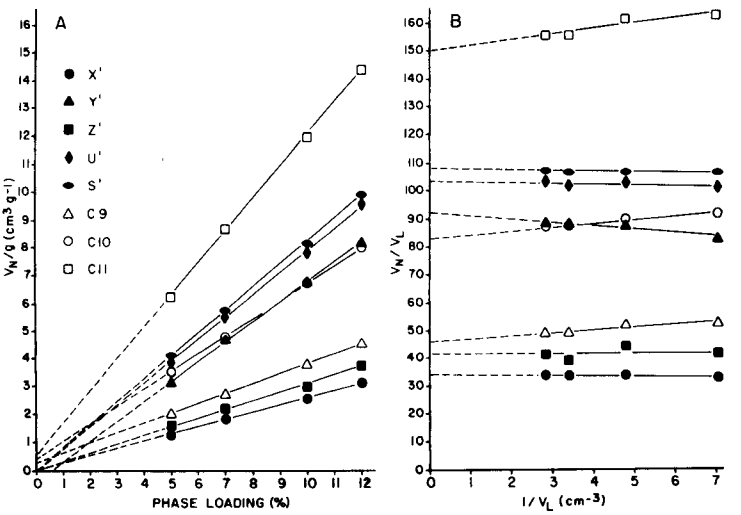

Fig. 4. Plots of V_N/g of column packing as a function of the percent phase loading (A) and V_N/V_L vs. $1/V_L$ (B) for McReynolds' probes on Ethoquad 18/25. V_N, net retention volume; V_L, volume of liquid phase.

The selectivity of Ethoquad 18/25 was determined by measuring McReynolds' constants (Table 2). Where necessary, the phase constants were corrected for contributions to retention resulting from gas-liquid phase adsorption. As shown in Fig. 4, all probes were retained largely by gas-liquid phase partitioning on Ethoquad 18/25; gas-liquid phase adsorption was most significant for the hydrocarbon retention-index markers and the proton-donor probes. The corrected retention-index values were obtained from the gas/liquid phase partition coefficients determined from plots of V_N/V_L vs. $1/V_L$ (V_N is the net retention volume and V_L the volume of liquid phase) as shown in Fig. 4, using the measured value for the phase density, $\rho = 0.9893$, at 120°C. Based on these values, Ethoquad is best characterized as a medium polar phase, considerably less polar than other liquid organic salts [1]. On a mass basis, this is presumably due to a reduction in the number of ionic groups contributing to retention caused by the large alkyl groups attached to the cation compared to the low-molecular-weight salts previously studied.

Thermodynamic approaches to the measurement of selectivity are based on the determination of the partial free energy of solution of either functional groups or specific test solutes [17]. Golovnya and co-workers [17, 18] calculated partial free energies of solution for the first five McReynolds' probes on a large number of stationary phases. As the densities of many common stationary phases remain unknown, they chose the expression on the left-hand side of the following equation for comparative purposes:

$$-(\Delta G + RT_c \ln \rho) = RT_c \ln (V_g T_c/273) \qquad (2)$$

where ΔG is the partial molar free energy of solution, R the gas constant, T_c the column temperature, ρ the stationary phase density at T_c, and V_g the specific retention volume.

By ignoring differences in stationary phase densities, an error of ±10% can be expected in their data [17]. Equation 2 was used to calculate values for $-[\Delta G + RT_c \ln \rho]$ for appropriate probes; results are summarized in Table 3. If these values are compared with the literature values, it is noted that Ethoquad 18/25 has general selectivity somewhere between those for the polyester and poly(ethylene glycol) stationary phases.

Substituting $\Delta G^m = \Delta H^m - T\Delta S^m$ into Eqn. 2, after utilizing the molal coefficient of Henry's Law to eliminate any adverse theoretical inconsistencies caused by a lack of a precise knowledge of the molecular weight of Ethoquad 18/25, yields [19, 20]:

$$\ln V_g = (\Delta H^m/R)\,(1/T) + (\Delta S^m/R) - \ln (1000/273\,R) \qquad (3)$$

where ΔH^m is the partial molal enthalpy of solution, ΔS^m the partial molal entropy of solution, and ΔG^m the partial molal free energy of solution. Thus, from a plot of $\ln V_g$ vs. $1/T$, the partial molal enthalpy of solution is obtained from the slope, and the partial molal entropy from the intercept. The partial molal free energy of solution can then be obtained from a knowledge of ΔH^m and ΔS^m. Values of ΔH^m, ΔS^m, and ΔG^m for a series of

TABLE 3

Partial molar and molal free energy of solution for McReynolds' probes on Ethoquad 18/25

Probe	Specific retention volume (cm^3)	Corrected specific retention volume (cm^3)	$-(\Delta G + RT_c \ln p)$ (cal mol^{-1})	$-\Delta G^m$ (cal mol^{-1})
Benzene	23.4	24.2	2773	2965
Butanol	61.8	65.3	3549	3742
2-Pentanone	27.1	26.7	2850	3043
Nitropropane	71.5	73.4	3641	3833
Pyridine	74.5	75.2	3659	3852
2-Methyl-2-pentanol	53.9	55.3	3419	3611
2-Octyne	48.7	48.5	3317	3509
Dioxane	38.6	38.9	3144	3336
cis-Hydrindane	97.9	98.4	3870	4062
n-Octane		18.0		2735
n-Nonane		32.5		3197
n-Decane		59.0		3663
n-Undecane		105.6		4117

TABLE 4

Thermodynamic constants for Ethoquad 18/25 obtained from a plot of ln V_g vs. $1/T$ at 120°C

Probe	Slope (cm^3 K)	Intercept (cm^3)	ΔH^m (cal mol^{-1})	ΔS^m (cal mol^{-1} K^{-1})	ΔG^m (cal mol^{-1})
Pyridine	4453 ± 105	−7.10 ± 0.26	−8849	−13.40	−3581
Bromobenzene	4951 ± 31	−7.44 ± 0.08	−9838	−14.08	−4304
Benzaldehyde	5383 ± 25	−7.87 ± 0.06	−10695	−14.93	−4824
Octanol	6799 ± 43	−10.79 ± 0.11	−13510	−20.75	−5353
Benzonitrile	5533 ± 50	−7.92 ± 0.13	−10995	−15.03	−5086
Acetophenone	5970 ± 83	−8.74 ± 0.21	−11862	−16.67	−5307
Benzodioxane	4931 ± 846	−5.61 ± 2.1	−9799	−10.44	−5695
Nitrobenzene	5983 ± 24	−8.45 ± 0.06	−11889	−16.09	−5562
Naphthalene	5973 ± 25	−8.28 ± 0.06	−11868	−15.75	−5676
2,6-Dimethylaniline	6738 ± 83	−9.78 ± 0.21	−13388	−18.72	−6027

selectivity test probes are given in Table 4 as well as some additional ΔG^m values for the McReynolds' test probes in Table 3. In its simplest form, it can be stated that the enthalpy term describes the nature of the intermolecular forces between solute and solvent molecules in the liquid organic salt, whereas the entropy term indicates the manoeuverability of a solute molecule in the liquid organic salt. Compared to literature values, the sign and magnitude of ΔS^m are similar to conventional non-ionic phases indicating similar freedom of motion for the solutes in Ethoquad 18/25 as observed for conventional phases. The partial molal free energies of solution are in

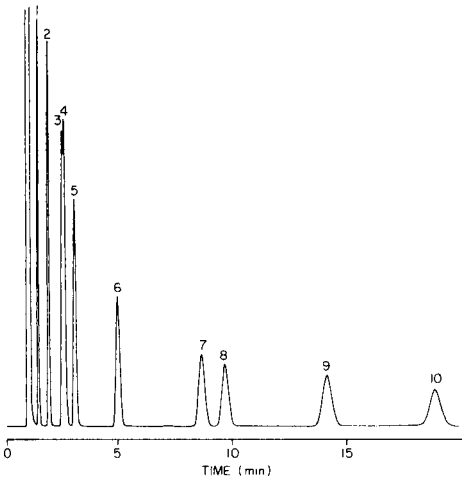

Fig. 5. Separation of a mixture of substituted benzenes on a 3 m (2 mm i.d.) column of 10% (w/w) Ethoquad 18/25 on Chromosorb W-AW (100—120 mesh) at 140°C with a nitrogen carrier flow rate of 15 ml min^{-1}. Peak identification: (1) benzene; (2) toluene; (3) ethylbenzene; (4) *p*-xylene; (5) chlorobenzene; (6) bromobenzene; (7) *o*-dichlorobenzene; (8) iodobenzene; (9) acetophenone; (10) nitrobenzene.

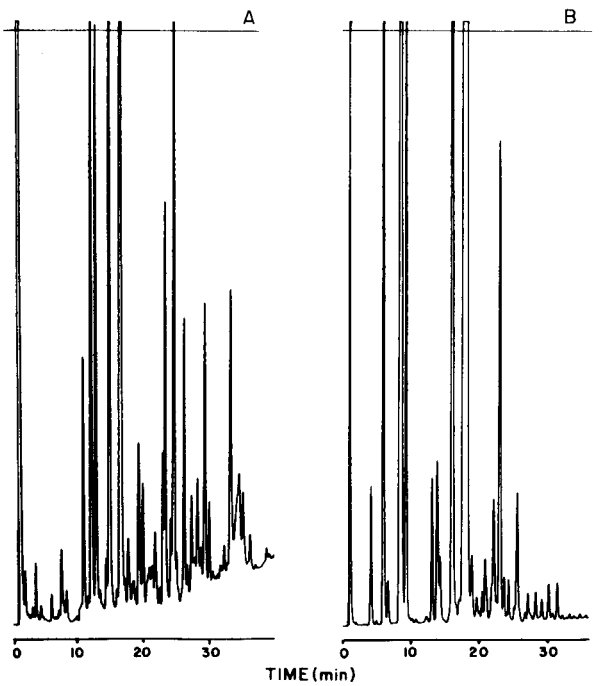

Fig. 6. Separation of oil of lavender (A) and bergamot (B) on the same column as described in Fig. 5. The column was held at 80°C for 4 min and then temperature-programmed at 4°C min^{-1} to 220°C.

keeping with the status of Ethoquad 18/25 as a phase of intermediate selectivity for the retention of dipolar and proton donor solutes.

The chromatographic properties of Ethoquad 18/25 are illustrated with a few selected examples of its general use. Figure 5 shows the separation of a mixture of substituted benzene derivatives on Ethoquad 18/25. Good peak shapes were obtained for the polar probes and the order of separation was in keeping with the previous theoretical discussion. Compared with the same mixture separated on TEHAB, nitrobenzene is now eluted quantitatively with good peak shape. Ethoquad 18/25 provides good separations of essential oil extracts as illustrated in Fig. 6 for lavender and bergamot and in Fig. 7 for lemon, rosemary and thyme. The essential oil extracts are rich in unsaturates, terpenes, and oxygenates of low to intermediate polarity that are well resolved on this phase.

In summary, the usefulness of TEHAB as a stationary phase is limited by its moderate vapor pressure, poor stability towards air, and by irreversible adsorption or reaction with dipolar and proton donor/acceptor solutes. Its poor chromatographic characteristics prevent any useful parallels being developed by using available spectroscopic data for evaluating intermolecular forces. In contrast, Ethoquad 18/25 is a very useful stationary phase of intermediate selectivity. Its low vapor pressure permits high temperature operation and Ethoquad 18/25 has the widest liquid temperature range of all

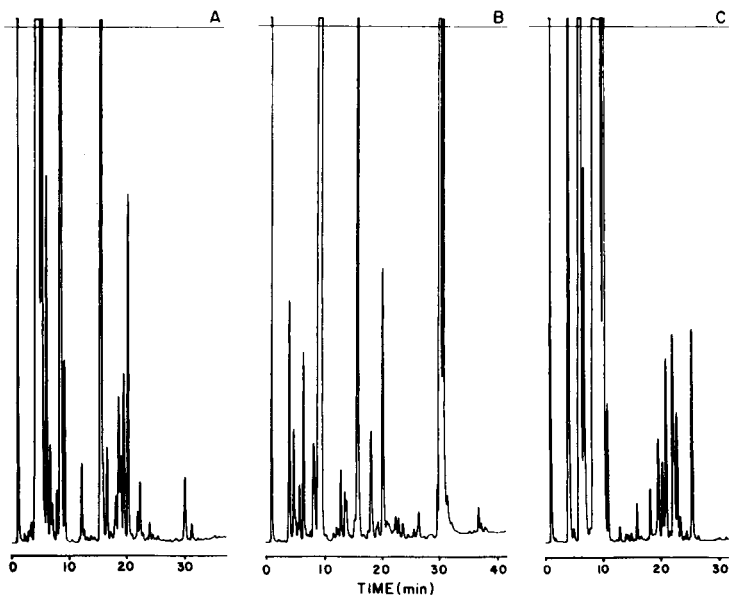

Fig. 7. Separation of oil of rosemary (A), thyme (B) and lemon (C) on the same column as described in Fig. 5. Column conditions: rosemary oil, 80° C for 4 min then programmed at 4°C min^{-1} to 200°C; thyme oil, 80°C for 4 min then programmed at 4°C min^{-1} to 210°C; lemon oil, 80°C for 3 min then programmed at 3°C min^{-1} to 185°C.

liquid organic salts studied to date. As a model for future synthesis of stationary phases, two points are noted. First, it should be feasible to synthesize asymmetrical alkylammonium cations of intermediate molecular weight with reasonable chromatographic properties that could also be used for spectroscopic studies of intermolecular interactions. For this purpose, salts of a defined structure and molecular weight that are liquids of moderate viscosity at room temperature are needed. Analogs of Ethoquad 18/25 seem to be the most promising approach at the moment. Second, to increase the polarity of liquid organic salts of high molecular weight, the use of cations with multiple ionic centers should be studied. This should establish the best compromise between the need to minimize vapor pressure while maintaining a high concentration of ionic groups to control selectivity.

REFERENCES

1 C. F. Poole, K. G. Furton and B. R. Kersten, J. Chromatogr. Sci., 24 (1986) 400.
2 C. L. Hussey, Adv. Molten Salt Chem., 5 (1983) 185.
3 C. F. Poole, B. R. Kersten, S. S. J. Ho, M. E. Coddens and K. G. Furton, J. Chromatogr., 352 (1986) 407.
4 F. Pacholec, H. T. Butler and C. F. Poole, Anal. Chem., 54 (1982) 1938.
5 M. E. Coddens, K. G. Furton and C. F. Poole, J. Chromatogr., 356 (1986) 59.
6 W. T. Ford, R. J. Hauri and D. J. Hart, J. Org. Chem., 38 (1973) 3916.
7 K. G. Furton and C. F. Poole, J. Chromatogr., 349 (1985) 235.
8 Physical and Chemical Characteristics of Armak Quaternary Ammonium Salts, Product Bulletin 81-6, Armak Industrial Chemicals, Chicago, IL, 1981.
9 C. F. Poole and S. A. Schuette, Contemporary Practice of Chromatography, Elsevier, Amsterdam, 1984, p. 42.
10 W. O. McReynolds, J. Chromatogr. Sci., 8 (1970) 685.
11 R. L. Martin, Anal. Chem., 33 (1961) 347.
12 W. T. Ford and D. J. Hart, J. Phys. Chem., 80 (1976) 1002.
13 W. T. Ford, R. J. Hauri and S. G. Smith, J. Am. Chem. Soc., 96 (1974) 4316.
14 A. L. McCellan, Tables of Experimental Dipole Moments, Vol. 2, Rahara Enterprises, El Cerrito, CA, 1974.
15 W. T. Ford and D. J. Hart, J. Am. Chem. Soc., 96 (1974) 3261.
16 A. J. DeStefano and T. Keough, Anal. Chem., 56 (1984) 1846.
17 R. V. Golovnya and T. A. Misharina, J. High Resolut. Chromatogr.-Chromatogr. Commun., 3 (1980) 51.
18 R. V. Golovnya and Y. N. Arsenyev, Chromatographia, 4 (1971) 250.
19 C. E. Figgins, B. L. Reinhold and T. H. Risby, J. Chromatogr. Sci., 15 (1977) 208.
20 D. F. Fritz and E. Sz. Kovats, Anal. Chem., 45 (1973) 1175.

Analytica Chimica Acta, 192 (1987) 63—75
Elsevier Science Publishers B.V., Amsterdam — Printed in The Netherlands

NEW PROBABILISTIC VERSIONS OF THE SIMCA AND CLASSY CLASSIFICATION METHODS
Part 1. Theoretical description

HILKO VAN DER VOET*,[a] and PIERRE M. J. COENEGRACHT

Chemometrics Research Group, Pharmaceutical Laboratories, A. Deusinglaan 2, NL-9713 AW Groningen (The Netherlands)

JAN B. HEMEL

Central Laboratory for Clinical Chemistry, University Hospital, P.O. Box 30001, NL-9700 RB Groningen (The Netherlands)

(Received 27th March 1986)

SUMMARY

The probabilistic SIMCA and CLASSY methods for multivariate classification are defined and explained in detail. The differences between the present algorithms and previous versions are described. Both probabilistic SIMCA and CLASSY methods construct principal-component class models and assume a normal distribution for the residuals. The methods differ in the distributional assumptions for the object scores within the class model space. Details are given for the construction of probability density functions which conform to the model assumptions, and which can be substituted in Bayes' theorem to obtain posterior classification probabilities.

An important aim in chemical pattern recognition is often the classification of unknown individuals into one of a number of previously defined classes. Apart from the classical statistical approach (SLDA, statistical linear discriminant analysis) many other classification methods have been designed, often with the purpose of avoiding the modelling assumptions which have to be made in SLDA [1]. In previous papers [2, 3], two of these classification methods, SIMCA and ALLOC, were discussed together with a proposed new hybrid method, CLASSY, which tries to combine the advantages of SIMCA and ALLOC. A probabilistic version of SIMCA was developed and evaluated. In the present series, a new probabilistic version of SIMCA (and the SIMCA part of CLASSY) is presented. This paper describes why the new algorithm is theoretically better than the previous one. Practical evaluation is given in Part 2 [4]. The original (non-probabilistic) SIMCA method has been described extensively [5—9]. Here only the information necessary for understanding the probabilistic versions is given.

[a]Present address: Agricultural Statistics Department, TNO Institute of Applied Computer Science (iTi-TNO), P.O. Box 100, NL-6700 AC Wageningen (The Netherlands).

0003-2670/87/$03.50

FORMULATION OF THE PROBLEM, BASIC NOTATION AND DATA SCALING

The general classification problem can be described as follows. There is a population of objects (cases, individuals), which is called the target population. The objects in the target population belong to classes. It is assumed here that each object belongs to exactly one class although it is possible to construct SIMCA models in which objects belong to several classes or to no class at all. It is assumed that a representative sample consisting of n objects with known class is drawn from the target population and that on each object the same p measurements are made. The results can then be arranged in an $n \times p$ data matrix $\mathbf{X}$. The number of objects sampled from class c is denoted by n_c; $\mathbf{X}_{ij}$ represents the measurement of variable j on object i, $\mathbf{X}_i$ represents the complete data vector of object i, and $\mathbf{X}_j$ represents all measurements on variable j. The sample for which the data are collected in $\mathbf{X}$, is called the training set or construction set because each classification method, be it SIMCA, SLDA or any other, constructs a classification rule based on these data. The purpose of any classification method, then, is to use these data for classifying other objects, the class of which is not known. These objects constitute the prediction set or test set. It is helpful to think of the data set as a collection of points (the objects) in a p-variate coordinate system (where each axis represents a variable). Principal component analysis (PCA), the mathematical technique which plays a key role in SIMCA, is best understood as an orthogonal rotation of the axes in the coordinate system.

Probabilistic classification is always based on the application of Bayes' formula which, in its simplest form, can be written as

$$P(c|\mathbf{X}_i) = P(\mathbf{X}_i|c) / \sum_{c=1}^{K} P(\mathbf{X}_i|c) \qquad (1)$$

where $P(\mathbf{X}_i|c)$ is the probability of finding an outcome $\mathbf{X}_i$ (which may be a vector) for an object i belonging to class c, and $P(c|\mathbf{X}_i)$ is the posterior probability that an object i with unknown class, but with data vector $\mathbf{X}_i$, belongs to class c; K is the total number of classes. For continuous variables, $P(\mathbf{X}_i|c)$ is zero, and is therefore replaced by a limit, the probability density ${}^{c}f_i(\mathbf{X})$. The problem of probabilistic classification is thus simplified and reduced to deciding on how the probability densities for the diverse classes can be estimated. To do this, it is necessary to formulate a model for the distribution of data vectors $\mathbf{X}_i$ from each class under consideration. The way in which this modelling is done is the basic difference between various probabilistic classification methods.

Data scaling

SIMCA uses PCA for the construction of class models. Principal components can only be usefully computed if the original variables are comparable, i.e., if the distances along the different axes have similar interpreta-

tions. It may be recalled that PCA selects the direction in the data space in which the object points are maximally separated.

It is therefore necessary to consider possible data scaling when SIMCA is used. The type of data determines which kind of scaling is appropriate. Roughly, there are three possibilities. First, when all variables are measured in the same units, and the order of magnitude of the measurement values is equal, scaling is not indicated. Secondly, when the variables are measured in different units and there is no information about the analytical precision of the measurements, it is customary to give all variables equal initial importance by autoscaling (subtraction of the mean and division by the sample standard deviation). It has been shown [10], that autoscaling is best done for each class separately (class autoscaling or class scaling). Thirdly, if the precision (reproducibility) of the variables (including any possible intra-individual variation) is known, there is a better procedure than autoscaling or class scaling: the measurement values are scaled so that all reproducibilities become equal; this is called reproducibility scaling.

In general, the scaling has the form

$$X^*_{ij} = (X_{ij} - ORIG_{cj})/SF_{cj} \tag{2}$$

where X_{ij} is the unscaled and X^*_{ij} the scaled value, $ORIG_{cj}$ the specified origin and SF_{cj} the scaling factor. Both $ORIG_{cj}$ and SF_{cj} may depend on the class c to which object i belongs, e.g., for class (auto) scaling:

$$ORIG_{cj} = (1/n_c) \sum_{i=1}^{n_c} X_{ij} \tag{3}$$

$$SF_{cj} = \{[1/(n_c - 1)] \sum_{i=1}^{n_c} (X_{ij} - ORIG_{cj})^2\}^{1/2} \tag{4}$$

The PC models which are calculated in SIMCA are centred on the class centroids. This means that $ORIG_{cj}$ is always computed by Eqn. 3. The choice of SF_{cj}, however, depends on the type of data, as discussed above.

NON-PROBABILISTIC SIMCA

The PC class models

In much of the following discussion only one class is needed. Therefore, class index c is dropped in the notation, e.g., n denotes the number of training objects from class c and A denotes the dimensionality of the class model.

The SIMCA classification method constructs a model for each class in the training set by applying PCA to the $n \times p$ matrix of the scaled data $\mathbf{X}^*$. PCA is best understood as a rotation of axes in the p-dimensional space such that the projections of the object points on the first PC axis (eigenvector) are maximally separated. Each successive PC axis is then chosen according to

the same criterion with the restriction that the axes should be orthogonal. In this way, p new orthogonal axes are obtained. The coordinates of the object points in this system are the component scores, denoted by t_{ik} for the score of object i on principal component axis k.

The variances of the scores on each eigenvector

$$s_k^2 = (1/n) \sum_{i=1}^{n} t_{ik}^2 \tag{5}$$

are important. If the eigenvectors are scaled to unit length (which is standard in PCA), the component variances s_k^2 are equal to the eigenvalues λ_k, which are computed in the PCA.

Basically, the class PC models are not intended to represent the data in another coordinate system but to approximate them in a coordinate system of lower dimensionality. This is achieved by selecting only some of the p PC axes. The number A of selected axes is then the dimensionality of the class model. There are several ways to select a value for $A (0 \leqslant A \leqslant p)$ such that the first A principal components of the class model provide a good approximation of the structural variation within the class. The original SIMCA method uses a cross-validation method for this purpose [11, 12], but other methods exist [13, 14]. Here it is simply assumed that a proper value of A for each class model is found.

The p-dimensional data space is thus divided (differently for each class) into two subspaces: an A-dimensional inside-model space (IMS) and a $(p - A)$-dimensional outside-model space (OMS). These spaces are orthogonal to each other because they are built from the first A and the remaining $p - A$ principal components, respectively.

The PC class model formed by SIMCA is contained in the IMS but it is restricted here also. The SIMCA class model is a rectangular hypervolume, called a hyperbox, formed by defining normal ranges in each of the A directions. The normal range in direction k is the interval $[t_k^-, t_k^+]$ with

$$t_k^- = \min_i(t_{ik}) - 0.5\, s_k \text{ and } t_k^+ = \max_i(t_{ik}) + 0.5\, s_k$$

Although a factor of 1.0 has been applied [5, 6], use of the factor 0.5, found in the SIMCA-3B programs [15], is continued here. The length of the hyperbox in direction k is then given by $l_k = t_k^+ - t_k^-$. The hyperbox thus encloses all training objects from the modelled class.

Distances in the outside-model space

Description of the position of an object in the OMS with respect to a class PC model is first discussed. The OMS formulae apply to both SIMCA and CLASSY and the discussion is thus simplified. In subsequent sections, the OMS formulae are extended to account for the IMS structure. The equations derived in this section are valid when the class hyperbox coincides with the IMS, i.e., when the length of the hyperbox in each dimension is infinite.

Therefore, this "OMS-only" model can also be called the "infinite hyperbox" model.

The distance from a point i in p space to a class model is found by projecting i orthogonally onto the IMS. The distance between i and the projection $\hat{i}$ will be denoted by d_i, which can be calculated either with the help of the PC coordinate system as $d_i = \left(\sum_{k=A=1}^{p} t_{ik}^2 \right)^{1/2}$ or with the help of the original coordinate system as $d_i = \left(\sum_{j=1}^{p} e_{ij}^2 \right)^{1/2}$. Here, $e_{ij} = X_{ij}^* - X_{\hat{i}j}^*$ and $X_{\hat{i}j}^*$ and X_{ij}^* are the coordinates of point $\hat{i}$ and point i on the original scaled variable j. Figure 1 illustrates this equivalence for a simple case ($p = 2, A = 1$).

Distances from point i to different class models can thus be calculated. It is unfair, however, to base a classification of i on a comparison of distances, when the class model dimensionalities A are not equal. For example, if there are a line and a plane in 3-dimensional space, then a randomly chosen point in this space will more often lie closer to the plane than to the line. This effect would give the classification procedure a positive bias for higher-dimensional models. To avoid this, one has to take account of the dimensionality of the OMS. The distance has to be calculated per dimension. In accordance with statistical theory, this is done by dividing d_i^2 (which is a sum of squares) by the number of OMS dimensions, $p - A$ (which can be interpreted as the number of degrees of freedom for the location of object i in the OMS): $s_i = [d_i^2/(p - A)]^{1/2}$. The resulting distance-per-dimension measure can then be seen as a standard deviation, which justifies the notation s_i. It is also sometimes called the object residual standard deviation (object RSD) in the SIMCA literature [6—9].

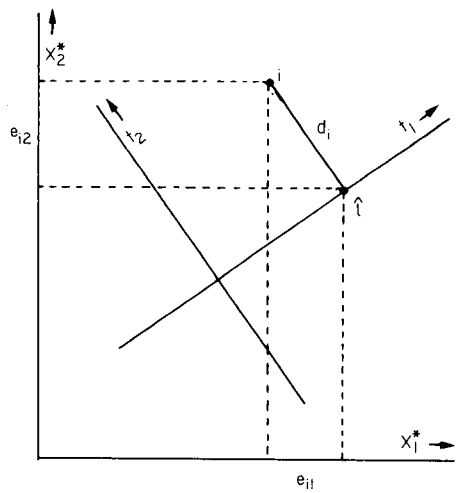

Fig. 1. An object i in a two-dimensional space and its projection $\hat{i}$ onto a one-dimensional class model.

To account for the hyperbox structure that exists within the IMS, non-probabilistic SIMCA augments s_i^2 with a term for each IMS dimension along which the projection of point i falls outside the normal range:

$$s_i^2(\text{augm}) = s_i^2 + \sum_{k=1}^{A} [(s_0^2/s_k^2)\, t_{ik}'^2] \qquad (6)$$

where $t_{ik}' = t_{ik} - t_k^+$ (when $t_{ik} > t_k^+$) or $= t_{ik} - t_k^-$ (when $t_{ik} < t_k^-$) or $= 0$ (otherwise). Thus t_{ik}' can be interpreted as the distance (if any) from point i to the hyperbox along IMS dimension k. In principle, the above formula describes a geometric addition of the OMS distance measure s_i and the IMS distances. The factor s_0^2/s_k^2 is introduced to make the terms in the right-hand side of Eqn. 6 compatible [6]. s_0 is the class residual standard deviation and is discussed below, under "Probabilistic SIMCA".

The need for probabilistic classification

The simplest form of classification is to force each test object into exactly one of the classes of the training set, i.e., pattern recognition on level 1 [16]. With non-probabilistic SIMCA, a forced classification is obtained by classifying each test object i into the class for which the value of s_i is lowest. There are two situations where classification on level 1 is clearly inappropriate. First, the test object may come from a class that was not represented in the training set. Often it will then behave as an outlier and the distances to all class models will be large. If detection of these outlying objects is possible, the pattern recognition is said to operate on level 2 [16]. Secondly, the test object may be close to more than one class model. This happens when the class models are not well separated from each other, which often happens in practice. In this case, it is a natural question to ask with what probability the test object could belong to each of the classes, but these probabilities are not given by the standard SIMCA method.

PROBABILISTIC SIMCA

Modelling the variation in the outside-model space

In probabilistic SIMCA, a statistical model is assumed for the distribution of the objects around the IMS. Based on this model, it is possible to compute the probability density of each class model at the coordinates of the test object. These probability densities specify the chance of finding an object of the considered class at that place, and they can be used both for the detection of outliers and for the calculation of classification probabilities, as will be shown below.

The model assumption on which probabilistic SIMCA is based can be formulated as follows: each test object i, which belongs to the same class as the objects with the help of which the class model was constructed, has component scores on the last $p - A$ PC axes, that are normally distrib-

uted with zero mean, with variance σ_0^2 equal in all directions, and with zero covariance between these directions. This can be written as:

$$(t_{i(A+1)} \ldots t_{ip})' \sim N^{p-A}\ (0, \sigma_0^2\, I) \tag{7}$$

where N^{p-A} denotes the $(p-A)$-variate normal distribution. It is thus assumed, that enough PCs have been included in the class model, so that the remaining dimensions contain only noise. The assumption of equal variance in all directions can be justified when an appropriate scaling (which is also necessary for the PCA) has been done.

It must be noted that this model depends on the data that are used to construct the principal components, i.e., on the training set. Whenever another training set is used, the centre of gravity and the direction of the PC axes will be somewhat different. The problems that arise have much to do with the distinction between principal component analysis (PCA) and factor analysis. In fact, the present assumptions would better fit into a factor analysis model, where the existence of factors (also called latent variables) is assumed initially. But the theoretical foundations of factor analysis are somewhat obscure [17] and many statisticians advocate the use of the computationally simpler PCA as an approximation to factor analysis [14, 17, 18]. In natural sciences, factor analysis is seldom applied although there are many applications of PCA under the name "factor analysis". The differences have been described [14, 18, 19].

Because of the dependence on the training set discussed above, the model specified in Eqn. 7 is in principle valid only for the scores of new (test) objects. For example, the assumption of equal variances is certainly not fulfilled for the training object scores, because the PCA guarantees decreasing variances for higher PC dimensions. Therefore the estimation of the parameter σ_0 with an estimator based on the training objects is statistically very difficult. Yet, this is done in the SIMCA method, because often only training objects will be available at the time of model construction.

In principle, an estimate of σ_0^2 which is the residual variance-per-direction, can be found by averaging the values of s_i^2. A training object, however, in contrast to a test object, pulls the class model closer to itself. This can be compared to the situation in linear regression where two points can always be perfectly fitted by a straight line. In the same way, $A + 1$ points can always be fitted with an A-dimensional PC model by a proper choice of one mean vector and A eigenvectors. Consequently, there is a loss of $A + 1$ degrees of freedom in estimating σ_0^2. The estimator is therefore computed as

$$s_0^2 = \left(\sum_{i=1}^{n} s_i^2\right)/(n-A-1) = \left(\sum_{i=1}^{n}\sum_{j=1}^{p} e_{ij}^2\right)/[(n-A-1)(p-A)] \tag{8}$$

s_0 is also called the class residual standard deviation (class RSD).

Similar considerations can be applied to a single training object: the total number of degrees of freedom $(n-A-1)(p-A)$ is then divided equally among the n training objects. In this way, one training object is assigned not $p-A$, but $(n-A-1)(p-A)/n$ degrees of freedom. When i

is a training object, s_i^2 should be corrected by multiplying by $n/(n-A-1)$ to remove the bias introduced by the model fitting.

In the following paragraphs, it is assumed that s_0 estimates the typical distance-per-dimension for all objects that belong to the class under consideration (although s_0 has been criticized as being usually too small [20]). The number of dimensions of a class model, A, has to be smaller than both p and $n-1$. Very often $(n-A-1)(p-A)$ is quite a large number, so that σ_0^2 can be directly replaced in approximate formulae by s_0^2.

Differences between the old and new algorithms for probabilistic SIMCA and CLASSY

The first version of probabilistic SIMCA, which was used (but only loosely described) earlier [2, 3], differed from the current version on four points. First, it was assumed that the OMS distance d_i could be modelled with a normal distribution around zero. This is, however, not an adequate description: d_i is the square root of a sum of squares of normally distributed residuals. It follows then, that d_i^2/σ_0^2 is χ^2-distributed with $p-A$ degrees of freedom. This can only be reduced to a normal distribution for $p-A=1$.

Secondly, in the old algorithm, the total probability density for a class model was calculated as the OMS density, but with the augmented distances s_i (augm) instead of s_i. There are at least two reasons why this should not be done: (1) the OMS density function thus calculated ceases to be a probability density function (which has special properties such as a unit area under the curve); (2) to compare densities of an object in different class models, it is necessary to translate the densities to the same coordinate system but the PCs defining OMS and IMS are generally different for each class model, and so OMS densities $f_i(t_{A+1} \ldots t_p)$ cannot be compared with each other. The only solution to this problem is to define IMS densities $f_i(t_1 \ldots t_A)$ in some suitable way, and then to make the necessary transitions to $f_i(t_1 \ldots t_p)$, $f_i(\mathrm{X}_1^* \ldots \mathrm{X}_p^*)$ and finally $f_i(\mathrm{X}_1 \ldots \mathrm{X}_p)$.

Thirdly, as indicated above, the comparison of densities in different class models has to be done with $f_i(\mathrm{X}_1 \ldots \mathrm{X}_p)$, i.e., the densities in the original, unscaled data space. This unscaling was not done in the previous algorithm. This will lead to different results for the new algorithm in the case of class autoscaling (where the applied scaling is different for each class).

Fourthly, in the first version of probabilistic SIMCA, the residual variances of each class model (s_0^2) were pooled to one overall residual variance. This has the drawback that the class models (which make use of s_0, see next section) are no longer completely independent of each other. An even more important argument for abolishing the pooling in the new version is that the different class-model OMSs cannot be compared directly (because of different PC modelling and possibly also different scaling).

These first, third and fourth points also apply to the old and new versions of the CLASSY method. The new algorithms for probabilistic SIMCA and CLASSY are described in detail below.

Probability densities in the outside-model space

Because principal components are always uncorrelated, it is not very stringent to add the assumption of independance, so that any multivariate probability density in the OMS is a simple product of $p - A$ univariate densities on these PCs. Moreover, because of the assumption that all directions in the OMS are equivalent, these univariate densities are all of the same type:

$$f_i(t_{A+1} \ldots t_p) = \prod_{k=A+1}^{p} f(t_{ik}) \tag{9}$$

with

$$f(t_{ik}) = (2\pi\sigma_0^2)^{-1/2} \exp\left[-\frac{1}{2} t_{ik}^2/\sigma_0^2\right] \tag{10}$$

This means that the OMS scores t_{ik} are normally distributed around zero with variance σ_0^2. Here, and in the remaining formulae, it will be assumed that s_0 has enough degrees of freedom to replace σ_0. Then, from Eqns. 9 and 10,

$$f_i(t_{A+1} \ldots t_p) = (2\pi s_0^2)^{-(p-A)} \exp\left[-\frac{1}{2} \sum_{k=A+1}^{p} t_{ik}^2/s_0^2\right] \tag{11}$$

or

$$f_i(t_{A+1} \ldots t_p) = (2\pi s_0^2)^{-(p-A)} \exp\left[-\frac{1}{2} (p-A) s_i^2/s_0^2\right] \tag{12}$$

The ratio in the exponent, $(p - A)s_i^2/s_0^2$, follows approximately a χ^2-distribution with $p - A$ degrees of freedom [14]. This can be used for outlier detection: an object i which is supposed to belong to a certain class, is declared to be an outlier if the above ratio exceeds the critical χ^2 value. This procedure is equivalent to an approximate F-test with the ratio s_i^2/s_0^2 and with $p - A$ and $(n - A - 1)(p - A)$ degrees of freedom [5, 6].

Probability densities in the inside-model space

The SIMCA IMS density $f_i(t_1 \ldots t_A)$ is defined as the product of A univariate densities:

$$f_i(t_1 \ldots t_A) = \prod_{k=1}^{A} f(t_{ik}) \tag{13}$$

The univariate density has to be defined such that there is a uniform distribution with the hyperbox limits t_k^- and t_k^+ and a normal error distribution beyond these limits (see Fig. 2). A function that meets these requirements is

$$f = (2\pi s^2)^{-1/2} \exp\left[-\frac{1}{2} t_{ik}'^2/s^2\right] \tag{14}$$

However, the area under the curve (AUC) does not equal 1, as required, but is larger by the area of a rectangle with length l_k and height $1/[(2\pi)^{1/2} s]$. Therefore the function f is corrected by dividing by $1 + l_k/[(2\pi)^{1/2} s]$. Rearrangement gives

$$f(t_{ik}) = [(2\pi s^2)^{1/2} + l_k]^{-1} \exp\left[-\frac{1}{2} t_{ik}'^2/s^2\right] \tag{15}$$

which satisfies the requirements for a probability density.

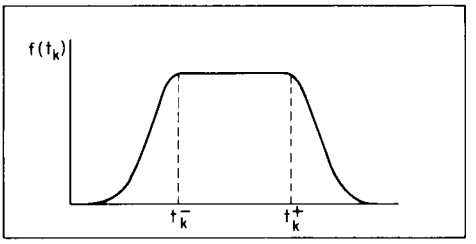

Fig. 2. SIMCA probability density function for each dimension of the IMS.

So far, no choice has been made for the parameter s; any choice is compatible with the requirements of a probability density function. It seems logical, however, to define $s = c\, s_k$, which means that the expected variation outside the hyperbox along IMS dimension k, is taken as proportional to the real variation along this dimension of the training objects inside the hyperbox.

Substitution of this definition in Eqn. 15, and of Eqn. 15 in Eqn. 13, gives the formula for the multivariate IMS density:

$$f_i(t_1 \ldots t_A) = \left\{ \prod_{k=1}^{A} [(2\pi c^2 s_k^2)^{1/2} + l_k] \right\}^{-1} \exp\left[-\frac{1}{2} \sum_{k=1}^{A} t_{ik}'^2/(cs_k)^2 \right] \qquad (16)$$

Multiplying the IMS density (Eqn. 16) by the OMS density (Eqn. 12) then yields the total probability density in the PC space:

$$f_i(t_1 \ldots t_p) = f_i(t_1 \ldots t_A) \times f_i(t_{A+1} \ldots t_p) \qquad (17)$$

Writing out this multiplication gives a formula with the following exponential part:

$$-\frac{1}{2}\left[(p - A)s_i^2/s_0^2 + \sum_{k=1}^{A} t_{ik}'^2/(cs_k)^2 \right] \qquad (18)$$

Now the effect of the proportionality constant c, which can still be chosen freely as part of the definition of the IMS model, can be clarified. One interesting possibility is to choose $c = (p - A)^{-1/2}$. In this case, the above exponential part can be written as $-\frac{1}{2}(p - A)s_i^2(\text{augm})/s_0^2$, so that $s_i(\text{augm})$, the augmented object RSD from non-probabilistic SIMCA, reappears in the density formula.

Generally, it can be seen from term 18 that c determines the weighting of the IMS dimensions versus the OMS dimensions. In non-probabilistic SIMCA, and in the probabilistic case with $c = (p - A)^{-1/2}$, standardized distances in any IMS dimension (t_{ik}'/s_k) are each given the same importance as the standardized distance-per-dimension in the OMS (s_i/s_0). It should be noted, however, that this relative weighting remains fairly arbitrary because of the also arbitrary hyperbox limits t_k^- and t_k^+. A disadvantage of choosing $c = (p - A)^{-1/2}$ is that the dimensionality of the OMS $(p - A)$ is introduced in

the model assumptions for the IMS. The IMS model thus becomes dependent on the total number of measured variables (p), while the IMS as such was constructed with only the first A principal components in order to be independent of however many noisy variables were measured. To avoid this, the proportionality constant was made $c = 1$. This means that each standardized IMS distance is given the same importance as the total standardized OMS distance $[d_i/s_0 = (p - A)^{1/2} s_i/s_0]$.

Classification with probabilistic SIMCA

The total density in the PC space, computed from Eqn. 17 with $c = 1$, can still not be used for comparing the fit of a test object to several different class models. The probability densities must be related to the same coordinate system. In standard PCA, the principal component axes (the eigenvectors) are scaled to length 1, which implies that the unit of length on these axes is the same as that of the variables on which the PCA was based. Therefore,

$$f_i(X_1^* \ldots X_p^*) = f_i(t_1 \ldots t_p) \tag{19}$$

The last step is to unscale the variables and find $f_i(X_1 \ldots X_p)$. This density function can be seen as the probability of finding a data vector X_i in the infinitesimal hyperspace $dX = dX_1 \cdot dX_2 \ldots dX_p$. In the same way, $f_i(X_1^* \ldots X_p^*)$ is the probability of finding a data vector in $dX^* = dX_1^* \cdot dX_2^* \ldots dX_p^*$. From Eqn. 2, it follows that $dX_j^* = dX_j/SF_{cj}$, and therefore also

$$dX^* = dX/\left(\prod_{j=1}^{p} SF_{cj}\right) \tag{20}$$

A suitable conversion can then be found by considering

$$\int_{-\infty}^{+\infty} \ldots \int_{-\infty}^{+\infty} f_i(X_1 \ldots X_p)\, dX = \int_{-\infty}^{+\infty} \ldots \int_{-\infty}^{+\infty} f_i(X_1^* \ldots X_p^*)\, dX^* = 1 \tag{21}$$

From Eqn. 20, the first equality can also be written as

$$\int_{-\infty}^{+\infty} \ldots \int_{-\infty}^{+\infty} f_i(X_1 \ldots X_p)\, dX = \left(1/\prod_{j=1}^{p} SF_{cj}\right) \int_{-\infty}^{+\infty} \ldots \int_{-\infty}^{+\infty} f_i(X_1^* \ldots X_p^*)\, dX \tag{22}$$

One solution of this equation is

$$f_i(X_1 \ldots X_p) = \left(1/\prod_{j=1}^{p} SF_{cj}\; f_i(X_1^* \ldots X_p^*)\right) \tag{23}$$

and Eqn. 23 is used for computing the total probability density of object i (with data vector X_i) in the original unscaled variable space.

At this stage, expressions that can be compared for different class models

have finally been obtained. If K classes are considered, it is possible to compute K probability densities for an object i, one for each class model. The final results from the computations in probabilistic SIMCA are then the posterior probabilities, which specify the probability (according to the SIMCA method) that object i belongs to class c. These posterior probabilities are found using Bayes' formula:

$$P(c|\mathbf{X}_i) = {}^{c}f_i(\mathbf{X}_1 \ldots \mathbf{X}_p) / \sum_{c=1}^{K} {}^{c}f_i(\mathbf{X}_1 \ldots \mathbf{X}_p) \tag{24}$$

This formula can be extended with prior probabilities and/or losses for misclassification, if required [21]. Without these, Eqn. 24 describes a situation where all classes are considered equally likely initially, and where classifying an object from class c_1 into class c_2 is considered equally bad for each c_1 and c_2 for which $c_1 \neq c_2$.

PROBABILISTIC CLASSY

CLASSY was developed to combine the advantages of the SIMCA and the ALLOC approaches to multivariate classification [2]. The construction of PC class models and the treatment of the OMS are both the same as in probabilistic SIMCA (see above). The treatment of the IMS is completely different: no hyperbox structure is assumed, but an estimate of the IMS density is based directly on the training objects (or rather their IMS scores $t_1, t_2, \ldots t_A$). The technique of this so-called kernel density estimation is the same as in the classification method ALLOC, where it is applied to the original values $\mathbf{X}_1$—$\mathbf{X}_p$ [21, 22].

The theory underlying kernel density estimation is available elsewhere [21]. The IMS density for CLASSY that follows from this method is

$$f_i(t_1 \ldots t_A) = [(2\pi)^{1/2}\ \mathrm{SMOOTH}]^{-A} \left(\prod_{k=1}^{A} s_k \right)^{-1} n^{-1} \sum_{ii=1}^{n}$$

$$\left\{ \exp \left[-\frac{1}{2} \sum_{k=1}^{A} ((t_{iik} - t_{ik})^2 / (\mathrm{SMOOTH}^2 s_k^2)) \right] \right\} \tag{25}$$

Here i is assumed to be a test object (i.e., not belonging to the class under consideration), ii is an index for the training objects of this class, and SMOOTH is the smoothness parameter, which plays an essential role in kernel density estimation.

The final steps in CLASSY classification are the same as for SIMCA (see the section on "Classification with probabilistic SIMCA"), i.e., multiplication of the IMS density by the OMS density (Eqn. 12), followed by the coordinate system transformations as specified by Eqns. 19 and 23, and finally the computation of the posterior probabilities by Eqn. 24.

In part 2 of this series [4], the new versions of both probabilistic SiMCA and CLASSY will be evaluated from their performance on three practical data sets.

REFERENCES

1 H. E. Solberg, Crit. Rev. Clin. Lab. Sci., 9 (1978) 209.
2 H. van der Voet and D. A. Doornbos, Anal. Chim. Acta, 161 (1984) 115.
3 H. van der Voet and D. A. Doornbos, Anal. Chim. Acta, 161 (1984) 125.
4 H. van der Voet, J. B. Hemel and P. M. J. Coenegracht, Anal. Chim. Acta, 191 (1986) 63.
5 S. Wold, Pattern Recognition, 8 (1976) 127.
6 C. Albano, G. Blomqvist, D. Coomans, W. J. Dunn III, U. Edlund, B. Eliasson, S. Hellberg, E. Johansson, D. Johnels, B. Nordén, M. Sjöström, B. Söderström, H. Wold and S. Wold, in A. Höskuldsson, K. Conradsen, B. Sloth Jensen and K. Esbensen (Eds.), Proc. Symp. on Appl. Stats., NEUCC, RECAU, RECKU and Danish Society of Theoretical Statistics, Copenhagen, 1981, p. 183.
7 S. Wold, C. Albano, W. J. Dunn III, K. Esbensen, S. Hellberg, E. Johansson and M. Sjöström, in J. Martens (Ed.), Proc. IUFOST Conf. Food Research and Data Analysis, Applied Science, London, 1983.
8 S. Wold, C. Albano, W. J. Dunn III, K. Esbensen, S. Hellberg, E. Johansson, W. Lindberg and M. Sjöström, Analusis, 12 (1984) 477.
9 S. Wold, C. Albano, W. J. Dunn III, U. Edlund, K. Esbensen, P. Geladi, S. Hellberg, E. Johansson, W. Lindberg and M. Sjöström, in B. R. Kowalski (Ed.), Chemometrics, Mathematics and Statistics in Chemistry, D. Reidel, Dordrecht, 1984, p. 17.
10 M. P. Derde, D. Coomans and D. L. Massart, Anal. Chim. Acta, 141 (1982) 187.
11 S. Wold, Technometrics, 20 (1978) 397.
12 H. T. Eastment and W. J. Krzanowski, Technometrics, 24 (1982) 73.
13 E. R. Malinowski and D. G. Howery, Factor Analysis in Chemistry, Wiley, New York, 1980.
14 P. E. Green, Analyzing Multivariate Data, The Dryden Press, Hinsdale, IL, 1978.
15 S. Wold, SIMCA-3B Manual, Department of Chemistry, Umeå University, S-90187 Umeå, Sweden, 1981.
16 C. Albano, W. J. Dunn III, U. Edlund, E. Johansson, B. Nordén, M. Sjöström and S. Wold, Anal. Chim. Acta, 103 (1978) 429.
17 D. J. Bartholomew, Biometrika, 71 (1984) 221.
18 C. Chatfield and A. J. Collins, Introduction to Multivariate Analysis, Chapman and Hall, London, 1980.
19 K. G. Jöreskog and H. Wold, in K. G. Jöreskog and H. Wold (Eds.), Systems under Indirect Observation, Part I, North-Holland, Amsterdam, 1981, p. 263.
20 D. Coomans, Ph.D. Thesis, Vrije Universiteit, Brussel, 1982, p. 271.
21 J. Hermans, J. D. F. Habbema, T. K. D. Kasanmoentalib and J. W. Raatgever, Manual for the ALLOC-80 Discriminant Analysis Program, Dept. of Medical Statistics, University of Leiden, Leiden, 1982.
22 D. Coomans, D. L. Massart, I. Broeckaert and A. Tassin, Anal. Chim. Acta, 133 (1981) 215.

Analytica Chimica Acta, 192 (1987) 77—83
Elsevier Science Publishers B.V., Amsterdam — Printed in The Netherlands

SPECTROFLUORIMETRIC FLOW-INJECTION DETERMINATION OF TERTIARY AMINES IN NON-AQUEOUS MEDIA

IAN R. C. WHITESIDE and PAUL J. WORSFOLD*

Department of Chemistry, University of Hull, Hull HU6 7RX (Great Britain)

ALBERT LYNES

Thornton Research Centre, Shell Research Ltd., P.O. Box 1, Chester CH1 3SH (Great Britain)

(Received 8th May 1986)

SUMMARY

The cyclic condensation of malonic acid with acetic anhydride in non-aqueous media is catalyzed selectively by tertiary amines. This derivatization reaction is adapted for flow injection analysis. A reaction pathway for the cyclization of a mixed anhydride condensate to form a fluorescent fully acylated phloroglucinol carboxylic acid is proposed. The effects of reaction parameters on the sensitivity of the reaction are described and calibration data are presented for ≤ 2.7 mM triethylamine, tripentylamine, *N,N*-diethylaniline and pyridine. A secondary amine (diethylamine) gave a negligible response, but both primary and secondary amines partially quenched the fluorescence induced by a tertiary amine.

Compounds containing a tertiary amine function have useful industrial applications, e.g., as corrosion inhibitors or organic reaction intermediates and in pharmaceutical preparations. However, commercial sources of these compounds are often impure or contain other additives, and a selective method for the determination of the tertiary amine content is therefore necessary. The presence of primary and secondary amines in particular can give rise to interferences. A further complication is that the sample matrix is often oil-based, and therefore a non-aqueous procedure is required.

A static method, based on the ability of the tertiary amine to catalyze the cyclic condensation of malonic acid and acetic anhydride to form a fluorescent adduct, was reported by Thomas [1] for the determination of alkaloids such as cocaine in pharmaceutical preparations. Its major limitations for routine analysis were the high temperature (80°C) and lengthy reaction time (15 min) required. A similar reaction, involving the tertiary amine-catalyzed condensation of citric acid and acetic anhydride to form a chromogenic adduct, was reported [2] as a post-column derivatization procedure for the determination of tertiary amines eluted under normal-phase conditions from a chromatographic column.

This paper describes a flow-injection procedure for the selective determination of tertiary amines in non-aqueous solution by derivatization with

0003-2670/87/$03.50

malonic acid and acetic anhydride to yield a fluorescent adduct. The reaction proceeds at room temperature (20°C) in a continuous flow, single-channel manifold at a sampling rate of 90 h^{-1}. It is readily combined with normal-phase high-performance liquid chromatography (h.p.l.c.) to provide sensitive and selective post-column derivatization of eluting components containing a tertiary amine group.

EXPERIMENTAL

Reagents, standards and preliminary tests

The derivatizing reagent consisted of various concentrations of malonic acid (up to 12%, w/v) in acetic anhydride, and was prepared daily by adding the appropriate amount of malonic acid (AnalaR; BDH) to acetic anhydride (50 ml) and gently stirring the mixture for 10 min.

For preliminary qualitative studies of the derivatization reaction, four compounds containing a tertiary amino group were used. Triethylamine (5 μl), diethylaniline (5 μl), pyridine (5 μl) and cocaine (5 mg) were added to separate 5-ml aliquots of 10% (w/v) malonic acid in acetic anhydride. After 5 min the fluorescence excitation and emission spectra of the solutions were scanned.

To optimize the malonic acid concentration for the derivatization reaction within a flow-injection manifold, solutions of pyridine (20 μl) and triethylamine (10 μl) in acetone (25 ml) were injected into acetic anhydride carrier streams containing 0, 1, 4, 8 and 12% malonic acid. To investigate the effect of different solvents on the fluorescence signal for the flow-injection procedure four stock solutions (3.0 mM) containing tributylamine (35 μl) in 50 ml of acetone, ethyl acetate, heptane or tetrahydrofuran were prepared. A glass syringe was used to dispense the tributylamine. Two further sets of standard solutions (1.2 mM and 2.1 mM) were prepared by serial dilution of the stock solutions with the appropriate solvent. The carrier stream for the flow-injection system for these, and all subsequent experiments, was 4% (w/v) malonic acid in acetic anhydride.

The effect of temperature (20°C and 45°C) on the rate of reaction was studied on a stock solution of triethylamine (35 μl) in tetrahydrofuran (100 ml) and five further solutions prepared by dilution of the stock solution with tetrahydrofuran. The relative sensitivity of the derivatization reaction for a range of compounds was studied by preparing stock solutions of triethylamine (35 μl), tripentylamine (80 μl), *N*,*N*-diethylaniline (40 μl), pyridine (20 μl) and diethylamine (20 μl) in tetrahydrofuran (100 ml). Further sets of standard solutions were prepared by dilution of the stock solutions with the tetrahydrofuran.

The stock solutions used in studies of the selectivity of the reaction for tertiary amines relative to primary and secondary amines were prepared from triethylamine (50 μl), hexylamine (250 μl) or diethylamine (250 μl) in tetrahydrofuran (25 ml). Test solutions were prepared by adding the hexylamine

or diethylamine stock solution (1, 2, 3, 4, 5 and 8 ml) to the triethylamine stock solution (1 ml) and diluting to 10 ml with tetrahydrofuran.

Instrumentation and procedures

The fluorescence spectra for the preliminary studies were obtained by using a scanning spectrofluorimeter (Perkin-Elmer LS-3000) and a 1-cm^2 cross-section quartz cell.

The flow-injection manifold used is shown in Fig. 1. The malonic acid/acetic anhydride carrier stream was pumped through a single-line manifold at 0.6 ml min^{-1} by a peristaltic pump (Gilson Minipuls 2) fitted with silicone rubber tubing (1.6 mm i.d., 4.8 mm o.d.; Watson Marlow). Teflon tubing (0.8 mm i.d.) was used for the 100-cm reaction coil and throughout the remainder of the system. Amine solutions (20 μl) were introduced into the reagent stream via a rotary teflon valve (Rheodyne 5020). The dispersion coefficient of the system was 7.4. The fluorescence of the stream was monitored by a filter fluorimeter (Perkin-Elmer LS-2) fitted with a 7-μl flow cell. For all quantitative measurements, the excitation wavelength was set at 400 nm with a 10-nm bandpass interference filter and the emission wavelength was set at 441 nm with a continuous interference filter.

The experiments at 45°C were done by passing the malonic acid/acetic anhydride reagent through a 200-cm coil upstream from the injection valve, and placing this 200-cm coil and the 100-cm coil in a water bath at 45°C.

RESULTS AND DISCUSSION

Qualitative study

Four tertiary amines were treated with 10% malonic acid in acetic anhydride at 20°C and the fluorescence excitation and emission spectra of the resultant mixtures were obtained. The wavelengths at which maximum excitation and emission, respectively, were observed were 396 and 443 nm for triethylamine, 394 and 440 nm for cocaine, 390 and 440 nm for pyridine, and 392 and 438 nm for diethylaniline. The results showed that the reaction proceeds at room temperature and that the predominant fluorescent product was the same in all four cases, so that its structure is therefore independent of the molecular structure of the tertiary amine.

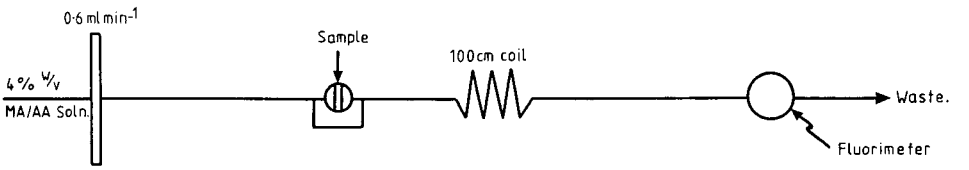

Fig. 1. Flow-injection manifold for the determination of tertiary amines at room temperature. Amine standards in tetrahydrofuran (20 μl) were injected. The distance from the injection valve to the detector was 100 cm.

A possible reaction pathway is shown below. Groth and Wallerberg [3] suggested that malonic acid and acetic anhydride react to produce a mixed anhydride condensate (**A** in the reaction scheme), which undergoes base-catalyzed cyclization between the two starred carbon atoms to produce a fluorescent, fully acylated phloroglucinol carboxylic acid. The various equilibria suggested in the proposed reaction scheme favour the formation of the final fluorescent product because of the stability of the enol form of the partially acylated phloroglucinol carboxylic acid relative to the keto form.

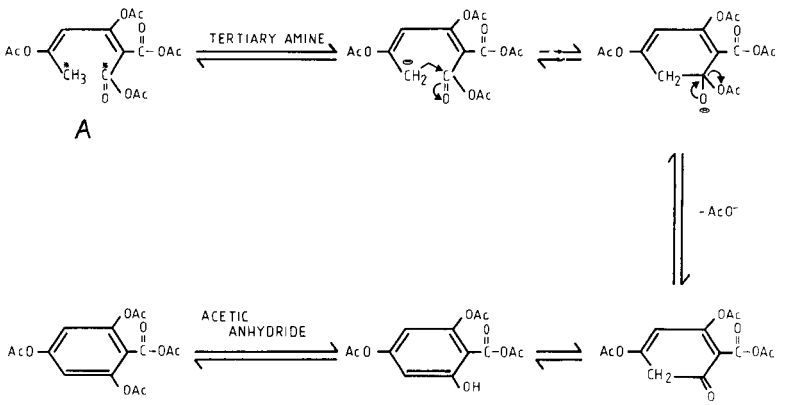

Primary and secondary amines are more likely to react directly with acetic anhydride to form *N*-substituted and *N,N*-disubstituted amides.

Optimization of reaction conditions

The effect of malonic acid concentration on the fluorescence emission intensity at 441 nm, when pyridine or triethylamine is used as the catalyst, is shown in Table 1. The optimum concentration in both cases was 4% (w/v). The decrease in signal at higher concentrations is probably due to further

TABLE 1

The effect of malonic acid concentration on fluorescence emission intensity for pyridine and triethylamine

Malonic acid conc. (%, w/v)	Pyridine		Triethylamine	
	Intensity[a]	RSD (n = 3)	Intensity[a]	RSD (n = 3)
0	1	—	1	—
1	238	1.6	269	2.8
4	940	0.5	293	1.0
8	213	0.7	120	2.1
12	65	3.8	68	3.7

[a]Arbitrary units.

reaction between malonic acid and the fully acylated phloroglucinol carboxylic acid.

The effect of the solvent on the fluorescence emission intensity is shown in Table 2 for tetrahydrofuran, acetone and ethyl acetate. The relative standard deviation (RSD) was typically less than 2.0% (n = 3) for the three solvents, but the results for heptane showed very poor reproducibility because of incomplete mixing of the sample with the carrier stream. The relative intensities observed can be related to solvent polarity, the least polar solvent, tetrahydrofuran [4], giving the highest signals. The wavelengths of maximum emission (441 nm in tetrahydrofuran, 453 nm in acetone and 455 nm in ethyl acetate) can also be related to solvent polarity. For the fully acylated phloroglucinol carboxylic acid, the $\pi - \pi^*$ transition will be favoured and the excited state will be more polar than the ground state [5]. More polar solvents are therefore more likely to stabilize the excited state, causing a red shift in the emission wavelength and a decrease in the fluorescence yield.

The effect of temperature on the emission intensity at 441 nm, in tetrahydrofuran, is shown in Table 3. The increased rate of reaction at 45°C more than compensates for the decrease in basicity [6] and the increase in non-radiative energy losses [7].

Calibration and interferences

Calibration and reproducibility data for five amines are given in Table 4. The two aliphatic tertiary amines, triethylamine and tripentylamine, gave much higher sensitivity than the two aromatic tertiary amines, *N,N*-diethylaniline and pyridine; the secondary amine, diethylamine, gave a negligible

TABLE 2

The effect of solvent on the fluorescence emission intensity

Tributylamine conc. (mM)	Intensity (arbitrary units)		
	Tetrahydrofuran	Acetone	Ethyl acetate
0	0.3	0.2	0.3
1.2	305	10.0	5.1
2.1	490	42	15.0
3.0	705	64	25.0

TABLE 3

The effect of temperature on the fluorescence emission intensity (in arbitrary units) from triethylamine (TEA)

TEA (mM)	0.3	0.5	0.7	1.0	1.5	2.5
Intensity (20°C)	—	62	—	155	320	678
(45°C)	120	300	515	—	—	—

TABLE 4

Calibration data for five amines

Amine	Conc. (mM)	Intensity[a]	RSD[b] (%)	Amine	Conc. (mM)	Intensity[a]	RSD (%)
Triethylamine[c]	0.5	62	1.9	*N,N*-Diethylaniline	1.5	3.8	20
	1.0	155	4.1		2.0	12.3	1.2
	1.5	320	0.0		2.5	26.2	0.6
	2.5	678	0.0	Pyridine[d]	2.0	26.3	2.2
Tripentylamine	0.5	27	1.3		2.5	73.7	2.1
	1.1	116	2.4	Diethylamine	1.0	1.1	—
	1.6	258	1.1		1.5	1.2	—
	2.2	410	5.0		1.9	1.3	—
	2.7	598	10.8				

[a]Arbitrary units. [b]n = 3. [c,d]Detection limits (3 σ) were: [c]ca. 0.005 mM; [d]0.04 mM.

signal. The poorer sensitivities of the aromatic amines can be related to their lower basicity and greater steric hindrance. The structure of the tertiary amine obviously has an effect on its catalytic efficiency and therefore, for quantitative analysis for several tertiary amines in a complex organic matrix, the flow-injection procedure would have to be incorporated as a post-column reaction after normal-phase h.p.l.c. separation. The RSD values were usually $\leqslant$5%.

The results for diethylamine in Table 4 indicate that secondary amines do not react with the malonic acid/acetic anhydride reagent to form a fluorescent adduct. When 10—77 mM diethylamine was present with 1.5 mM triethylamine, however, the resulting fluorescence signal was quenched by ca. 10% for all diethylamine concentrations as compared with the signal from triethylamine alone. Similarly, when 8—60 mM hexylamine was present with 1.5 mM triethylamine, the resulting fluorescence signal was quenched by ca. 20% for all hexylamine concentrations as compared with the signal from triethylamine alone. This indicates that primary and secondary amines can cause a negative interference, possibly by affecting the reaction pathway, and that for complex mixtures the reaction should be preceded by normal-phase h.p.l.c. separation. Indeed, the flow injection technique should be seen as a convenient way of developing reactions that can subsequently be used in the post-column mode in conjunction with h.p.l.c.

The authors thank Thornton Research Centre, Shell Research Limited, for an Extra-Mural Research Grant in support of this work, and Dr. K. J. Toyne for helpful discussions about the mechanism of the reaction.

REFERENCES

1 A. D. Thomas, Talanta, 22 (1975) 865.
2 M. Kudoh, I. Matoh and S. Fudano, J. Chromatogr., 261 (1983) 293.
3 A. B. Groth and G. Wallerberg, Acta Chem. Scand., 20 (1966) 2628.
4 J. F. Lawrence, Organic Trace Analysis by Liquid Chromatography, Academic Press, New York, 1981, p. 121.
5 W. R. Seitz, Crit. Rev. Anal. Chem., 8 (1980) 367.
6 G. Perrault, Can. J. Chem., 46 (1968) 2021.
7 E. P. Kirkby and R. F. Steiner, J. Phys. Chem., 74 (1970) 4480.

Analytica Chimica Acta, 192 (1987) 85—93
Elsevier Science Publishers B.V., Amsterdam — Printed in The Netherlands

HISTIDINE AS THE FUNCTIONAL GROUP FOR A CHELATING ION EXCHANGER

CHUEN-YING LIU
Department of Chemistry, National Taiwan University, Taipei 107 (Taiwan)
(Received 21st March 1986)

SUMMARY

In the chelating ion exchanger synthesized, the amino group of histidine is attached chemically via the azide method to the carboxyl group of Amberlite IRC-50. A flow system based on a spectrophotometric detector, with 4-(2-pyridylazo)resorcinol as reagent, is described for fast assays of eluted cations. The pH dependence of the metal extraction is reported for Ag(I), Au(III), Cu(II), Fe(III), Hg(II), Ni(II) and Zn(II) ions. The resin exhibits no affinity for the alkali or alkaline earth metals. The uptake of traces of the specified elements from synthetic samples by a short (90 mm) column of the histidine-containing resin was in the range 94—100% and the retained metals were readily eluted by means of 2 M hydrochloric or hydrobromic acid. In column operation, mercury was quantitatively recovered even in the presence of large excesses of various ligands. The recoveries of the trace metals were good at the usual pH of natural waters.

Ion exchangers have been widely used for the preconcentration of metal ions from various matrices [1]. In particular, chelating resins are valuable because of their selectivity for a large number of metals over the alkali and alkaline earth metals. Imidazole derivatives play an important role in biological systems, e.g., in several hydrolases [2] and hemoproteins [3—5]. Therefore, several studies have been published about imidazole-containing polymers. Polymers with chemically bound imidazole groups are of interest from different points of view. As weakly basic polymers, or after quaternization as polymers with strongly basic properties, they can be applied as ion exchangers [6, 7]. They have also been tested as catalysts in the hydrolysis of esters and used as ligands for complexing metallic ions [8]. Histidine [2-amino-3-(4′-imidazolyl)-propanoic acid] contains four different functional groups which are potential sites of coordination to metal ions, i.e., the charged carboxyl group, the uncharged amino group, and the two nitrogens in the imidazole ring. A marked change in their chelating behavior and properties would be expected on introducing more functional groups into the molecule. In spite of the voluminous research on metal/histidine complexes [9], there are few reports about histidine-containing polymers, especially with regard to their chelating properties. It was therefore thought to be of interest to synthesize a histidine-containing polymer and to test its properties in an ion exchanger.

0003-2670/87/$03.50

In this paper, a new chelating resin containing histidine groups, prepared from the common cation-exchange resin, Amberlite IRC-50, is reported. The complexation of various metal ions and the extractive properties of the resin are described.

EXPERIMENTAL

Apparatus and reagents

The flow system for the detection of transition metal ions is shown in Fig. 1. The system consisted of two Milton—Roy pumps (Model 396 Simplex), a Cheminert rotary injection valve (Model R-6031SV-K) equipped with a 100-μl sample loop, a polyhistidine resin column (90 × 4 mm i.d.), a LDC/Milton Roy Spectromonitor D variable-wavelength detector and a Yokogawa automatic recorder. The flow rate was 0.53 ml min^{-1} for pump 1 and 0.07 ml min^{-1} for pump 2.

4-(2-Pyridylazo)resorcinol (PAR) was used for the detection of metal ions. The aqueous reagent contained 2×10^{-4} M PAR, 1 M ammonium acetate and ammonia solution (d = 0.88) (15 ml l^{-1}). It was found advisable to degas the reagent and store it under nitrogen to prevent oxidation. Table 1 lists the absorption maxima for several cation complexes.

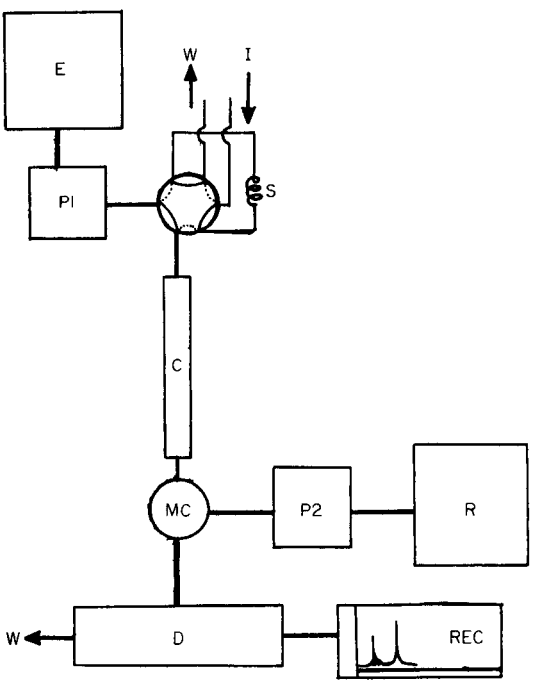

Fig. 1. Schematic diagram of the flow system for the determination of transition metals: E, eluent tank; P1, P2, pumps; I, injection; S, sample loop; C, resin column; MC, mixing chamber; R, reagent reservoir; D, detector; Rec, recorder; W, waste.

TABLE 1

Absorption maxima for complexes of metal cations with PAR

Complex metal	Cu	Pb	Ni	Co	Fe	U	Hg
λ_{max} (nm)	507	529	501	530	510	529	527.5

Amberlite IRC-50 (16—30 mesh; Rohm and Haas) was extracted with methanol, dried, ground and sieved. The 30—60 mesh and 60—100-mesh fractions were washed with 12 M hydrochloric acid, water and acetone successively, and used in the synthesis.

Synthesis of the histidine-containing resin

The derivatized resin was prepared by the following reaction sequence [10].

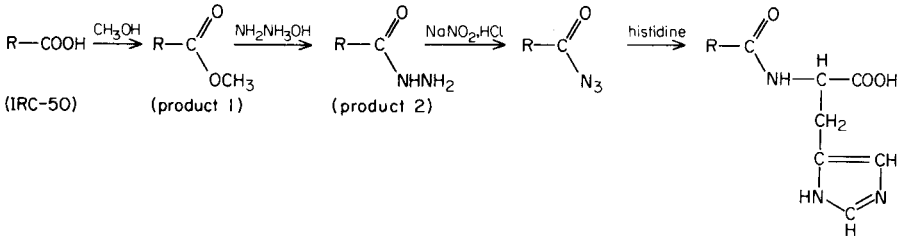

To 60 g of the pre-treated Amberlite IRC-50 resin was added 600 ml of methanol containing 15 ml of 18 M sulfuric acid as catalyst. The resulting mixture was refluxed at 70°C for 20 h. The product was cooled to room temperature and then collected by filtration under suction and washed sequentially with water and methanol until no sulfate ion appeared in the filtrate. The above procedures were repeated to obtain a higher yield. Product 1 was mixed with 400 ml of methanol. Then 25 ml of hydrazine hydrate was added dropwise and the mixture was left to react at room temperature for 30 h. The product was washed with water until no hydrazine appeared in the filtrate. To product 2 was added 500 ml of 0.42 M hydrochloric acid. While the mixture was constantly agitated in a freezing mixture of salt and ice, a solution of 100 ml of 0.2 M sodium nitrite was added dropwise. After the addition was complete, the mixture was stirred at 0°C for 30 min, and 33 g of L-histidine was added. Then 50 ml of triethylamine (0°C) was added to adjust the pH to 8.0—8.5. The reaction mixture was kept at 0°C for 48 h and stirred. 50 ml of 1 M ammonium chloride and 1 M ammonia solution was added to remove the unreacted azide. The final product was collected by suction filtration and washed sequentially with 0.1 M hydrochloric acid, water and methanol to remove any unreacted starting material.

Resin characterization

Water regain. The method of Parrish [11] was used.

Hydrogen ion capacity. Total acidic hydrogen content was determined by back-titration. A 0.2-g sample of the resin in the acidic form was added to 10.0 ml of 0.10 M sodium hydroxide and the mixture was equilibrated for 2 h at room temperature with stirring. After filtration with suction, the excess of alkali was titrated with 0.10 M hydrochloric acid.

Procedure for determination of acidity constants. Air-dried resin in the hydrogen form (0.200 g) was shaken in polyethylene bottles for 48 h with 2 M potassium chloride containing different amounts of 0.10 M sodium hydroxide at constant ionic strength of 0.1 M. The total volume of the solution was 25.0 ml.

Metal ion uptake as a function of pH

A batch technique was used, the chelating functions always being in excess to the metal. Dry resin (0.3 g) was suspended with 50 ml of 1.00×10^{-3} M solution of the cation perchlorate. The pH was adjusted by adding 0.1 M perchloric acid or 0.1 M sodium hydroxide. Suspensions were stirred for 48 h and then filtered. The concentrations of metal ions in the solution were determined spectrophotometrically.

The spectrophotometric methods used were as follows [12]: cuprizone [bis(cyclohexanone)oxalyldihydrazone] for copper, Nitroso-R salt (1-nitroso-2-hydroxy-3,6-naphthalenedisulfonic acid, disodium salt) for cobalt, dimethylglyoxime for nickel, xylenol orange for zinc and 1,10-phenanthrolinium chloride for iron.

Resin capacity and sorption isotherm

The procedure used above to study the variation of metal ion uptake with pH was applied, except that pH was kept fixed at 5.5 for the duration of the equilibration and that the metal ion concentration varied for each trial.

Concentration of trace metals

For all column studies, a 90 × 4-mm column of the histidine-containing resin was used. For the recovery of trace metals, the sample was deionized water containing various amount of metal ion buffered to pH 6.0. Triplicate 250-ml samples were passed through resin columns at a flow rate of 3 ml min^{-1}. After collection, the complexed metals were stripped from the column with 5 ml of 2 M hydrochloric acid or 2 M hydrobromic acid. They were determined spectrophotometrically.

The effect of ligands on the recovery of the ions was examined for 250-ml portions of deionized water to which were added 1 mg l^{-1} of each metal ion and a large excess of the ligand under study.

RESULTS AND DISCUSSION

Characterization of resin

In order to verify the presence of histidine groups in the synthesized resin, the infrared spectra of the resin shown in Fig. 2 were obtained with KBr pellets after each step in the synthesis. The i.r. spectrum of the Amberlite

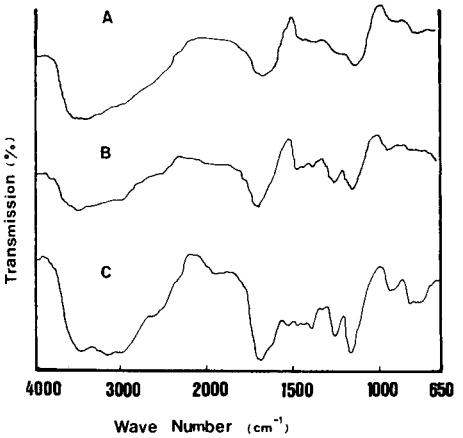

Fig. 2. Infrared spectra: (A) Amberlite IRC-50; (B) esterified product; (C) resin containing histidine groups.

IRC-50 showed bands at 3500—2500 and 1670 cm^{-1} (—COOH), whereas the spectrum of the esterified product exhibited bands at 1700, 1250 and 1150 cm^{-1} (—COOR). The spectrum of the final product showed bands at 1530 cm^{-1} (imidazolium group).

Elemental analysis gave 51.35% C, 7.3% H, 2.2% N and 39.1% O. The content of 2.2% nitrogen means that each 1 g of resin contains 1.59 mmol of nitrogen.

Table 2 shows the physical and chemical characteristics of the histidine-containing resin. The acidity constants were obtained by the direct algebraic method from the titration curve. The pK_a value of 5.8 is assigned to the imidazolium group, and is close to the value for the imidazolium group of the monomeric histidine [13].

Metal ion uptake as a function of pH

The extraction behavior of the resin toward various cations [Fe(III), Ni(II), Cu(II), Zn(II), Ag(I), Hg(II), and Au(III)] was investigated in aqueous solution over the pH range 0—6. The data from these experiments are presented in Fig. 3. Over this pH domain, alkali and alkaline earth metal ions were not extracted and therefore exhibit no affinity for the histidine function. Generally, the uptake of the other cations increased with pH and was quantitative over pH 5 for the tested metals.

These data for the percent extracted vs. pH can be summarized in terms of the half-extraction pH ($pH_{1/2}$). A comparison of the $pH_{1/2}$ values (Table 3) with the available stability constants [9] for the corresponding histidine monomer shows quite good agreement; the order of the stability constants is Fe(III) > Cu(II) > Zn(II) > Ni(II), while Au(III) > Hg(II) > Ag(I). Therefore, the $pH_{1/2}$ values can be considered as a good indication of the affinity of the

TABLE 2

Physical and chemical characterization of the histidine-containing resin

Bead size	60—100 mesh	Cobalt capacity[a]	1.06
Water regain	49 mmol g^{-1}	Copper capacity[a]	2.06
Nitrogen content	1.59 mmol g^{-1}	Mercury capacity[a]	1.50
Hydrogen ion capacity	1.42 mmol g^{-1}	Nickel capacity[a]	1.33
pK_a (imidazolium group)	5.80	Silver capacity[a]	1.24
		Zinc capacity[a]	1.55

[a] At pH 5.5, all given as mmol g^{-1}.

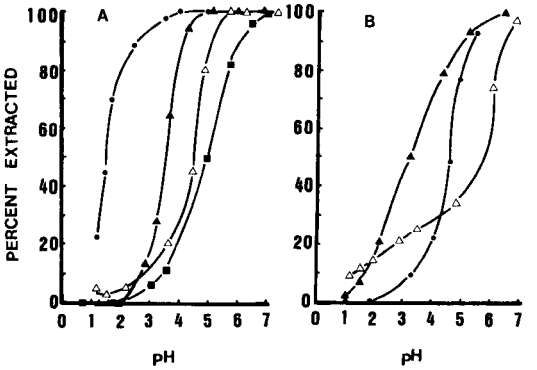

Fig. 3. Metal uptake as a function of pH. In A: (▲) Cu(II); (●) Fe(III); (■) Ni(II); (△) Zn(II). In B: (△) Ag(I); (▲) Au(III); (●) Hg(II).

metal ion for the resin. There is a wide difference between the $pH_{1/2}$ values of the different cations. Thus, the resin can be used for metal ion preconcentration and for selective separation and recovery, according to the equilibration pH. The results indicate that all the cations under examination can be preconcentrated effectively at the natural pH of environmental water, i.e., without the previous addition of any pH-adjusting reagents.

Resin capacity and sorption isotherms

The sorption isotherms of the resin were examined to establish the behavior of its chelating sites during saturation and its maximal capacity (Table 2). The results are plotted in Fig. 4. Some metals exhibit an uptake which exceeds the resin capacity as determined by the nitrogen content. This may be due to the chelating properties of the unreacted carboxylic acid of the polymer matrix.

TABLE 3

pH for 50% extraction ($pH_{1/2}$) of ions by the histidine-containing resin

Metal ion	Ag(I)	Ni(II)	Cu(II)	Zn(II)	Hg(II)	Fe(III)	Au(III)
$pH_{1/2}$	5.7	5.0	3.6	4.5	4.6	1.5	3.2

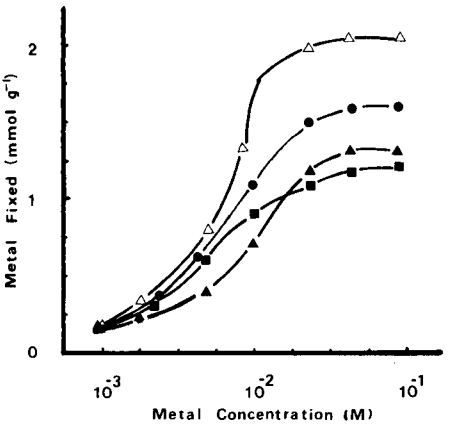

Fig. 4. Metal uptake as a function of metal concentration: (■) Ag(I); (△) Cu(II); (▲) Ni(II); (●) Zn(II).

Trace metal studies

In recent years, there has been increasing concern over the health hazard caused by pollution of the environment by heavy metals and numerous procedures have been developed for the determination of these metals. Chelating ion-exchange resins of different types have proved beneficial for preconcentration [1]. To demonstrate the usefulness of the histidine-containing resin for concentrating heavy metals and noble metals, the recovery of seven trace metals was tested for synthetic samples. The results (Table 4) showed excellent recovery for all.

The effects of complexing agents on the recoveries of Fe(III), Cu(II), Hg(II) and Ag(I) at 1 mg l^{-1} concentrations was studied by adding an excess

TABLE 4

Recovery of trace metals from aqueous media on the histidine-containing resin

Metal ion	Amount added[a] (μmol)	Amount found[b] (μmol)	Recovery (%)	Metal ion	Amount added[a] (μmol)	Amount found[b] (μmol)	Recovery (%)
Ag(I)	5.0	4.75	95	Ni(II)	5.0	4.80	96
	0.5	0.45	90		0.5	0.46	93
Cu(II)	5.0	4.90	98	Zn(II)	5.0	4.80	96
	0.5	0.48	96		0.5	0.47	94
Fe(III)	5.0	4.95	99	Au(III)	5.0	3.10	62
	0.5	0.48	96		0.5	0.35	70
Hg(II)	5.0	5.00	100		0.5	0.47[c]	94
	0.5	0.49	97				

[a]In 250 ml of pH 6.0, 0.1 M hexamine buffer. [b]Elution with 2 M HCl, except where indicated. [c]Elution with 2 M HBr.

TABLE 5

Recoveries of trace metals in the presence of various ligands with the histidine-containing resin

Ligand	Amount added (mg l^{-1})	Recovery (%)[a]			
		Fe(III)	Cu(II)	Hg(II)	Ag(I)
Sodium acetate	60	98 (6.1)	98 (6.2)	100 (4.9)	95 (6.5)
KH_2PO_4	136	57 (6.2)	97 (6.4)	100 (5.9)	92 (6.5)
Citric acid	210	46 (3.5)	98 (6.0)	100 (4.5)	89 (6.3)
	2100	36 (2.5)	—	30 (3.3)	—
Ammonium tartrate	185	84 (4.4)	75 (6.1)	100 (4.1)	81 (6.7)
	1850	80 (4.9)	—	97 (5.0)	78 (6.3)

[a]Metal ion present at the 1 mg l^{-1} level. The numbers in parentheses indicate the pH of the solution tested.

TABLE 6

Recovery of mercury (140 $\mu g\ l^{-1}$) from binary mixtures with other metal ions in a sample volume of 250 ml

Metal ion	Me:Hg[a]	Hg found ($\mu g\ l^{-1}$)	Recovery (%)	Metal ion	Me:Hg[a]	Hg ($\mu g\ l^{-1}$)	Recovery (%)
Ag(I)	10	131	94	K(I)	10^3	140	100
Cu(II)	10	119	85	Mn(II)	10	143	102
Cd(II)	10	139	99	Na(I)	10^3	140	100
Co(II)	10	137	98	Ni(II)	10	136	97
Fe(III)	10	133	95	Zn(II)	10	137	98

[a]Molar ratio.

of various ligands. As shown in Table 5, the recovery of mercury was almost unaffected by the ligands studied.

Because the results of Tables 4 and 5 showed that mercury could be recovered quantitatively and selectively, the recovery of mercury from binary synthetic mixtures was tested. The results given in Table 6 showed that there was little effect from other metal ions except copper(II) ion.

Conclusion

The results prove that the resin containing histidine groups has potential for the preconcentration of mercury from natural water or biological samples. Considerable work is still needed to increase the versatility of the preconcentration system by detailed studies of chemistries involved.

The financial support of this work by the National Science Council of the Republic of China is gratefully acknowledged.

REFERENCES

1 A. Mizuike, Enrichment Techniques for Inorganic Trace Analysis, Springer-Verlag, Berlin, 1983.
2 C. J. Gray, Mechanism der Enzymkatalyse, Akademie Verlag, Berlin, 1976, pp. 83, 174 and 190.
3 B. Chance, R. W. Estabrook and T. Yonetani, Hemes and Hemoproteins, Academic Press, New York, 1966, pp. 64, 273 and 371.
4 E. Antonini and M. Brunori, Hemoglobin and Myoglobin in their Reactions with Ligands, North-Holland Publ. Co., Amsterdam, 1971, pp. 23, 77, 88 and 349.
5 H. Rein, O. Ristau and K. Ruckpaul, Biochim. Biophys. Acta, 393 (1975) 373.
6 Ch. A. Feldt and G. T. Kekish, U.S. Patent 3047516 (1962); Chem. Abstr., 58 (1963) 1605b; U.S. Patent 3234150 (1966); Chem. Abstr., 64 (1966) 17812g.
7 H. P. Gregor, P. Teyssie, G. K. Hoeshele, R. Feinland, M. Shida and A. Tsuk, J. Am. Chem. Soc., 87 (1965) 5525.
8 G. Manecke and R. Schlegel, Makromol. Chem., 177 (1976) 3191.
9 L. D. Pettit, Pure Appl. Chem., 56 (1984) 247.
10 Y. S. Klausner and M. Bodanszky, Synthesis, (1974) 549.
11 J. R. Parrish, J. Appl. Chem., 15 (1965) 280.
12 J. Fries and H. Getrost, Organic Reagents for Trace Analysis, E. Merck, Darmstadt, 1977.
13 L. D. Pettit and J. L. M. Swash, J. Chem. Soc., Dalton Trans., (1976) 588.

Analytica Chimica Acta, 192 (1987) 95—101
Elsevier Science Publishers B.V., Amsterdam — Printed in The Netherlands

ETUDE DE LA COMPLEXATION DES LANTHANIDES TRIVALENTS PAR LES SIX ISOMÈRES DE L'ACIDE DIAMINOCYCLOHEXANE-TÉTRAACÉTIQUE

Partie 4. Détermination des Constantes de Formation des Complexes 1:1 des Lanthanides Trivalents avec Quatre Isomères. Influence des Facteurs Géométriques sur la Stabilité des Complexes et la Sélectivité des Agents Chélatants

J. CHARLIER, E. MERCINY et J. FUGER*

Laboratoire de Chimie Analytique et Radiochimie, Université de Liège, B4000-Sart Tilman-Liège (Belgique)

(Reçu le 8 juillet 1986)

RÉSUMÉ

Les auteurs déterminent, par titrage coulométrique suivi potentiométriquement, dans un milieu de force ionique égal à 1 (KCl) et à 25°C, les constantes de stabilité des complexes de stoechiométrie 1:1 avec les lanthanides trivalents des isomères *cis*-1,2, *trans*-1,3 *cis*-1,3 et *cis*-1,4 de l'acide diaminocyclohexane-*N,N,N',N'*-tétraacétique. Ils étudient l'influence de la structure moléculaire sur le pouvoir chélatant de ces agents complexants et montrent qu'il faut compter avec les facteurs géométriques.

SUMMARY

(*Study of the complexation of trivalent lanthanides by the six isomers of diaminocyclohexanetetraacetic acid. Part 4. Formation constants of the 1:1 complexes of four isomers and the effect of stereochemical factors on complex stability.*)

The stability constants of the 1:1 complexes of the trivalent lanthanides with the *cis*-1,2, *cis*-1,3, *trans*-1,3 and *cis*-1,4 isomers of diaminocyclohexane-*N,N,N',N'*-tetraacetic acid are reported for an ionic strength of 1 mol l^{-1} (KCl) at 25°C; the values were obtained by coulometric titration with potentiometric detection. The interrelationships between the molecular structure of the chelating agents and the stability constants are discussed, and the importance of stereochemical factors is emphasized.

Dans les publications précédentes [1—3], nous rendions compte du protocole de synthèse des isomères de l'acide diaminocyclohexanetétraacétique (DCTA) et de leurs constantes d'acidité dans un milieu de force ionique égal à 1 (KCl) et à 25°C. Nous déterminions également les constantes de formation des complexes de stoechiométrie 1:1 avec les lanthanides trivalents pour deux de ces ligands, le *trans*-1,2-DCTA et le *trans*-1,4-DCTA, dans le même milieu. Dans ce travail, nous étudions les propriétés complexantes vis-à-vis des lanthanides trivalents des quatre autres isomères du DCTA; nous tentons d'établir une relation entre la structure moléculaire et le pouvoir complexant de ces divers isomères.

0003-2670/87/$03.50

Les caractéristiques physicochimiques de ces composés ont été détaillées précédemment de même que les techniques expérimentales et les méthodes de mesure et de calcul pour l'interprétation des courbes de titrage potentiométrique en vue de déterminer les constantes de formation des complexes [1—3]. La zone de pH ($2 < pH < 6$) que nous considérons pour l'interprétation des courbes de titrage potentiométrique est limitée du côté des pH élevés par la précipitation de l'hydroxyde de lanthanide. D'autre part, il est inutile de travailler en milieu trop acide. En effet, les constantes de formation des complexes sont relativement faibles et par conséquent, la quantité de complexe formé ne devient significative qu'aux environs de pH égal à 2. Ainsi, par exemple, pour le complexe samarium/*trans*-1,4-DCTA dont la constante de stabilité vaut $10^{-8,56}$, le pourcentage de complexation du cation à pH 2 vaut 4,5.

RÉSULTATS ET DISCUSSION

Le Tableau 1 reprend les valeurs des constantes de formation des complexes de stoechiométrie 1:1 des agents étudiés avec les lanthanides trivalents. A la Fig. 1, nous reportons ces valeurs en fonction du nombre atomique des lanthanides. Deux constatations s'imposent: comme souligné précédemment [2] et si on exclut le cas des deux isomères du 1,2-DCTA, l'ordre de grandeur des constantes de formation (K) des complexes 1:1 des isomères du DCTA avec les terres rares fait ressortir une analogie de comportement avec les acides aminodiacétiques. Quant à la sélectivité, elle est intermédiaire entre celle des acides diaminotétraacétiques et celle des acides aminodiacétiques en général. En ce qui concerne le *trans*-1,2-DCTA, son comportement et ses propriétés sont parfaitement connues [4—6]; il se comporte comme un acide hexadenté, tous les sites actifs participent à la complexation de l'ion métallique provoquant ainsi, tout comme l'EDTA, le départ d'au moins 6 molécules d'eau. On attribue généralement à sa plus grande rigidité ses performances supérieures à celles de l'EDTA. Nous l'avons repris dans le Fig. 1 et le Tableau 1 à titre purement comparatif pour souligner combien, tout en ayant la même formulaire moléculaire, il a un comportement différent de celui des autres isomères du DCTA. La Fig. 1 montre que, d'une manière générale, l'allure de la courbe de log K en fonction du nombre atomique des lanthanides est quasi-monotone du lutétium au gadolinium et du samarium au lanthane avec une discontinuité plus ou moins marquée suivant les cas, au niveau du gadolinium. Si l'on admet généralement que cette discontinuité est due à une variation du nombre de molécules d'eau d'hydratation, les avis divergent quant à l'espèce concernée par cette déshydratation. Rappelons, en effet, à ce sujet que plusieurs hypothèses ont été formulées: ainsi, selon certains, c'est le nombre de molécules d'eau fixées sur l'ion non complexé qui varie avec le rayon des lanthanides tandis que pour d'autres, c'est le nombre de molécules d'eau de l'ion complexé qui est différent. Il faut se rappeler également que log K résulte d'une contri-

TABLEAU 1

Constantes de formation des complexes de stoechiométrie 1:1 des agents étudiés avec les lanthanides trivalents[a]

Lanthanides	*Cis*-1,2-DCTA			*Cis*-1,3-DCTA			*Trans*-1,3-DCTA			*Cis*-1,4-DCTA			*Trans*-1,4-DCTA			*Trans*-1,2-DCTA	
	Log K	pK_{a_1}	pK_{a_2}	Log K	pK_{a_1}	pK_{a_2}	Log K	pK_{a_1}	pK_{a_2}	Log K	pK_{a_1}	pK_{a_2}	Log K	pK_{a_1}	pK_{a_2}	Log L	pK_{a_2}
Lanthane	3,71	4,88	7,62	6,24	6,30	8,75	7,02	5,55	7,87	7,13	6,76	7,61	7,3	5,8	7,4	16,3	2,4
	±0,01	±0,05	±0,05	±0,05	±0,2	±0,1	±0,2	±0,4	±0,3	±0,02	±0,05	±0,05	±0,2	±0,3	±0,3	±0,1	±0,1
Cérium	—	—	—	6,50	5,92	8,42	7,36	5,40	7,78	7,64	6,20	7,30	7,5	5,84	7,3	16,97	2,28
				±0,02	±0,08	±0,1	±0,1	±0,05	±0,05	±0,02	±0,05	±0,05	±0,1	±0,08	±0,1	±0,05	±0,05
Praséodyme	—	—	—	6,78	5,76	8,29	7,48	5,34	7,76	7,47	6,07	7,30	7,76	5,89	7,18	17,30	2,18
				±0,02	±0,05	±0,05	±0,02	±0,02	±0,01	±0,02	±0,03	±0,02	±0,02	±0,05	±0,06	±0,02	±0,04
Néodyme	4,41	—	7,02	7,08	5,39	8,19	7,55	5,25	7,67	7,51	6,14	7,38	7,96	5,91	7,03	17,73	2,11
	±0,02		±0,03	±0,01	±0,02	±0,02	±0,01	±0,02	±0,02	±0,02	±0,02	±0,02	±0,01	±0,03	±0,03	±0,01	±0,01
Samarium	4,72	4,83	6,85	7,44	5,21	7,71	8,05	5,35	7,50	8,02	6,06	7,07	8,56	6,02	6,45	18,50	1,78
	±0,03	±0,08	±0,08	±0,01	±0,02	±0,01	±0,01	±0,01	±0,01	±0,01	±0,02	±0,02	±0,01	±0,01	±0,02	±0,01	±0,02
Europium	—	—	—	7,60	5,15	7,61	—	—	—	—	—	—	—	—	—	—	—
				±0,01	±0,02	±0,02											
Gadolinium	4,37	—	7,00	7,28	5,36	7,91	7,95	5,12	7,48	8,35	5,80	6,57	8,56	5,95	6,41	18,97	1,66
	±0,02		±0,2	±0,01	±0,01	±0,01	±0,01	±0,01	±0,02	±0,01	±0,01	±0,01	±0,01	±0,01	±0,01	±0,01	±0,02
Terbium	—	—	—	7,82	5,18	7,19	8,22	5,06	7,43	8,80	5,75	6,28	8,79	5,82	6,28	19,62	1,38
				±0,01	±0,01	±0,01	±0,01	±0,01	±0,01	±0,01	±0,01	±0,01	±0,01	±0,01	±0,01	±0,04	±0,05
Dysprosium	4,70	4,48	6,72	8,18	5,21	7,08	8,41	4,83	7,28	8,96	5,78	6,15	9,03	5,75	6,14	19,98	1,35
	±0,01	±0,05	±0,04	±0,01	±0,01	±0,01	±0,01	±0,01	±0,01	±0,01	±0,01	±0,01	±0,01	±0,01	±0,01	±0,02	±0,03
Holmium	—	—	—	8,21	5,00	7,09	8,52	4,61	7,16	9,13	5,61	5,94	9,27	5,66	6,03	20,29	1,30
				±0,01	±0,01	±0,01	±0,01	±0,01	±0,01	±0,01	±0,01	±0,01	±0,01	±0,01	±0,01	±0,02	±0,03
Erbium	—	—	—	8,21	5,05	7,10	8,70	4,51	7,04	9,43	5,63	6,09	9,46	5,62	5,86	20,63	1,24
				±0,01	±0,01	±0,02	±0,01	±0,01	±0,01	±0,02	±0,03	±0,02	±0,01	±0,01	±0,01	±0,02	±0,04
Thulium	4,40	5,13	6,93	8,30	4,98	7,12	8,66	4,44	7,12	9,47	5,42	5,75	9,69	5,56	5,70	20,98	1,22
	±0,03	±0,08	±0,08	±0,01	±0,01	±0,01	±0,01	±0,01	±0,01	±0,01	±0,01	±0,01	±0,01	±0,01	±0,01	±0,02	±0,03
Ytterbium	—	—	—	8,42	4,85	7,04	8,72	4,23	7,12	9,69	5,23	5,58	9,83	5,49	5,67	21,28	1,16
				±0,01	±0,01	±0,01	±0,01	±0,01	±0,01	±0,01	±0,01	±0,01	±0,01	±0,01	±0,01	±0,03	±0,03
Lutétium	4,81	—	6,44	8,42	4,82	7,02	—	—	—	9,77	5,35	5,5	9,90	5,44	5,67	21,52	1,11
	±0,01		±0,05	±0,01	±0,01	±0,01				±0,01	±0,01	±0,01	±0,01	±0,01	±0,01	±0,03	±0,04

[a]Titrage coulométrique suivi potentiométriquement (1 M KCl; 25,00 ± 0,01° C). Log K = log $[LnL^-]/[Ln^{3+}][L^{4-}]$; pK_{a_1} = —log $[LnLH][H^+]/[LnLH_2^+]$; pK_{a_2} = —log $[LnL^-][H^+]/[LnLH]$. La précipitation des hydroxydes $Ln(OH)_3$ limite l'interprétation des courbes de titrage en général à pH < 6,5 au niveau du lanthane et à pH < 6 au niveau du lutétium. L'erreur commise sur la détermination des différentes constantes est calculée comme précédemment [1].

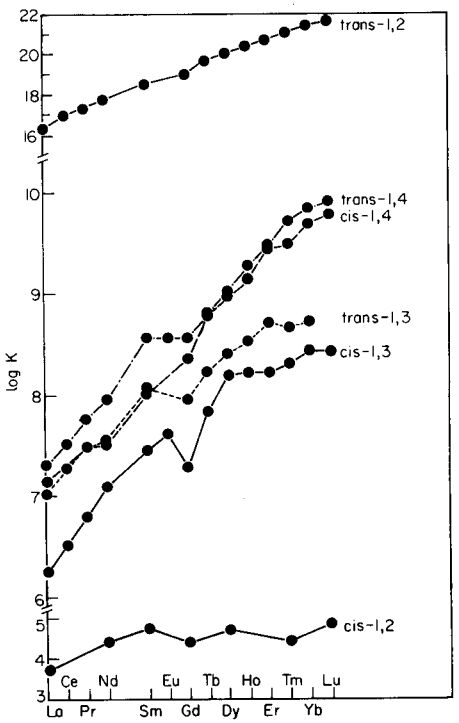

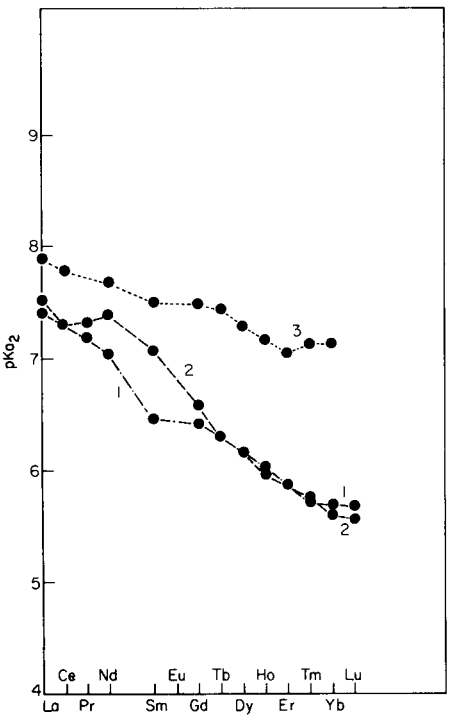

Fig. 1. Evolution du logarithme de la constante de stabilité (log K) en fonction du nombre atomique des lanthanides pour les complexes des isomères du DCTA.

Fig. 2. Evolution de pK_{a_2} de l'espèce LnLH en fonction du nombre atomique des lanthanides pour le *trans*-1,4-DCTA (courbe 1), le *cis*-1,4-DCTA (courbe 2) et le *trans*-1,3-DCTA (courbe 3).

bution enthalpique et d'une contribution entropique, toutes deux directement fonctions de l'hydratation du cation. En effet, de par la perte d'une molécule d'eau, la distance cation–site de coordination diminue. Par conséquent, l'enthalpie de formation du complexe devient plus négative tandis que l'entropie augmente. Ainsi ΔG devient plus négatif et donc log K augmente.

Si l'on analyse les résultats de façon plus détaillée, on note que le *cis*-1,2-DCTA se caractérise par des valeurs très faibles des constantes de formation de ses complexes avec les terres rares et par une sélectivité quasiment nulle pour les éléments allant du samarium au lutétium. Les constantes qu'il donne sont environ un ordre de grandeur plus petites que celles obtenues avec les acides aminodiacétiques. Ceci illustre l'influence de la taille du chélatant et de sa rigidité sur la stabilité des complexes puisque deux groupements iminodiacétiques s'ils sont mal situés sont moins performants qu'un seul. Ceci n'est concevable qu'en tenant compte d'empêchements stériques qui maintiennent le cation trivalent à une grande distance des sites les plus actifs, c'est-à-dire les deux atomes d'azote.

Les constantes obtenues avec le *cis*-1,3-DCTA sont aussi particulièrement faibles, notamment comparées à celles obtenues pour le *trans*-1,3-DCTA. De nouveau, la géométrie de la molécule est telle que les encombrements stériques sont prépondérants et maintiennent le cation à une grande distance des sites coordinatifs. Pour s'en convaincre, il suffit de se rappeler que ce composé, tout comme d'ailleurs le *cis*-1,2-DCTA, forme aisément un anhydre [3].

En comparant les isomères *trans*-1,3-DCTA, *cis*-1,4-DCTA et *trans*-1,4-DCTA, on s'aperçoit qu'au niveau des terres cériques, les valeurs de log K du *trans*-1,3-DCTA et du *cis*-1,4-DCTA sont très proches les unes des autres mais plus faibles que celles du *trans*-1,4-DCTA, tandis qu'au niveau des terres yttriques, les isomères du 1,4-DCTA tendent vers les mêmes valeurs et se différencient nettement du *trans*-1,3-DCTA qui forme avec Ln^{3+} des complexes moins stables. En étudiant les modèles moléculaires [7], on remarque, d'une part, que le *trans*-1,3-DCTA a une distance N—N maximale de 5,1 Å, le *cis*-1,4-DCTA de 5,9 Å et le *trans*-1,4-DCTA de 6,1 Å; et, d'autre part, que la rigidité des chaînes iminodiacétiques va croissant du *cis*-1,4-DCTA au *trans*-1,4-DCTA et au *trans*-1,3-DCTA. Pour les terres cériques, on peut donc dire que l'on a affaire à de gros ions hydratés qui maintiennent les deux atomes d'azote à leur distance maximale quelle que soit le rigidité des chaînes iminodiacétiques. Une distance de 5,1 Å entre les sites coordinatifs apparaît donc équivalente, sur le plan de la stabilité des complexes formés, à une distance de 5,9 Å, alors qu'une distance de 6,1 Å entre les deux atomes d'azote permet sans doute une meilleure pénétration de l'ion hydraté. Au niveau des terres yttriques, les différences observées semblent, par contre, être dues à la rigidité différente des agents chélatants; celle-ci, moins forte pour les isomères 1,4-DCTA leur permet de mieux "envelopper" le cation.

D'un autre côté, si on examine l'évolution de la constante d'acidité (pK_{a2}) de l'espèce LnLH pour le *trans*-1,4-DCTA, le *cis*-1,4-DCTA et le *trans*-1,3-DCTA (Fig. 2), on note également une similitude des valeurs au niveau des terres cériques, alors qu'au niveau des terres yttriques, les valeurs sont nettement plus faibles pour le *trans*-1,4-DCTA et le *cis*-1,4-DCTA que pour le *trans*-1,3-DCTA. Ceci peut s'interpréter de deux manières différentes. Soit, on considère que le nombre de molécules d'eau d'hydratation de l'ion Ln^{3+} est différent pour les terres cériques et les terres yttriques; il serait de 9 du lanthane au néodyme, de 8,8 pour le samarium, de 8,3 pour l'europium et redeviendrait constant et égal à 8 du terbium au lutétium [8]. Dans ces conditions, le *trans*-1,4-DCTA et le *cis*-1,4-DCTA, de moins grande rigidité, pourraient mieux "envelopper" les cations lourds puisque leur sphère d'hydratation serait plus petite. Par conséquent, l'effet enthalpique est favorisé par la diminution de la distance Ln—N et il en résulte une augmentation de la stabilité du complexe, ce qui se traduit par une diminution importante de pK_{a2}. Soit, on considère que la sphère d'hydratation est la même pour tous les ions non complexés mais que le *trans*-1,4-DCTA et le *cis*-1,4-DCTA, contrair-

ement au *trans*-1,3-DCTA, seraient capables de déplacer une molécule d'eau supplémentaire grâce à leur plus grande flexibilité.

Cependant, si on regarde plus attentivement les courbes de pK_{a2} en fonction de Z pour ces trois agents chélatants, on constate que, si jusqu'au samarium, la pente de la courbe est sensiblement la même pour ces trois acides, à partir du gadolinium, par contre, pK_{a2} diminue beaucoup plus fortement pour le *cis*-1,4-DCTA et le *trans*-1,4-DCTA. On peut dès lors imaginer que, du lanthane au néodyme, on a affaire à de gros ions en solution qui maintiennent les deux atomes d'azote à leur distance maximale. Au niveau du samarium, le rayon ionique hydraté diminuant légèrement, le composé ayant la distance N—N maximale la plus grande (c'est-à-dire, le *trans*-1,4-DCTA) commence à se "replier" pour mieux envelopper le cation. C'est donc pour ce dernier que la diminution de pK_{a2} au niveau du samarium est la plus importante. Ensuite, du terbium au lutétium, la dimension de l'ion hydraté ayant plus fortement diminué, chaque agent chélatant commence à se "rétracter" dans les limites permises toutefois par leur mobilité respective.

Mis à part le *cis*-1,2-DCTA, les divers isomères du DCTA présentent une sélectivité appréciable, plus faible cependant que celle de l'EDTA (à l'exception du *trans*-1,2-DCTA qui présente une plus grande sélectivité), mais qui peut néanmoins être mise à profit pour une séparation chromatographique des terres rares. Notons à ce sujet qu'il n'est pas nécessaire d'avoir des composés très stables pour réaliser de bonnes séparations car, plus le complexe est stable, plus la cinétique des réactions est faible et c'est un facteur dont il faut, sans aucun doute, tenir compte. En effet, c'est non seulement le facteur de séparation, et par conséquent la sélectivité, qui importe dans ce domaine mais, plus encore, les cinétiques de complexation et de décomplexation qui agissent sur la valeur de la hauteur équivalente à un plateau théorique (HEPT) et influencent l'efficacité des séparations [9—13].

Dans un premier temps, les chercheurs ont cru que, plus le nombre de pôles de coordination était élevé, plus on augmentait du même coup la stabilité des complexes formés et la sélectivité des agents chélatants. En réalité, il n'en est rien. Si, en effet, des composés tels l'acide triéthylènetétranitrilohexaacétique (TTHA) [14] forment des complexes très stables avec les lanthanides, ils présentent cependant une sélectivité très faible, voire quasi nulle, car le nombre élevé de pôles de coordination provoque la déshydratation totale des lanthanides du lanthane au lutétium, de sorte que, seule, la contraction du rayon ionique intervient dans la sélectivité. Bien plus, avec des agents tels l'acide diéthylènetrinitrilopentaacétique (DTPA) [14], on observe une diminution de log K pour les terres yttriques, diminution qui s'explique par le fait que pour les ions plus petits, il n'est plus possible, pour des raisons purement stériques, de fixer la totalité des sites actifs sur le cation.

En définitive, l'expérience a montré que le meilleur compromis entre la stabilité des composés et la sélectivité de l'agent complexant était réalisé, pour les composés non cycliques, avec des acides à six fonctions coordinatives tels l'EDTA.

Toutefois, il est raisonnable de penser que les performances optimales ne sont pas encore atteintes dans ce domaine. C'est pourquoi nous avons envisagé l'étude de composés cycliques sur lesquels viennent se fixer les fonctions iminodiacétiques. Ainsi, après avoir étudié les isomères du DCTA, nous envisageons l'étude des isomères de l'acide cyclopentanetétraacétique de même que ceux de l'acide cycloheptanetétraacétique en vue de déterminer l'influence de la rigidité intrinsèque du cycle sur les performances de l'agent chélatant.

BIBLIOGRAPHIE

1 E. Merciny et J. Fuger, Anal. Chim. Acta, 160 (1984) 87.
2 E. Merciny et J. Fuger, Anal. Chim. Acta, 166 (1984) 199.
3 J. Charlier, E. Merciny et J. Fuger, Anal. Chim. Acta, 178 (1985) 299.
4 G. Schwarzenbach, R. Gut et G. Anderegg, Helv. Chim. Acta, 37 (1954) 937.
5 T. Moeller et T. M. Hseu, J. Inorg. Nucl. Chem., 24 (1962) 1635.
6 G. Anderegg, Helv. Chim. Acta, 46 (1963) 1833.
7 Framework Molecular Models, Prentice-Hall, Engelwood Cliffs, NJ, 1965.
8 A. Habenschuss et F. H. Spedding, J. Chem. Phys., 70 (1979) 2797; 73 (1980) 442.
9 P. Glentworth, B. Wiseall, C. L. Wright et J. Mahmood, J. Inorg. Nucl. Chem., 30 (1968) 967.
10 G. A. Nyssen et D. W. Margerum, Inorg. Chem., 9 (1970) 1814.
11 W. D'Olieslager et A. Oeynen, J. Inorg. Nucl. Chem., 40 (1978) 1565.
12 E. Brücher et G. Laurenczy, J. Inorg. Nucl. Chem., 43 (1981) 2089.
13 E. Merciny, Thèse de doctorat, Université de Liège (1968).
14 A. E. Martell, Critical Stability Constants, Vol. 1: Amino Acids, Plenum Press, New York, 1974.

Analytica Chimica Acta, 192 (1987) 103—107
Elsevier Science Publishers B.V., Amsterdam — Printed in The Netherlands

Short Communication

AUTOMATED DETERMINATION OF MOLYBDENUM(VI) IN SEAWATER BY MEANS OF CONSTANT-CURRENT REDUCTION OF THE ADSORBED 8-QUINOLINOL COMPLEX IN A COMPUTERIZED FLOW POTENTIOMETRIC STRIPPING ANALYZER

CHI HUA, DANIEL JAGNER* and LARS RENMAN

Department of Technical Analytical Chemistry, Chemical Center, University of Lund, P.O. Box 124, S-221 00 Lund (Sweden)

(Received 17th June 1986)

Summary. Molybdenum(VI) in seawater is determined by means of potentiostatic adsorption of the 8-quinolinol complex onto a mercury film electrode at —0.2 V vs. SCE and subsequent reduction of the complex by means of constant-current stripping in 5 M calcium chloride medium with a fully automated stripping analyzer. A single stripping peak at —0.42 V vs. SCE was obtained. The molybdenum(VI) concentration in reference seawater NASS-1, with a certified value of 11.5 ± 1.9 μg l^{-1}, was found to be 8.9 ± 1.3 μg l^{-1} ($n = 10$).

Progress in adsorptive stripping analysis has increased the number of elements that can be determined by electrochemical stripping techniques [1]. In addition to the well known determinations of nickel and cobalt as their dimethylglyoxime complexes, methods for the determination of uranium, iron, copper and vanadium have been proposed by van den Berg and coworkers [2—5] and for aluminium by Wang et al. [6]. These procedures are based on differential cathodic stripping voltammetry after adsorptive accumulation of a suitable metal complex onto a hanging mercury drop electrode. Even though adsorptive accumulation for 1 min is normally sufficient, the whole analytical procedure is somewhat time-consuming because it requires sample deoxygenation by inert gas bubbling. Furthermore, changing and cleaning of electrodes between samples are more difficult to automate in a batch system than in a flow system. The determination of nickel and cobalt as their dimethylglyoxime complexes has successfully been transferred to a flow system based on constant-current reduction with simultaneous recording of the potential vs. time transient at a mercury film electrode [7]. The flow approach not only simplifies the procedure but it also makes it possible to optimize the chemical conditions both during adsorptive accumulation and during constant-current stripping.

The purpose of this work was to attempt to transfer the batch system for the determination of molybdenum(VI) proposed by van den Berg [8] to a computerized analyzer for potentiometric and constant-current stripping methods in order to obtain a fully automated procedure for the determination of molybdenum(VI) in seawater.

0003-2670/87/$03.50

Experimental

Instrumentation. The main parts of the flow system, which has been described in detail elsewhere [9], consist of a thin-layer cell with a glassy carbon working electrode (3-mm diameter) into which six different solutions can be sucked by means of a peristaltic pump. During operation, the electrode potential, the flow rate, the magnitude of the constant current, and operation of the six inlet valves and sampler are under computer control. After recording of the stripping and background curves, the controlling computer program localizes the stripping peak potential, integrates the peak over a pre-chosen potential width and finally reports, digitally and graphically, the results obtained by either the standard addition or calibration graph procedures. All potentials mentioned below are measured against the saturated calomel electrode (SCE).

Reagents. All reagents used were of analytical grade and all dilutions were made with Millipore-Q water. A stock solution of 8-quinolinol (0.20 M) was prepared by dissolving the reagent in 0.45 M hydrochloric acid. A stock solution of molybdenum(VI) (1 g l^{-1}) was prepared by dilution of Titrisol (Merck) standard solution. Nearly saturated aqueous calcium chloride solution (5 M) was prepared from calcium chloride dihydrate (Merck, p.a.). Seawater reference samples from southeast Bermuda (NASS-1) and off Halifax harbour (CASS-1) were purchased from the National Research Council of Canada.

Procedure for seawater. Add 50 μl of 8-quinolinol stock solution to 5 ml of the seawater sample and adjust to pH 2.6 with sodium hydroxide solution. Repeat the procedure with another aliquot of the sample to which 10 μg l^{-1} of molybdenum(VI) has been added and transfer the solutions to two inlet tubes of the analyzer.

The first step in the automated procedure is formation of a fresh mercury film for 30 s in a 2.5 M calcium chloride solution containing 200 mg l^{-1} mercury(II). During plating, the potential is decreased from −0.5 V to −1.0 V in steps of 0.1 V and between the first two potential decrements the potential is switched off for 3 s. The sample (or in the next cycle, the sample with standard addition) is then allowed into the cell at a flow rate of 2 ml min^{-1} and adsorptive accumulation proceeds at −0.20 V for 15 s. Finally, 5 M calcium chloride containing 0.8% (v/v) acetic acid is sucked into the cell for 30 s at a flow rate of 2.5 ml min^{-1}, after which a reductive current of 6 μA is applied. The stripping potential vs. time transient is monitored at a real-time rate of 19.2 kHz until the potential reaches a value of −0.9 V. After 2 s at this potential, a potential of −0.2 V is applied for 2 s after which the background is recorded.

In the evaluation procedure, the program subtracts the background from the primary stripping curve, localizes the position of the peak potential in the pre-chosen region, −0.300 to −0.500 V, integrates the peak area in the region ±70 mV around the peak potential and displays the stripping curve graphically on printer/plotter and strip-chart recorder together with the

value obtained for the stripping time. An average filter of 30 mV is used in the digital display [9]. After analysis of the sample containing the standard addition, the program also reports the final result. The complete procedure can be repeated automatically the required number of times, after which the evaluation program reports the mean value and relevant standard deviations.

During data evaluation, the flow cell is cleaned with a mixture of ethanol and hydrochloric acid (9:1 v/v) and with 5 M hydrochloric acid. In this solution the old mercury film is removed by applying a potential of +0.15 V for 5 s.

Results and discussion

Complex formation. The complex formation between 8-quinolinol (HL) and molybdenum(VI), which is the predominant oxidation state for molybdenum in seawater, has been little investigated. Based on kinetic measurements, Knowles and Diebler [10] suggested the overall reaction

$$H^+ + HL + MoO_4^{2-} \rightleftharpoons H_2MoO_4L^-$$

with a logarithmic stability constant of 10.29. In these measurements, the total molybdenum(VI) concentration was, however, in excess of total 8-quinolinol concentration. Bantysh et al. [11] suggested the equilibria

$$MoOOH^{3+} + L^- \rightleftharpoons MoO(OH)L^{2+} \quad (\log K = 16.44)$$

$$MoOOH^{3+} + 2L^- \rightleftharpoons MoO(OH)L_2^+ \quad (\log K = 30.02)$$

for the molybdenum(VI)/8-quinolinol system.

In an attempt to establish the composition of the complex responsible for the adsorption process, the total concentration of 8-quinolinol was varied in the range 0.6—5 mM and the pH in the range 2—5 in a 0.25 M NaCl solution containing 10 $\mu g\ l^{-1}$ molybdenum(VI). Assuming that only one complex is responsible for the adsorption, a plot of the ratio between complexed and uncomplexed molybdenum(VI) gave results in very good agreement with the reaction suggested by Knowles and Diebler [10], i.e., a monoligand complex would appear to be responsible for the adsorption. Consequently, this model was used for optimizing the experimental conditions in the sample solution. In order to elucidate the speciation of the solution in detail, a much more extensive investigation, beyond the scope of this work would be necessary.

The reduction process. In seawater medium, the batch process yields two reductive stripping peaks. According to van den Berg [8], the first peak corresponds to the reduction of Mo(VI) to Mo(V) and the second peak is related to further reduction to Mo(III). In the 10 M chloride stripping medium used here, only one stripping peak was obtained, the potential being approximately —0.42 V vs. SCE. Constant-current stripping does not give any detailed information of the number of electrons involved in the reduction. By comparison with other well characterized reductions it can, however, be concluded that two, or possibly three, electrons are involved in

the reduction process. It is thus reasonable to assume that complexation between Mo(IV) [or possibly Mo(III)] and chloride ions is responsible for the stabilization of the oxidation state formed during the initial reduction step, thus preventing further reduction. This is supported by the fact that the reduction potential obtained in this study is more positive than that obtained by van den Berg [8] and that a decrease in the chloride concentration of the stripping medium decreases the stripping potential.

Adsorption potential. The effect of the adsorption potential on the electrode response was investigated by varying the potential in the region —0.1 to —0.4 V vs. SCE in 0.25 M sodium chloride at a pH of 2.6 and a total 8-quinolinol concentration of 2 mM. Optimum response was obtained between —0.15 and —0.25 V in agreement with the observations made by van den Berg [8].

Linear range. The linear range of the adsorption process was investigated by analyzing reference seawater (NASS-1) with adsorption times between 10 and 50 s and again after standard additions of 0—20 $\mu g\ l^{-1}$ molybdenum(VI) at a fixed deposition time of 15 s. In both series, the adsorption potential was —0.20 V and the solution was at pH 2.6 with a total 8-quinolinol concentration of 2 mM. The stripping peak area varied linearly with deposition time up to 40 s and with standard additions up to 15 $\mu g\ l^{-1}$. Because the concentration of molybdenum in the seawater was ca. 10 $\mu g\ l^{-1}$, it was concluded that linear response is obtained if the product of the deposition time and the molybdenum concentration is less than 400 s $\mu g\ l^{-1}$.

Analysis of seawater. Figure 1(a) shows the stripping curves obtained on the

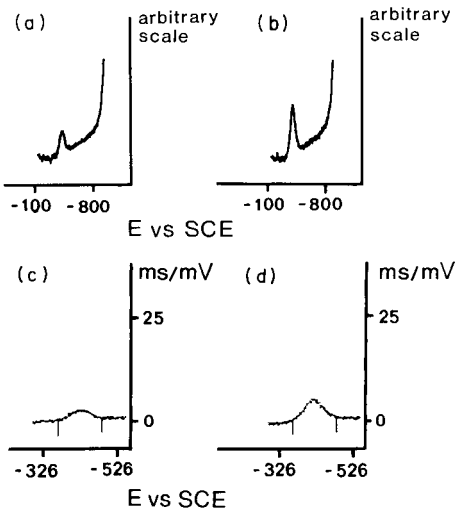

Fig. 1. Constant-current reductive stripping curves obtained on the strip-chart recorder after 15 s of potentiostatic deposition at —0.20 V: (a) in reference seawater NASS-1; (b) after a standard addition of 10 $\mu g\ l^{-1}$ Mo(VI). (c,d) Same results displayed on the printer/plotter.

strip-chart recorder after 15 s of deposition in reference seawater NASS-1, and Fig. 1(b) after the standard addition of 10 $\mu g\ l^{-1}$ Mo(VI). Figure 1(c,d) shows the same plots as obtained on the printer/plotter. Ten consecutive analyses of NASS-1 yielded an average molybdenum concentration of 8.9 $\mu g\ l^{-1}$ with a standard deviation of 1.3. This is lower than, though not significantly different from, the certified value of 11.5 ± 1.9 $\mu g\ l^{-1}$. The corresponding value obtained for CASS-1, which is not certified for molybdenum, was 7.9 ± 1.4 $\mu g\ l^{-1}$.

Interferences. Interferences can be caused either by overlapping stripping peaks from other metal/8-quinolinol complexes or by competitive adsorption of surface-active substances present in the sample. Even though 8-quinolinol is far from being a selective reagent, very few easily reducible elements are capable of forming complexes with it at pH values below 3. Addition of 20 $\mu g\ l^{-1}$ cadmium(II), lead(II) and copper(II) to 0.25 M sodium chloride solutions yielded no stripping peaks, indicating that neither these elements, nor the reagent itself, interferes with the determination.

Coastal surface waters contain organic matter (0.01—0.5 mg l^{-1}) with a surface activity similar to that of Triton X-100. Addition of 0.5 and 2.5 mg l^{-1} Triton X-100 to reference seawater NASS-1 decreased the sensitivity by about 20 and 80%, respectively. However, the recovery obtained with the standard addition method was 98% at a Triton X-100 concentration of 0.5 mg l^{-1}, so it can be concluded that competitive adsorption is a problem only in highly contaminated waters. For such samples, ultraviolet radiation prior to the measurement step is recommended.

REFERENCES

1 J. Wang, Stripping Analysis, VCH Publishers, Deerfield Beach, Florida, 1985.
2 C. M. G. van den Berg and Z. Q. Huang, Anal. Chim. Acta, 164 (1984) 209.
3 C. M. G. van den Berg and Z. Q. Huang, J. Electroanal. Chem., 177 (1984) 269.
4 C. M. G. van den Berg, Anal. Chim. Acta, 164 (1984) 195.
5 C. M. G. van den Berg and Z. Q. Huang, Anal. Chem., 56 (1984) 2383.
6 J. Wang, P. A. M. Farias and J. Mahmoud, Anal. Chim. Acta, 172 (1985) 57.
7 H. Eskilsson, C. Haraldsson and D. Jagner, Anal. Chim. Acta, 175 (1985) 79.
8 C. M. G. van den Berg, Anal. Chem., 57 (1985) 1532.
9 L. Renman, D. Jagner and R. Berglund, Anal. Chim. Acta, 188 (1987) 137.
10 P. F. Knowles and H. Diebler, Trans. Faraday Soc., 64 (1968) 977.
11 A. I. Bantysh, E. V. Dobizha and D. A. Knyazev, Zh. Neorg. Khim., 12 (1967) 2165.

Analytica Chimica Acta, 192 (1987) 109—113
Elsevier Science Publishers B.V., Amsterdam — Printed in The Netherlands

Short Communication

STORAGE AND STABILITY OF MERCURY AND METHYLMERCURY IN SEA WATER

RIAZ AHMED[a] and M. STOEPPLER*

Institute of Applied Physical Chemistry (ICH-4), Nuclear Research Centre (KFA) Jülich, P.O. Box 1913, 5170 Jülich (Federal Republic of Germany)

(Received 11th July 1986)

Summary. The long-term storage behavior of mercury and methylmercury at ng l^{-1} levels in sea water was studied at pH 4.0, 6.0, 8.0 and 10.0, and with 2% (v/v) hydrochloric or nitric acid added. Partial complexation and disappearance of mercury and methylmercury were observed; some of the lost mercury became detectable (by cold-vapour atomic absorption spectrometry) after prolonged storage.

Mercury and its compounds received much attention after the Minamata tragedy in which many people died after consuming fish which was contaminated with mercury. As fish was the source of this disease, the determination of mercury and its compounds in all species of fish likely to be used as food became very important. There are very many studies on the determination of mercury and its compounds in fish [1] and it is now well known that most of the mercury in fish occurs as methylmercury [1, 2]. Logically, the source of mercury for sea-water fish cannot be other than sea water itself. Much work has been done on the determination of mercury in sea water [3, 4] and, in some parts of the Mediterranean, the levels of mercury in fish were found to be far above the safe threshold. However, recent studies showed that the amounts of mercury reported earlier for sea water were too high [5, 6] and that the bioaccumulation of mercury by fish in the Mediterranean is higher than that in the Atlantic Ocean [7]. It has also been reported that the amount of methylmercury in sea water is only about 1% of the total mercury present [8]. Compared to the mercury level in fish, which is about 90% methylmercury, this shows an enormous bioaccumulation in the marine food chain [2, 9].

There are some problems in the determination of mercury in water samples which are obvious from interlaboratory intercomparisons [10, 11]. One of the problems is loss of mercury from solutions. This has been studied extensively for ionic mercury [12, 13], but problems associated with losses and stability of methylmercury have not been investigated in detail, simply because of the very low amounts of methylmercury and the associated

[a]Permanent address: NCD-PINTSTECH, P.O. Nilore, Islamabad, Pakistan.

0003-2670/87/$03.50

analytical problems. Some data on the storage and stability of methylmercury are available [14, 15], but the concentrations used were at the $\mu g\ l^{-1}$ level, which is much more than the actual content of mercury in sea water. The behavior of methylmercury in water systems has been shown to be complex, as will be reported elsewhere. Thus it was considered necessary to study the storage and stability of methylmercury in sea-water samples at low levels, close to the actual concentrations of mercury in sea water, under different conditions. This communication deals with the storage and stability of mercury and methylmercury in sea water at different pH values and in the presence of acids.

Experimental

All the chemicals used were of Suprapur grade (Merck). Decanted sea water was used; samples were placed in brown glass bottles, spiked with mercury(II) and methylmercury chloride at $ng\ l^{-1}$ levels and stored in the dark. The pH was adjusted with hydrochloric acid and sodium hydroxide.

Glass storage bottles were first cleaned by filling with aqua regia, then rinsed and filled with (1 + 5) nitric acid for a week. This acid solution was analyzed for any mercury. Clean bottles were further washed twice with mercury-free deionized water.

Mercury was determined by cold-vapor atomic absorption spectrometry (a.a.s.) [16, 17]; the procedure had a detection limit of 0.1 $ng\ l^{-1}$ and a linear range of 0—10 ng of mercury. Ionic mercury was determined in the usual way. The reduction mixture (10% tin(II) chloride/20% sulfuric acid) did not decompose methylmercury. Total mercury was determined after samples had been u.v.-irradiated for 4 h. The difference between ionic and total mercury was considered to be methylmercury. Sea water itself was analyzed for total mercury after treatment with (1 + 17) nitric acid and u.v.-irradiation for 6 h.

Results and discussions

Samples were stored in the dark for a total period of 3 months and analyzed at defined intervals. Figure 1A shows the storage behavior of mercury and methylmercury at pH 4.0. As can be seen, nearly 40% of added methylmercury was not detectable by the a.a.s. procedure after one day. So much methylmercury should not be decomposed so quickly in sea water, which contains normally about 3% sodium chloride. This disappearance of methylmercury is in agreement with other studies in this laboratory, which showed that in the presence of L-cysteine a major fraction of mercury was converted to an undetectable species. Sea water may contain some humic substances with sulfhydryl groups. After the initial loss, there was a gradual decomposition of methylmercury over the whole storage period, but there was some increase in total mercury which suggests that some mercury was restored to a detectable form. At pH 6.0 (Fig. 1B), the general behavior was similar except that long storage produced no increase in detectable mercury, and

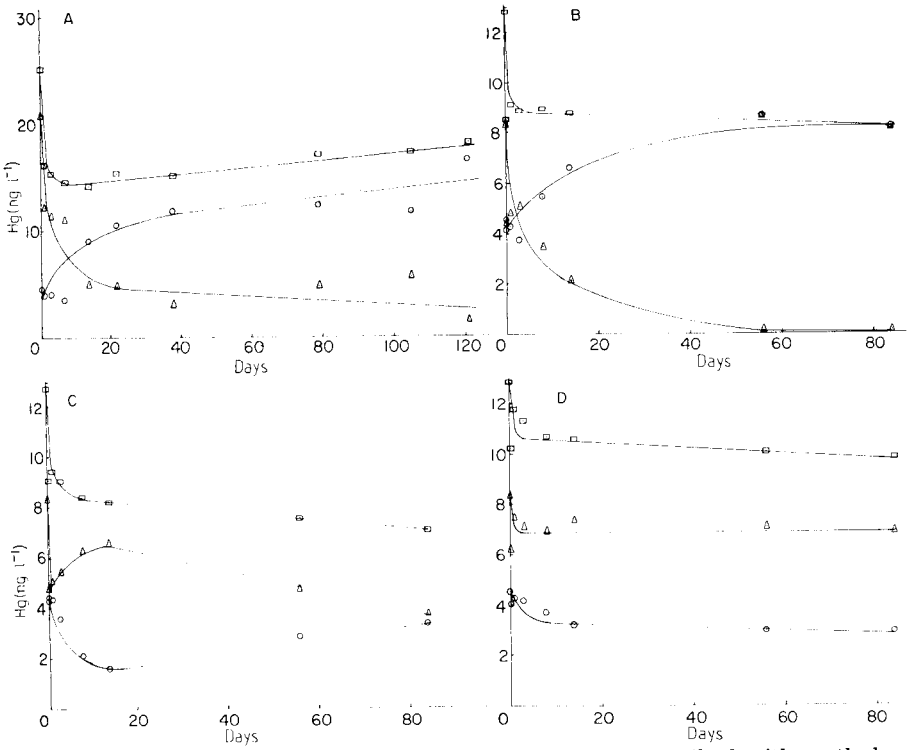

Fig. 1. Storage studies of sea water at different pH values, spiked with methylmercury and 4.0 ng l^{-1} mercury. (A) pH 4.0, 20.6 ng l^{-1} methylmercury; (B) pH 6.0, 8.24 ng l^{-1} methylmercury; (C) pH 8.0, 8.24 ng l^{-1} methylmercury; (D) pH 10.0, 8.24 ng l^{-1} methylmercury. (⊙) Ionic mercury; (△) methylmercury; (⊡) total mercury.

that the rate of decomposition of methylmercury was faster than at pH 4.0.

At pH 8.0 (Fig. 1C), the initial loss of methylmercury was similar to that at pH 4.0 or 6.0, but the rate of decomposition of methylmercury was slower, because methylmercury is relatively stable at the higher pH. After the initial conversion of nearly 40% of added methylmercury to an undetectable form, some of it was slowly restored to a detectable form during about 17 days; then methylmercury slowly decomposed to ionic mercury. There was also a gradual decrease in total mercury. At pH 10.0 (Fig. 1D), the initial disappearance of methylmercury was much less than at pH 4 or 6, which suggests that methylmercury is less reactive at this pH. After the initial loss, methylmercury remained stable for the whole storage period. There were some initial losses in total mercury and ionic mercury as well.

In the presence of 2.0% (v/v) hydrochloric acid (Fig. 2A), methylmercury was quite stable but there was an initial loss of ionic mercury which was later restored. In other work, similar data were found for rain-water samples.

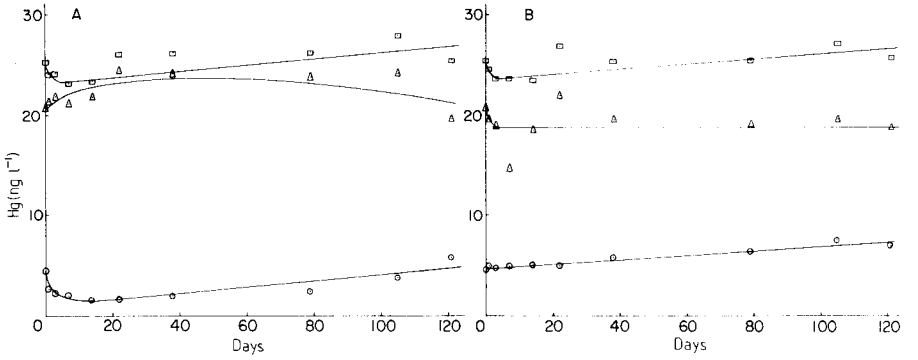

Fig. 2. Storage studies of sea water spiked with 4.0 ng l^{-1} mercury and 20.6 ng l^{-1} methylmercury. (A) 2% (v/v) hydrochloric acid added; (B) 2.0% (v/v) nitric acid added. (⊙) Ionic mercury; (△) methylmercury; (⊡) total mercury.

Commonly, when mercury is to be determined, water samples are acidified for immediate analysis. This means that some of the mercury may not be detected. When sea water was stored in the presence of 2.0% (v/v) nitric acid, there was no initial loss of ionic mercury but there was an initial loss of methylmercury although to a lesser extent than at pH 4 or 6 (Fig. 2B).

It can be concluded that reliable determination of mercury and methylmercury in sea water is difficult. Sea water appears to contain some complexing substances, probably organic compounds with sulfhydryl groups, that convert mercury or methylmercury to a form undetectable by cold-vapor a.a.s. Therefore, the results for mercury and methylmercury in sea water will not be accurate if mercury complexation is not eliminated by appropriate acidification.

One of the authors (R.A.) acknowledges financial support from the Federal Ministry of Research and Technology (BMFT), F.R.G., through the International Bureau of KFZ-Karlsruhe.

REFERENCES

1 W. Schreiber, Sci. Total Environ., 31 (1983) 283.
2 H. Egan, Proc. Anal. Div. Chem. Soc., April (1978) 117.
3 J. Olafsson, Anal. Chim. Acta, 68 (1974) 207.
4 W. F. Fitzgerald, W. B. Lyans and C. D. Hunt, Anal. Chem., 46 (1974) 1882.
5 K. May and M. Stoeppler, in G. Müller (Ed.), Proc. Int. Conf. Heavy Metals Environ., Vol. 1, CEP Consultants, Edinburgh, 1983, p. 241.
6 S. R. Aston and S. W. Fowler, Sci. Total Environ., 43 (1985) 13.
7 M. Bernhard, in K. J. Irgolic and A. E. Martell (Eds.), Environmental Inorganic Chemistry, VCH Publishers, Weinheim, 1985, p. 348.
8 J. Yamamoto, Y. Kaneda and Y. Hikasa, Int. J. Environ. Anal. Chem., 16 (1983) 1.
9 R. Ahmed, Ph.D. Thesis, Islamabad, 1982.
10 AQC Committee, Analyst, 110 (1985) 103.

11 J. Olafsson, Mar. Chem., 11 (1982) 129.
12 See, e.g., D. R. Christmann and J. D. Ingle, Jr., Anal. Chim. Acta, 86 (1976) 53.
13 M. Stoeppler and H. W. Dürbeck, in Umweltprobenbank, Bd. I, 2, Umweltbundesamt, Berlin, 1981, p. 85.
14 K. R. Olson, Anal. Chem., 49(1) (1977) 23.
15 M. Stoeppler and W. Matthes, Anal. Chim. Acta, 98(2) (1978) 389.
16 K. May, M. Stoeppler and K. Reisinger, Environ. Anal. Chem., in press.
17 K. May, R. Ahmed, K. Reisinger, B. Torres and M. Stoeppler, in T. D. Lekkas (Ed.), Proc. Int. Conf. Heavy Metals Environ., Vol. 2, CEP Consultants, Edinburgh, 1985, p. 513.

Analytica Chimica Acta, 192 (1987) 115—117
Elsevier Science Publishers B.V., Amsterdam — Printed in The Netherlands

Short Communication

IRON(III) AS RELEASING AGENT FOR COPPER INTERFERENCE IN THE DETERMINATION OF SELENIUM BY HYDRIDE-GENERATION ATOMIC ABSORPTION SPECTROMETRY

RAGNAR BYE
Department of Chemistry, University of Oslo, Box 1033, Blindern, Oslo 3 (Norway)
(Received 2nd June 1986)

Summary. Iron(III) has a very effective releasing effect on the depressive interference from copper(II) on the determination of selenium by hydride-generation atomic absorption spectrometry. In solutions with 100 mg l^{-1} Cu(II), 10 μg l^{-1} Se(IV) and 2.0 mol l^{-1} HCl, the absorbance obtained was much higher when 8 g l^{-1} Fe(III) was added than for any earlier releasing agent.

Of the elements that interfere seriously in the determination of selenium by hydride-generation a.a.s., copper and nickel are important, as these are common elements in metallurgical samples. When copper is analyzed for selenium by this technique, selenium has been separated from the matrix by coprecipitation with hydrated iron oxide [1, 2] or lanthanum hydroxide [3]. Alternatively, copper can be removed electrolytically prior to the generation of hydrogen selenide [4]. As such steps include risks of loss of analyte, it would be better if selenium in copper samples could be determined in the sample solution without prior separation.

It was recently demonstrated that iron(III) could minimize the serious interference from nickel(II) in the determination of selenium by hydride-generation a.a.s. [5, 6]. Copper depresses the selenium signals even more strongly than nickel does. Many attempts have been made to overcome this problem by using various complexing agents, but no method appears to be completely successful. In view of the promising results for nickel, it was decided to examine whether iron(III) could be used to decrease the interference from large amounts of copper.

Experimental

Equipment and solutions. A Perkin-Elmer 300 atomic absorption spectrometer was used with a discharge lamp for selenium operated at 6 W. The selenium signals were measured at 196.0 nm and recorded on a Radiometer Servograph REC-51 recorder. The Perkin-Elmer MHS-10 hydride generation system and a 10-cm single-slot burner with an air/acetylene flame (10.5/3.5 l min^{-1}) were used as recommended by the manufacturer. Argon (99.99%) was used as purging gas for the generating system.

0003-2670/87/$03.50

The salts used for the test solutions were copper(II) chloride dihydrate and iron(III) chloride hexahydrate, both analytical grade. The sodium tetrahydroborate solution (3% w/v) was prepared by dissolving the salt (Fluka, p.a. grade) in 1% (w/v) sodium hydroxide solution; it was filtered before use. A selenium(IV) standard solution (5 mg l^{-1}) was prepared by diluting a 1000 mg l^{-1} solution prepared from sodium selenite (Fluka, p.a. grade).

Procedure. The test solutions containing the chosen concentrations of iron(III), copper(II), selenium(IV) and hydrochloric acid were prepared in 100-ml volumetric flasks; three 10-ml aliquots at each concentration were examined; the means of these data are reported.

Results and discussion

The effect of iron(III) was examined on three sets of solutions containing 10 μg l^{-1} selenium(IV), 100 mg l^{-1} copper(II), and increasing concentrations of iron(III), up to 8 g l^{-1}, in 1, 2 and 4 mol l^{-1} hydrochloric acid. The results (Fig. 1) show that the absorbances increased up to 4 g l^{-1} iron(III). The increase at lower iron concentrations was most pronounced for the 2 and 4 mol l^{-1} acid solutions, probably because of increased formation of chlorocopper(II) complexes at the higher chloride concentrations [7]. With >4 g l^{-1} iron(III), further increase in absorbance was small at all acid concentrations, and 4 mol l^{-1} hydrochloric acid gave the lowest signals, probably because of increasing concentrations of species such as $FeCl_4^-$ and $FeCl(H_2O)_5^{2+}$. The results in Fig. 1 could be explained by the relative effects of hydrogen ions and chloride ions on the copper and iron species.

The influence of the concentration of copper(II) (up to 1.6 g l^{-1}) on the selenium signals in the presence of 8 or 16 g l^{-1} iron(III) was investigated for solutions containing 10 μg l^{-1} selenium(IV) in 2 mol l^{-1} hydrochloric acid. The results obtained showed that the signals decreased continuously with increasing concentration of copper(II) in both cases and that an iron(III) concentration of 16 g l^{-1} had no advantage over 8 g l^{-1}. But quite

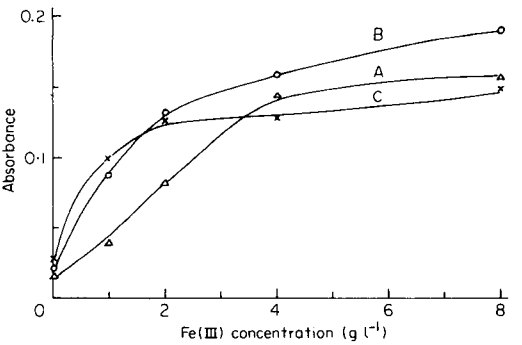

Fig. 1. Influence of the concentration of iron(III) on measurements of 100 ng of Se(IV) in 100 mg l^{-1} Cu(II) solutions at different acidities: (A) 1.0, (B) 2.0, (C) 4.0 mol l^{-1} hydrochloric acid.

satisfactory results were obtained with 8 g l^{-1} iron(III); for instance, the absorbance was 0.05 for 10 μg l^{-1} selenium(IV) at a copper(II) concentration of 600 mg l^{-1} and 0.22 at 100 mg l^{-1} copper(II). Similarly high sensitivities for selenium in the presence of such concentrations of copper do not seem to have been achieved previously. For example, in previous work with thiourea, which was then considered one of the most effective masking agents, the absorbance was ca. 0.08 for 10 μg l^{-1} selenium(IV) in the presence of 100 mg l^{-1} copper(II) [8]. Further work on methods for the determination of selenium in copper (and nickel) samples by adding iron(III) is in progress.

REFERENCES

1 K. Ohta and M. Suzuki, Anal. Chim. Acta, 77 (1975) 288.
2 K. Siu and S. S. Berman, Anal. Chem., 56 (1984) 1808.
3 M. Bèdard and J. D. Kerbyson, Can. J. Spectrosc., 21 (1976) 64.
4 R. Bye, Anal. Chem., 57 (1985) 1481.
5 B. Welz and M. Melcher, Analyst, 109 (1984) 577.
6 R. Bye, Analyst, 111 (1986) 111.
7 P. N. Vijan and D. Leung, Anal. Chim. Acta, 120 (1980) 141.
8 R. Bye, L. Engvik and W. Lund, Anal. Chem., 55 (1983) 2457.

Analytica Chimica Acta, 192 (1987) 119—124
Elsevier Science Publishers B.V., Amsterdam — Printed in The Netherlands

Short Communication

SPECTROPHOTOMETRIC STUDY OF A TERNARY ZIRCONIUM/FLUORIDE/ALIZARIN COMPLEX WITH APPLICATION TO THE DETERMINATION OF ZIRCONIUM

R. LÓPEZ NUNEZ, M. CALLEJÓN MOCHÓN* and A. GUIRAÚM PÉREZ

Department of Analytical Chemistry, Faculty of Chemistry, University of Seville, 41012 Seville (Spain)

(Received 18th February 1986)

Summary. A ternary zirconium/fluoride/alizarin complex is extracted into methyl isobutyl ketone. The apparent molar absorptivity at 556 nm is 1.52×10^5 l mol^{-1} cm^{-1}. The r.s.d. is 1.3% for 10 μg Zr (n = 12). There are several interferences, some of which can be masked with EDTA.

Alizarin and alizarin red S have been used widely for the spectrophotometric determination of zirconium [1]. Recently, anthraquinones were used to form ternary metal complexes in the presence of other organic [2—5] and inorganic [6, 7] ligands to enhance sensitivity and selectivity. This communication reports an investigation of the conditions affecting the formation and extraction into methyl isobutyl-ketone (MIBK) of a zirconium/fluoride/alizarin complex with subsequent spectrophotometric determination of zirconium in the organic phase.

Experimental

Apparatus. Perkin-Elmer Model 554 and Coleman 55 spectrophotometers were used with 1.0-cm glass or quartz cells. A Beckman Model 70 pH meter was used with a combination glass electrode. Extractions were done with a Selecta Model Vibromatic 384 mechanic shaker.

Reagents. All reagents used were of analytical-reagent grade. Distilled/deionized water was used throughout. A stock zirconium solution (1 mg ml^{-1}) was prepared by dissolving zirconium(IV) chloride in 1 M hydrochloric acid. The solution was standardized by titration with EDTA, with eriochrome black T, as indicator [8]. Other zirconium solutions were prepared by dilution with water. Alizarin (0.1104 g) was dissolved in 100 ml of MIBK to give a 4.6×10^{-3} M solution, which was stable for at least two months. This solution was diluted as required. A 1 M buffer was prepared by dissolving 37.0 g of ammonium fluoride and enough ammonia to give pH 8.9 in 1 l of water; it was stored in a polyethylene bottle.

Recommended procedure. Place 15 ml of zirconium solution containing ⩽20 μg of zirconium, 25 ml of pH 8.9 buffer and 10 ml of 1.15×10^{-3} M

0003-2670/87/$03.50

alizarin solution in MIBK in a 100-ml separating funnel, and shake for 10 min. Separate the phases and centrifuge the organic phase. Measure its absorbance at 556 nm against a reagent blank in 1.0-cm cells.

Determination of zirconium in a magnesium alloy. Weigh accurately about 0.5 g of alloy into a 100-ml Erlenmeyer flask and dissolve in 3 M hydrochloric acid. Transfer the solution to a 100-ml volumetric flask and dilute to the mark with 3 M hydrochloric acid. Remove a 25-ml aliquot, and add to it 5 ml of aqueous 2.5×10^{-2} M cupferron solution. Extract the precipitate twice with 10-ml portions of MIBK, transfer the extract to a 25-ml volumetric flask and dilute to volume with MIBK. Take 0.5 ml of the solution, add to it 2 ml of 2.7×10^{-2} M disodium EDTA and proceed as in the recommended procedure.

Results and discussion

Alizarin in MIBK reacts with zirconium in alkaline media in the presence of fluoride to produce a violet complex in the organic phase. The absorption spectra of the complex extracted into MIBK and of a sample prepared in the same way without zirconium, both measured against the solvent as reference, are given in Fig. 1. These spectra have the greatest difference in absorbance at 556 nm. Spectra obtained similarly for solutions containing zirconium, alizarin and ammonium chloride at pH 8.9, and zirconium, alizarin and 0.1 M sodium hydroxide (to obtain the required pH) were practically the same as that of the alizarin solution. These observations

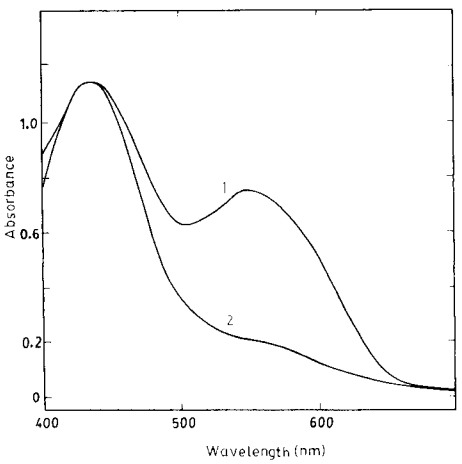

Fig. 1. Absorption spectra measured against MIBK: (1) zirconium/fluoride/alizarin complex (7.6×10^{-6} M Zr and 4.6×10^{-4} M alizarin, pH 8.9); (2) reagent blank.

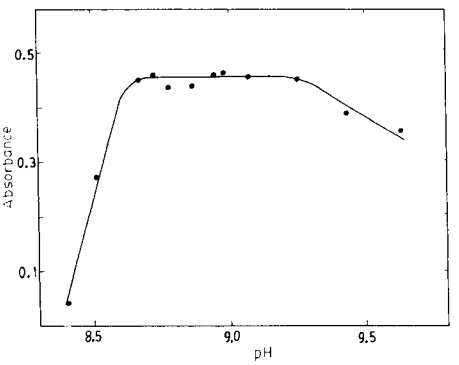

Fig. 2. Effect of the formation and extraction of the complex (reagent blank subtracted). (Buffer solutions (25 ml) of pH 8.4—9.6 were used with 3.7×10^{-6} M Zr and 4.6×10^{-4} M alizarin.)

can be interpreted as indicating the formation of a mixed-ligand complex in MIBK.

Effect of pH and other variables. To establish the optimum pH range for complex formation and extraction, zirconium was allowed to react with 1 M ammonium fluoride in solutions of pH 8.4—9.6, and the complex formed was extracted into MIBK in the presence of alizarin. Figure 2 shows that constant, maximum absorbance was obtained at pH 8.7—9.2.

The effect of fluoride concentration was investigated by addition of x ml of ammonium fluoride/ammonia buffer and $(25 - x)$ ml of ammonium chloride/ammonia buffer (both of pH 8.9), so that the ionic strength was always the same; otherwise the recommended procedure was used. The extent of formation of extractable complex increased with increasing fluoride concentration up to 0.5 M; absorbances then remained constant with up to 0.8 M fluoride so that rigorous control of the fluoride concentration is not necessary, provided that it is >0.5 M.

It was considered that the concentration of alizarin in the organic phase would affect the extraction of the ternary complex. In order to establish the optimal concentration, 4.6×10^{-5} M to 1.16×10^{-3} M alizarin was added to the solutions prepared as in the recommended procedure. At least a 40-fold molar excess of the reagent over zirconium was necessary in order to obtain maximum absorbance.

The shaking time was varied from 1 to 45 min while the other variables were kept constant. Maximum constant absorbance was obtained after 5 min; therefore a 10-min shaking period is recommended. The absorbance of the organic phase was practically constant over the volume range 3:1—4:1 aqueous/organic phase. The 4:1 ratio was chosen.

Composition of the complex. The metal/fluoride ratio in the complex was determined as follows. The complex in MIBK solution was washed three times with ammonium chloride/ammonia buffer (pH 8.9) and destroyed with 1 M hydrochloric acid. The alizarin remained in the organic phase. The aqueous phase containing the zirconium and fluoride was made up to a standard volume. Zirconium was determined by the method proposed in this work (the extraction for zirconium in triplicate determinations was 92—95%), and the fluoride was determined spectrophotometrically by the cerium(III)/alizarin complexan method [9]. The metal/fluoride ratio was found to be 1:2.

The equilibrium shift method was applied to estimate the metal/alizarin ratio, keeping the concentration of fluoride in excess. Because the extracted species must be uncharged, the charge must be neutralized by deprotonated ligands. Thus, the equilibrium between an aqueous solution containing zirconium (M^{n+}) and fluoride, and an organic solution containing alizarin (H_2A) could be formally expressed as

$$M^{n+}_{aq} + m(H_2A)_0 + pF^-_{aq} \rightleftharpoons Q_0 + q\,H^+_{aq}$$

where Q represents the ternary complex and $p = 2$. The extraction constant is

$$k_{ex} = [Q]_0 [H^+]^q_{aq} / [M^{n+}]_{aq} [H_2A]^m_0 [F^-]^p_{aq}$$

and the distribution coefficient $D = [Q]_0 / \Sigma [M^{n+}]_{aq}$. As zirconium forms fluoride and hydroxide complexes, $D = \alpha [Q]_0 / [M^{n+}]_{aq}$, where $1/\alpha = 1 + k_{1OH} [OH^-] + k_{2OH} k_{1OH} [OH^-]^2 + \ldots + k_{1F} [F^-] + k_{2F} k_{1F} [F^-]^2 + \ldots + k_{1OH1F} k_{1OH} [OH^-] [F^-] + \ldots$, k_{ij} being the consecutive stability constants for the fluoride and hydroxide complexes. Thus α is a function of pH and fluoride concentration.

Substitution, solving for D and taking logarithms gives

$$\log D = \log k_{ex} + \log \alpha + q \text{ pH} + m \log [H_2A]_0 + p \log [F^-]_{aq}$$

Plotting log D vs. log $[H_2A]_0$ at constant pH and fluoride concentration yields the slope equal to the ligand/metal ratio m in the extracted species. The slope of 2.79 obtained (r = 0.9877, 7 points) over the range log D = −1.4 to −0.1 indicates a 1:3 zirconium/alizarin ratio. The distribution coefficient was evaluated by assuming that the zirconium is totally complexed when the alizarin concentration is very high. Then $D = A\ r/(A_{max} - A)$ where r is the volume ratio of the aqueous phase to the organic phase, A is the absorbance of the extract for each concentration of the alizarin, and A_{max} is the absorbance of the extract for a large excess of alizarin.

The results obtained indicated that the mole ratio of zirconium/fluoride/alizarin in the ternary complex is 1:2:3. On the basis of other works [6, 10] it is supposed that two of the alizarin ligands are protonated, so that the complex is of the type $ZrF_2A(H_2A)_2$, where H_2A is alizarin.

Determination of zirconium. The calibration graph obtained by the recommended procedure was linear in the range 0–20 μg of zirconium. The apparent molar absorptivity at 556 nm calculated from the slope of the calibration graph was 1.52×10^5 l mol^{-1} cm^{-1}, and the Sandell sensitivity was 0.6 ng Zr cm^{-2}. The precision was estimated from 12 results for 10 μg of zirconium, which had a mean absorbance of 0.419 vs. the reagent blank, with a standard deviation of 0.0025 (relative standard deviation 1.3%). The absorbance of the reagent blank at 556 nm measured vs. MIBK was 0.138 ± 0.002 (12 measurements).

To study possible interferences, 40 ml of solution containing the diverse ion and 10 μg of zirconium was treated as in the procedure. The tolerance levels are shown in Table 1; in some cases these levels can be increased by addition of EDTA.

The method was satisfactorily applied to the determination of zirconium in a standard Ce-Zn-Zr-Mg alloy (BCS 307). Zirconium and rare earths were precipitated with cupferron [11] and separated by extraction with MIBK. About 96% of the zirconium cupferronate was extracted into MIBK. A small portion of the extract was analyzed for zirconium by the recommended procedure, after addition of EDTA to prevent interference from rare earths. The reported zirconium value for the alloy was 0.56%; the value found (± standard deviation) by triplicate determinations was 0.543 ± 0.003%. The alloy also contained 2.84% total rare earths, 2.08% zinc, 0.05% copper, 0.006% manganese and 0.02% iron.

TABLE 1

Maximum tolerance ratios for foreign ions in the determination of 10 μg of zirconium in 40 ml of solution

Tolerance ratio[a]	Ion
2500	EDTA
1000	$Cr(VI)$, Br^-, I^-, BrO_3^-, IO_3^-, SCN^-, $C_2O_4^{2-}$, NO_2^-, NO_3^-, HPO_4^{2-}, AsO_2^-, SO_4^{2-}, SO_3^{2-}, $S_2O_3^{2-}$, SeO_3^{2-} acetate, citrate, tartrate, ascorbate
500	$P_2O_7^{4-}$, ClO_4^-, CN^-, phthalate
100	La^{3+}, Ni^{2+}, Ag^+, Hg^{2+}, Mo(VI), W(VI), $B_4O_7^{2-}$, AsO_4^{3-}, ClO_3^-
50	Be^{2+}, Mg^{2+}, Bi^{3+}, Zn^{2+}, Cd^{2+}, Th^{4+}, Ca^{2+}[b], Pb^{2+}[b], Cr^{3+}[b], Mn^{2+}[b], Co^{2+}[b], Cu^{2+}[b], Sr^{2+}[b], Ba^{2+}[b], Al^{3+}[b]
10	Tl^+[b], $S_2O_8^{2-}$, IO_4^-
5	Ce^{4+}, V(V), U(VI)
1	Y^{3+}
<1	Fe^{3+}[b], Sn^{2+}[b], Ti^{4+}[b], In^{3+}[b], Ga^{3+}[b]

[a]Ratio (w/w) of diverse ion to Zr. [b]In presence of 1.7×10^{-3} M EDTA.

TABLE 2

Comparison of some spectrophotometric methods for zirconium

Reagent	Wavelength (nm)	Molar absorptivity (10^4 l mol^{-1} cm^{-1})	Ref.
Arsenazo-III	665	12.0	12
3,5-Dibromo-PADAP/ antipyrine	600	13.5	13
Chlorophosphonazo	675	21.0	14
Br-BTAE/NaLS[a]	520	44.0	15
Fluoride/alizarin	556	15.2	present method

[a]Br-BTAE/NaLS ñ 2-(6-bromo-2-benzothiazolylazo)-5-diethyldiaminophenol sodium lauryl sulphate.

The new method is compared with other sensitive methods [12—15] for zirconium in Table 2. The proposed method is one of the most sensitive for determining zirconium. It has the advantages, also, of reasonable selectivity, good reproducibility and highly stable reagent solutions.

REFERENCES

1 Z. Marczenko, Spectrophotometric Determination of Elements, Ellis Horwood, Chichester, 1976, pp. 611—619.
2 V. A. Nazarenko and G. V. Flyantikova, Zh. Anal. Khim., 27(12) (1972) 2369.
3 D. Y. Zulfugardy and I. R. Guseinov, Azerb. Khim. Zh., 2 (1972) 173.
4 E. T. Beschetnova and L. G. Anisimova, Fiz-Kim. Metody Anal. Kontrolya Proizvod, Mezhvuz. Sb., 2 (1976) 40.
5 N. L. Shestidesyatnaya and N. M. Milgaeva, Koord. Khim., 4(10) (1978) 1544; 7(9) (1981) 1380.

6 M. Roman Ceba, A. Arrebola Ramirez and J. J. Berzas Nevado, Talanta, 29 (1982) 142.
7 R. López Núñez, M. Callejón Mochón and A. Guiraúm Pérez, Talanta, 33 (1986) 587.
8 F. Bermejo and A. Prieto, Aplicaciones Analíticas del AEDT y Analogos, Ed. Univ. Santiago de Compostela, Santiago de Compostela, 1975, pp. 365—66.
9 M. Hanocq and L. Molle, Anal. Chim. Acta, 40 (1968) 13.
10 H. E. Zittel and T. M. Florence, Anal. Chem., 39 (1967) 320.
11 J. Stary and J. Smizanska, Anal. Chim. Acta, 29 (1963) 545.
12 S. B. Savvin, Talanta, 8 (1961) 672; 11 (1964) 1, 7.
13 S. I. Gusev, N. F. Garrilova and L. V. Poplevina, Zh. Anal. Khim., 32 (1977) 1363.
14 T. Yamamoto, H. Muto and Y. Kato, Bunseki Kagaku, 26 (1977) 515.
15 Zhang Chao-Ping, Qi Da-Yonh and Zhov Tian-ze, Talanta, 29 (1982) 1119.

Analytica Chimica Acta, 192 (1987) 125—128
Elsevier Science Publishers B.V., Amsterdam — Printed in The Netherlands

Short Communication

SPECTROPHOTOMETRIC DETERMINATION OF ZIRCONIUM IN STEELS WITH XYLENOL ORANGE

ABDUL MAJEED and M. S. KHAN
Chemistry Department, Islamia University, Bahawalpur (Pakistan)
E. K. BALLANTYNE (retired)
British Steel Corporation Clydebridge Works, Cambuslang, Glasgow (Great Britain)
(Received 26th April 1984)

Summary. Zirconium (0.005—0.25%) is determined after acid dissolution of the steel, and fusion of insoluble matter with sodium carbonate and sodium hydrogensulphate. Niobium and other interfering ions are removed by mercury cathode electrolysis. Residual small amounts of iron(III) are masked with ascorbic acid.

Zirconium has many useful properties (e.g., its ability to increase corrosion resistance and mechanical strength of alloys at low and elevated temperatures) which have made its determination important in special steels. Its transparency to thermal neutrons has made zirconium very useful as a construction material in nuclear reactors. There are numerous gravimetric, titrimetric and spectrophotometric methods for the determination of zirconium in steel. Classical methods [1, 2] are time-consuming and of uncertain accuracy. Small amounts are best determined spectrophotometrically; numerous reagents have been proposed [3]. Polymerization and hydrolysis of zirconium species are complicating factors, so it is desirable to use only those reagents which react in fairly acidic media, in which such complications are minimized. The determination of zirconium with alizarin sulphonate is not very sensitive and procedures based on arsenazo-III and xylenol orange seem to have been preferred in most recent work [3, 4]. In the proposed method, xylenol orange is used as the chromogenic reagent for the determination of zirconium in steel; electrolysis at a mercury cathode is used to remove interfering metals [5].

Experimental

Apparatus and reagents. A Unicam SP600 spectrophotometer was used. All reagents were of analytical grade, unless otherwise stated. Distilled water was used throughout. Xylenol orange (0.05% w/v) was prepared in 0.01 M hydrochloric acid. The stock zirconium solution (1 mg ml^{-1}) was prepared by dissolving 0.3533 g of $ZrOCl_2 \cdot 8H_2O$ in 1.25 M sulphuric acid and diluting

0003-2670/87/$03.50

to 100 ml with the same acid. A more dilute standard (20 μg ml^{-1} Zr) was made by diluting 10 ml of the 1 mg ml^{-1} solution to 500 ml with 1.25 M sulphuric acid.

Procedure. Weigh accurately ca. 0.5 g of steel into a 150-ml beaker, add 25 ml of 1.25 M sulphuric acid and 40 ml of water. Heat gently for >1 h. Add 10 drops of 15% (v/v) hydrogen peroxide and again heat gently until the sample is completely dissolved. Continue heating to decompose the excess of hydrogen peroxide. Cool and filter through a Whatman no. 540 filter paper. Retain the filter paper and precipitate for the determination of acid-insoluble zirconium.

To determine acid-soluble zirconium, dilute the filtrate to 75 ml with water, add 24 ml of mercury to the beaker and apply mercury cathode electrolysis [5], regulating the air flow so as to stir the solution. Iron, chromium, copper, nickel and cobalt are removed during this electrolysis. Use potassium hexacyanoferrate(II) to check that most of the iron has been removed; residual iron(III) can be reduced by addition of ascorbic acid. When most of the iron(III) has been removed, remove the beaker from the electrolysis apparatus while the current is still passing. Filter the solution through a Whatman no. 540 filter paper and wash the filter paper with water, taking care not to let the volume exceed 80 ml. Transfer the solution to a 100-ml volumetric flask, add 15 ml of 1.25 M sulphuric acid and dilute to volume with water. Pipette a 20-ml aliquot of this solution to a 50-ml volumetric flask, and add 5 ml of fresh 5% (w/v) ascorbic acid solution to reduce any iron(III) or molybdenum(VI) remaining after electrolysis. Add 2 ml of the xylenol orange solution and dilute to 50 ml with water. Measure the absorbance, after 10—30 min, at 540 nm in a 20-mm cuvette, against a blank prepared from zirconium-free high-purity iron (Johnson Matthey) taken through the whole procedure.

To determine acid-insoluble zirconium, ash the filter paper in a platinum crucible, treat the residue with 2 ml of 2.5 M sulphuric acid and 2 ml of 40% hydrofluoric acid and evaporate to dryness. Fuse the residue with 0.5 g of sodium carbonate and 0.5 g of sodium hydrogensulphate. When cool, treat the fused mass with 1 ml of concentrated hydrochloric acid and 2 drops of concentrated nitric acid, evaporate to dryness very carefully and add 1 ml of concentrated hydrochloric acid. Dissolve the residue in water and transfer to a 100-ml volumetric flask containing 40 ml of 1.25 M sulphuric acid. Dilute to volume with water, shake well and continue as for the acid-soluble zirconium determination by pipetting 20 ml into a 50-ml flask, adding 5 ml of 5% ascorbic acid, etc. Any traces of iron(III) which may be present are reduced by ascorbic acid and do not interfere, so that electrolysis is not required. Run a blank, using the residue from the high-purity iron.

Calibration. Weigh accurately 0.5 g of high-purity iron (99.46% iron; Johnson Matthey) into each of six 100-ml beakers. To the first beaker, add 25 ml of 1.25 M sulphuric acid. To the others, add 5, 10, 15, 20 and 25 ml of the diluted zirconium standard, making up to 25 ml with 1.25 M sulphuric

acid where necessary. Add 40 ml of water to each beaker and continue as for the determination of acid-soluble zirconium. Use the solution containing no zirconium as the blank for the spectrophotometric measurements.

Results and discussion

The spectrophotometric procedure gave a linear calibration for zirconium over the range 0.005—0.25% zirconium in steel; in the equation $y = mx + c$, $m = 6.33$, $c = 0.018$, with a correlation coefficient of 0.9981 (5 results). The method was applied to some standard steels. A comparison of the results with the certified value (Table 1) indicates the good accuracy of the method. If the samples contained more than 0.20% zirconium, the sample weight should be decreased to 0.25 g. The relative standard deviation was always within 3%.

Most probably, zirconium in steel exists as a solid solution in the iron. The digestion time for the dissolution of zirconium was found to be critical. The acid-insoluble fraction decreased with increasing digestion time until a constant value was obtained. Therefore the sample must be digested for at least 1 h during dissolution.

In the present work, xylenol orange was preferred as the chromogenic reagent on account of its high sensitivity and selectivity. Its use was first suggested by Cheng [6]. The zirconium/xylenol orange complex formed is stable between 10 and 30 min after preparation. It is recommended that a fresh reagent solution should always be used. The decomposition of xylenol orange in aqueous solutions was discussed by Pribil [7]. The ageing of zirconium solutions is also critical. For example, West [8] observed that a freshly prepared solution of zirconium reacts very rapidly with xylenol orange; as the ageing time lengthened, the rate of the chromogenic reaction decreased. When the zirconium solutions used here were kept overnight before testing, very little colour developed within 60 min. Large concentrations of xylenol orange should be avoided because they increase the absorbance [1]. It is possible that other than 1:1 complexes may be formed. In the present work, a 0.05% solution was used because it has been recommended by previous workers [1, 3]; 2 ml of the 0.05% xylenol orange

TABLE 1

Determination of zirconium in NBS steel samples

NBS no.	Zirconium (%)		Niobium (%)
	Present method[a]	Certified value	(Certified value)
1261	0.0089 ± 0.0002	0.0090	0.022
1262	0.1940 ± 0.0006	0.1990	0.29
1263	0.0490 ± 0.0003	0.0490	0.049
1264	0.0660 ± 0.0004	0.0680	0.157

[a]Mean and standard deviation for 10 samples.

solution was found to be satisfactory for up to 0.2% zirconium in steel, which was the maximum amount used in the standards.

Interferences. Interferences from various ions have been reported [1, 3, 4, 6]. In the present work, it was checked that alkali metals, alkaline earth metals, beryllium and iron(II) did not interfere. The following metal ions were tolerated in concentrations (by weight) 100 times higher than zirconium: Mn(II), Bi(III), Sn(II), Cr(III), Zn(II), Cd(II), and Pb(II). Ten times higher concentrations were tolerated for Co(II), Ti(IV), Mo(VI) and Fe(III). The effects of larger concentrations of iron(III) could be suppressed by ascorbic acid. Large amounts of Fe, Cr, Ni, Cu and Nb were removed by electrolysis. Titanium up to 0.25% did not interfere; above this amount, titanium caused negative errors. Niobium also interfered, forming a coloured complex with xylenol orange. However, no increased absorbance was observed in niobium-containing steel samples after electrolysis (Table 1), and it was concluded that niobium was removed by the mercury cathode electrolysis. This was also true for concentrations of copper more than twice that of zirconium. Interference by niobium could also be decreased by using 2.5 M sulphuric acid. Similarly, at lower acidities hafnium interfered. Hafnium complexes absorb appreciably in 0.25 M sulphuric acid but at higher acid concentrations the absorbance diminishes and in 1.25 M acid no absorbance was observed.

REFERENCES

1 A. K. Mukherji, Analytical Chemistry of Zirconium and Hafnium, Pergamon Press, Oxford, 1970.
2 W. C. Alford, L. Shapiro and K. Charles, Anal. Chem., 23 (1951) 1149.
3 See, e.g., Z. Marczenko, Spectrophotometric Determination of Elements, Horwood, Chichester, 1976, pp. 609—621.
4 F. D. Snell, Photometric and Fluorimetric Methods of Analysis, Part 2, Wiley, New York, 1978, pp. 1135—1172.
5 R. B. Hahn and J. L. Johnson, Anal. Chem., 29(6) (1957) 902.
6 K. L. Cheng, Talanta, 2 (1959) 61.
7 R. Pribil, Talanta, 3 (1959) 200.
8 T. S. West, in Trace Characterization, Chemical and Physical, Proceedings of the First Materials Research Symposium, N.B.S. Monograph 100, 1967, p. 234.

Analytica Chimica Acta, 192 (1987) 129—132
Elsevier Science Publishers B.V., Amsterdam — Printed in The Netherlands

Short Communication

THE SPECTROPHOTOMETRIC DETERMINATION OF IRON(III) IN A FLOW-INJECTION SYSTEM WITH A MIXED SOLVENT

T. J. CARDWELL*, D. CARIDI and R. W. CATTRALL

Analytical Laboratories, Department of Chemistry, La Trobe University, Bundoora, Victoria 3083 (Australia)

I. C. HAMILTON

Analytical Laboratories, Department of Chemistry, Footscray Institute of Technology, Footscray, Victoria 3011 (Australia)

(Received 2nd July 1986)

Summary. A fast and sensitive flow-injection procedure is described for the determination of iron(III). The complexing agent is ammonium diisopropyldithiophosphate in a 1:1 (v/v) isopropanol/water carrier stream. The linear range is 0.05—15 mg l^{-1} iron(III) with a detection limit of 0.01 mg l^{-1} and the injection rate is about 400 h^{-1}.

Several spectrophotometric procedures have been used in flow injection analysis for the determination of iron [1—10]. Some have been based on the measurement of total iron and others have measured iron(II) and/or iron(III) species in solution. In many of these procedures, 1,10-phenanthroline has been used as the reagent. For the determination of total iron, iron(III) in the sample was reduced by ascorbic acid [1, 2] or on-line in a Jones reductor mini-column [3] for reaction with 1,10-phenanthroline. In the absence of a reducing agent, iron(II) has been determined directly with the same chromogenic reagent [2—6]. Faizullah and Townshend [3] described the simultaneous spectrophotometric determination of iron(II) and iron(III) by splitting the sample into two streams; one portion was passed through a Jones reductor and a delay coil before recombining with the other stream to merge with a reagent stream to give two responses, one for iron(II) and the other for total iron, and so iron(III). Lynch et al. [6] used two reagents, thiocyanate and 1,10-phenanthroline, in parallel streams for the spectrophotometric determination of iron(II) and iron(III), but this procedure required two spectrophotometers.

Other reagents that have been recommended for the spectrophotometric determination of iron(II) or total iron include 2,4,6-tripyridyl-1,3,5-triazine with hydroxylammonium chloride to reduce iron(III) [7] and 2-(3,5-dibromo-2-pyridylazo)-5-[*N*-ethyl-*N*-(3-sulfopropyl)amino] phenol with ascorbic acid as the reducing agent [8]. Iron(III) has been determined with β-resorcyclic acid, sulfosalicylic acid and potassium thiocyanate [9] or as the

0003-2670/87/$03.50

chloro-complex in strong hydrochloric acid media [10]. All these procedures rely on the formation of water-soluble iron species for spectrophotometric detection. As numerous reagents produce iron complexes with limited solubility in water, this communication deals with a sensitive flow-injection procedure based on one such complex. Iron(III) is determined by measuring the absorbance of a dialkyldithiophosphate complex in an aqueous-alcoholic medium.

Experimental

Reagent and solutions. Ammonium diisopropyldithiophosphate was synthesized by the procedure described for the diethyl salt [11]. The ligand solution was prepared by adding phosphorus pentasulfide to an excess of isopropanol (Nanograde, Mallinckrodt) and ammonia gas was bubbled through the mixture to produce the salt. Excess of solvent was removed by evaporation and the white solid was purified by recrystallization from isopropanol/diethyl ether. The crystals were collected and washed with diethyl ether.

A 1000 mg l^{-1} stock solution of iron(III) was prepared by dissolving 1 g of iron wire (May and Baker, 99.3%) in 100 ml of 8 M nitric acid and diluting to 1 l with Nanopure deionized water (Barnstead). Iron(III) standard solutions were prepared by dilution of the stock solution with isopropanol water and 8 M nitric acid so that the final solutions were in 1:1 (v/v) isopropanol/water with pH < 3. The carrier stream was 0.01 M ammonium diisopropyldithiophosphate in 1:1 (v/v) isopropanol/water adjusted to pH < 3 with nitric acid. All solutions were degassed by sonication before use.

Equipment. A single-channel flow-injection manifold was assembled. A Gilson Minipuls-II peristaltic pump was used to deliver the carrier stream which was filtered in the reservoir through a small sintered glass filter (porosity 4). The flow rate was 1 ml min^{-1}. Solvaflex pump tubing (Technicon) was required on the peristaltic pump because of its compatibility with the components of the ligand carrier solution. A Rheodyne 7125 injector fitted with a 5-μl sample loop made from teflon tubing (0.3 mm i.d.) was used for sample introduction into the carrier stream. The reaction coil had a total length of 35 cm and consisted of 10 cm of teflon tubing (0.3 mm i.d.) butt-jointed through a zero volume union to the end of the stainless steel inlet tubing (250 × 0.23 mm i.d.) of the detector flow cell. The iron(III) chelate was detected with a Waters Associates Model 441 absorbance detector at 365 nm.

Results and discussion

Iron(III) reacts with ammonium diisopropyldithiophosphate in acidic aqueous media to produce an intense blackish-green crystalline precipitate of composition $Fe[S_2P(OC_3H_7)_2]_3$. The complex is soluble in a 1:1 (v/v) water/alcohol mixture, and so can be used for the spectrophotometric determination of iron(III).

Preliminary studies showed that complexation was rapid when samples of iron(III) were injected into a carrier stream which contained ammonium diisopropyldithiophosphate in 1:1 (v/v) isopropanol/water adjusted to pH < 3 with nitric acid. The optimum concentration of ligand in the carrier stream was found to be 0.01 M; higher concentrations gave large background absorbances at high detector sensitivities apparently caused by refractive index differences between the sample and the carrier stream. For sample concentrations of iron(III) below 1 mg l^{-1}, the peak responses must be corrected for background even with the 0.01 M ligand concentration. Results reported below have been corrected for background absorbance. Spectral scans of both the ligand and the metal complex in the solvent used as the carrier stream showed an absorption band maximum for the metal complex at 365 nm (molar absorptivity 8.5×10^3 l mol^{-1} cm^{-1}); there was no interference from the ligand at this wavelength. Excellent sensitivities were achieved in the flow-injection procedure by using a 5-μl sample loop and a 35-cm reaction coil. Figure 1 shows the calibration curve obtained for injections of samples containing up to 100 mg l^{-1} iron(III). The upper limit in the linear range is about 15 mg l^{-1} iron(III) and the curvature of the plot is due to insufficient complexing agent in the carrier stream.

Excellent linearity was achieved for a series of standards in the range 0.05—15 mg l^{-1} iron(III) with a correlation coefficient of 0.9993. The limit of detection was 0.01 mg l^{-1} and the precision was acceptable (r.s.d. < 2% for all the standards). At a carrier flow rate of 1 ml min^{-1}, the residence time for each injection is less than 10 s so that a very high injection rate (350—400 h^{-1}) is theoretically possible. The linear range of 0.05—15 mg l^{-1} iron(III) is comparable to the range (0.1—30 mg l^{-1}) reported for flow-injection determinations of iron(II) with 1,10-phenanthroline [1—4] and for

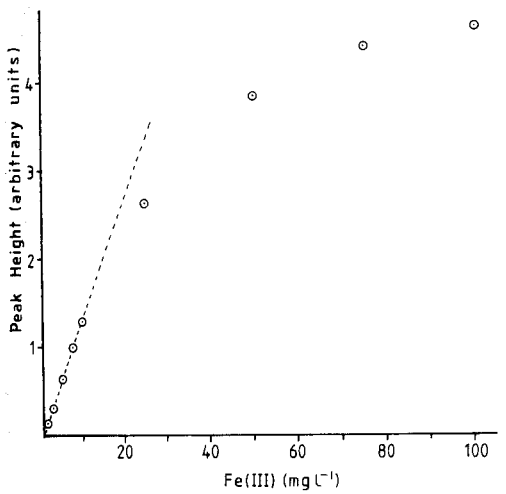

Fig. 1. Plot of peak heights against concentration of iron(III) standards.

iron(III) with potassium thiocyanate (0.5–180 mg l^{-1}) [6]. The manifold can be modified if required to analyse samples in a linear range extending above 15 mg l^{-1}. A linear range of 1–100 mg l^{-1} iron(III) was achieved by increasing the concentration of the ligand salt in the carrier stream to 0.1 M. However, the sample throughout was then lower (200 h^{-1}) because it was necessary to increase the length of the reaction coil (100 cm) to attenuate the absorbance by introducing increased dispersion in the manifold.

It is of interest to note that the excellent sensitivity and high sample throughput achieved with the low-dispersion (D = 1.2–1.3) single-channel manifold could not be reproduced when the stainless-steel flow cell in the Waters detector was replaced by a teflon flow cell of equivalent volume which was constructed here. This can be attributed to the unusual design of the Waters flow cell which has a severely restricted inlet giving excellent mixing of the sample plug with the carrier stream immediately prior to detection. With the home-made flow cell, the signal was almost undetectable because mixing was poor in the short transfer line from injector to detector and in the relatively unrestricted inlet to the cell. Of course, any flow cell can be used if a system with higher dispersion is used to ensure mixing of the sample plug with the carrier stream. This was demonstrated in a dual-channel system where the sample was injected into a carrier stream of 1:1 isopropanol/water, adjusted to pH 2 with nitric acid, which then merged with a reagent stream containing ammonium dithiophosphate in the same medium. However, as the dispersion was much greater in this manifold, both the sensitivity and the sample throughput were reduced compared with the single-channel system.

The use of restrictors in flow-injection manifolds to improve mixing and sample throughput is under investigation.

We are grateful to the Australian Research Grants Scheme for financial support for this project.

REFERENCES

1 J. Moratti, F. J. Krug, L. C. R. Pessenda and E. A. G. Zagatto, Analyst, 107 (1982) 659.
2 B. P. Bubnis, M. R. Straka and G. E. Pacey, Talanta, 30 (1983) 841.
3 A. Faizullah and A. Townshend, Anal. Chim. Acta, 167 (1985) 225.
4 J. L. Burguera and M. Burguera, Anal. Chim. Acta, 161 (1984) 375.
5 T. P. Lynch, N. J. Kernoghan and J. N. Wilson, Analyst, 109 (1984) 839.
6 T. P. Lynch, N. J. Kernoghan and J. N. Wilson, Analyst, 109 (1984) 843.
7 Tecator, Application Note, No. 72 (1984).
8 H. Wada, G. Nakagawa and K. Oshita, Anal. Chim. Acta, 153 (1983) 199.
9 D. J. Leggett, N. H. Chen and D. S. Mahadevappa, Indian J. Chem., 20A (1981) 1051.
10 T. Mochizuki, Y. Toda and R. Kuroda, Talanta, 29 (1982) 659.
11 R. G. Cavell, E. D. Day, W. Byers and P. M. Watkins, Inorg. Chem., 11 (1972) 1759.

INTERNATIONAL JOURNAL OF BIO-MEDICAL COMPUTING

Aims and Scope

International Journal of Biomedical Computing provides an international forum for the presentation of original work, interpretative reviews, commentaries and discussion of fundamental research and new developments in the apllication of the various types of computers (digital, analogue and hybrid) to medicine in particular and the biosciences in general, such as: biochemistry, nuclear magnetic resonance and other techniques in imaging, X-ray dosage, hospital administration, dietetics, pathological data, epidemiology, instrumentation, physiology, cybernetics, sociology, psychology, information storage and retrieval in medical practice and hospitals.

The International Journal of Biomedical Computing is of vital importance for everyone engaged in basic and clinical research, medical information handling, or computer applications.

1987 – Vols. 20, 21 (2 vols. in 8 issues)
Subscription Price: US $ 296.00 including postage and handling
ISSN 0020-7101

ELSEVIER

Send your orders to:

Elsevier Scientific Publishers Ireland, Ltd., P.O. Box 85, Limerick, Ireland

Requests for free sample copies should be sent to:

In the U.S.A. and Canada
Journal Information Center
ELSEVIER SCIENCE PUBLISHERS,
52 Vanderbilt Avenue, New York, NY 10017, U.S.A.

In all other countries:
ELSEVIER SCIENTIFIC PUBLISHERS
IRELAND LTD.,
P.O. Box 85, Limerick, Ireland

The US $ price is definitive.

0003-2670/87/$03.50

rinted in The Netherlands

CONTENTS

(Abstracted, Indexed in: Anal. Abstr.; Biol. Abstr.; Chem. Abstr.; Curr. Contents Phys. Chem. Earth Sci.; Life Sci.; Index Med.; Mass Spectrom. Bull.; Sci. Citation Index; Excerpta Med.)